ABSTRACT

DONG, LAURA BETH. Polystyrene Hydrogenation in Supercritical CO_2-Decahydronaphthalene Using Porous Catalysts. (Under the direction of Dr. George W. Roberts and Dr. Douglas J. Kiserow).

The heterogeneous hydrogenation of polystyrene (PS) was studied in a slurry batch reactor. Mixtures of supercritical carbon dioxide ($scCO_2$) and decahydronaphthalene (DHN) were used as the solvent for the polymer. Several palladium-based porous catalysts were identified for PS hydrogenation at 150^{o}C. Relatively high degrees of hydrogenation were obtained with monometallic palladium catalysts for the reaction conducted in neat DHN. The 5% Pd/SiO_2 was twice as active in hydrogenating PS as 5% Pd/Al_2O_3. However, when either palladium catalyst was used in $scCO_2$-DHN, hydrogenation ceased within 15 minutes of CO_2 addition to the reactor. Detected in the gas phase at the end of CO_2-containing reactions, carbon monoxide (CO) was formed via the reverse water-gas shift (RWGS) reaction and poisoned hydrogenation sites. Physical mixtures consisting of a hydrogenation catalyst (5% Pd/Al_2O_3 or 5% Pd/SiO_2) and a methanation catalyst (65% $Ni/SiO_2/Al_2O_3$ or 5% Ru/Al_2O_3) were effective in reducing CO levels. However, when the "salt-and-pepper" catalyst was used, aromatic ring hydrogenation levels in $scCO_2$-DHN were consistently lower than those obtained in neat DHN.

A bimetallic catalyst in which the hydrogenation and methanation functions are located on the same support (e.g., 1.6% Ru/4.2% Pd/SiO_2 or 5% Pd/5% Ru/SiO_2) was successfully used to reduce CO levels and to hydrogenate PS in $scCO_2$-DHN. The

success of the bimetallic catalyst in hydrogenating PS in scCO_2-DHN over the salt-and-pepper approach was attributed to the differences in internal mass transfer resistances for PS hydrogenation and the RWGS reaction. Because of their smaller molecular diameters, CO_2 and H_2 are able to access the active sites in the catalyst interior and form CO. However, the much larger polymer molecules had very little or no access to the catalyst interior and could not react on the poisoned sites. When the methanation function was proximate to the hydrogenation metal, as in the case of the bimetallic catalyst, CO was methanated before it poisoned hydrogenation sites.

Polymer size effects on heterogeneous PS hydrogenation were determined by varying polymer molecular weight and by using CO_2 to tune polymer coil size in DHN. The ability to tune polymer coil size by varying CO_2 concentration was demonstrated in high pressure dynamic light scattering experiments. A nearly two-order-of-magnitude increase in the rate of hydrogenation in neat DHN was observed when PS molecular weight decreased from 160 kDa to 24 kDa. For a 160 kDa PS, the rate of hydrogenation increased with CO_2 concentration; an order-of-magnitude change was observed when CO_2 pressure was increased from 0 psig to 2200 psig. The improvements in reaction rate in either neat or CO_2-expanded DHN were found to be directly related to increases in PS diffusivity and decreases in polymer coil diameter, both of which are functions of polymer molecular weight and solvent quality.

Polystyrene Hydrogenation in Supercritical CO_2-Decahydronaphthalene Using Porous Catalysts

by
Laura Beth Dong

A dissertation submitted to the Graduate Faculty of
North Carolina State University
in partial fulfillment of the
requirements for the Degree of
Doctor of Philosophy

Chemical Engineering

Raleigh, North Carolina

2010

APPROVED BY:

_____	_____
Ruben G. Carbonell	Alan E. Tonelli
_____	_____
George W. Roberts (Chair of Advisory Committee)	Douglas J. Kiserow (Co-chair of Advisory Committee)

BIOGRAPHY

Laura Beth Dong was born on September 20, 1981, in Greenwood, Mississippi. She grew up in Webb, Mississippi. In May 2000, she graduated from Lee Academy (Clarksdale, Mississippi). The following fall, she entered the Chemical Engineering program at Mississippi State University (MSU).

While an undergraduate at MSU, she was involved in many College of Engineering and Chemical Engineering student organizations, serving as president of the MSU student chapter of AIChE and Omega Chi Epsilon. She also worked as an undergraduate research assistant on the remediation of small-arms training range soils. She graduated summa cum laude in May 2004 with a Bachelor of Science in Chemical Engineering, with minors in Mathematics and Chemistry.

In August 2004, she entered the Chemical and Biomolecular Engineering (CBE) graduate program at North Carolina State University. In Spring 2005, she was named a National Science Foundation Graduate Research Fellow. She served as president of the CBE Graduate Student Association and as a Graduate Student Recruiting Captain for the department. For her doctoral dissertation research, she has worked under the direction of Dr. George W. Roberts on the hydrogenation of polystyrene in supercritical carbon dioxide-expanded solvents.

ACKNOWLEDGEMENTS

First and foremost, I would like to express my gratitude to my advisor, Dr. George Roberts, for his constant guidance, encouragement, and patience. It has been an honor to learn from you. I would also like to acknowledge the helpful input of my committee members, Dr. Doug Kiserow, Dr. Ruben Carbonell, and Dr. Alan Tonelli.

I would also like to thank Dr. John van Zanten for his helpful discussions regarding dynamic light scattering; Joshua Manasco and Sara Arvidson for their help with DSC measurements; and Salomon Turgman for the *many* hours he has spent with the GPC. Also, special thank you's go out to Kit Yeung and Hai Bui, whose handyman and craftsmanship skills have performed small miracles, and Dr. Gary McVicker for sharing his knowledge of catalysis.

My appreciation also goes out to past and current colleagues in the Roberts research group and the Kenan CO_2 Center- particularly, Nathan Cain, my "partner in crime"; Jaehoon Kim for introducing me to GPC; Tamer Ahmed for help with GC measurements; Dawei Xu for acclimating me to polystyrene hydrogenation; and Paul Chin, Xenia Tombokan, Shaun Tann/er, and Alan Chang for their fellowship. I am also thankful for the contributions of several undergraduate researchers.

To my Fun Lunch crew, thank you for riding the ups and downs of graduate research with me. A "You are awesome!" goes out to the Melvins for their friendship. Mike, I am so lucky to have your love and support. I am also grateful for the love and support of my parents- Ronald and Linda- and my sisters- Melanie and Brittany.

TABLE OF CONTENTS

LIST OF FIGURES

LIST OF TABLES

CHAPTER 1 :

INTRODUCTION

1.1. Motivation and Objectives

Hydrogenated polymers exhibit increased thermal and oxidative stability and better solvent resistance than their unsaturated counterparts [1, 2]. The complete hydrogenation of the aromatic rings of polystyrene (PS) creates a polymer with improved physical properties [3, 4]. Hydrogenating PS creates a product with lower density, lower water absorption, increased transparency, and a higher glass transition temperature (T_g) than PS itself [3]. Some reports indicate that the T_g of fully hydrogenated PS is 147^{o}C [3, 5], which is comparable to that of poly(bisphenol A carbonate) (BPA-PC). Combined with the improved transparency, the increase in T_g may make hydrogenated PS competitive with BPA-PC in some applications. For example, hydrogenated PS been identified as useful for optical media storage [6, 7]. Some have called hydrogenated PS the "poor man's polycarbonate" since the product is much less costly and less toxic than BPA-PC, and the process does not involve the toxic chemicals used in traditional BPA-PC synthesis methods.

Previous researchers have used supported rhodium, nickel, palladium, and platinum catalysts to hydrogenate PS [5-10]. Due to the large size of polymer molecules, the mass transfer challenges associated with heterogeneously-catalyzed, small-molecule reactions are magnified in heterogeneous polymer hydrogenation. Polymer solutions are

very viscous, and polymer diffusivity is relatively low. These undesirable mass transfer conditions can result in lower reaction rates. In heterogeneously-catalyzed reactions, polymer molecules also have the challenge of diffusing through the pores and reacting. When the reactant molecule is comparable to the diameter of the catalyst pores, hindered reactant diffusion has been shown to affect reaction kinetics [11-14]. When the polymer coil is larger than the diameter of the catalyst pore, the reactant will be unable to access the catalyst interior.

One way to reduce transport effects in heterogeneously-catalyzed PS hydrogenation is to use supercritical CO_2 ($scCO_2$) as a solvent or co-solvent [15-17] . Transport property enhancements associated with the use of $scCO_2$ have been documented [18]. Since PS is not soluble in CO_2 at reasonable pressures, it is not feasible to use neat $scCO_2$ as a reaction medium. However, the use of a CO_2-expanded liquid (CXL) as a reaction medium can result in lower solution viscosities and higher reactant diffusivities. As a result, reaction rates should increase. Besides the positive effects on mass transfer, other advantages of using a CXL are increased H_2 solubility in hydrogenations and reduced organic solvent waste. The use of a CXL also creates a means of tuning reaction conditions by varying the system pressure.

When a batch reactor is used, one potential disadvantage to conducting hydrogenations in a CXL is catalyst deactivation that occurs via carbon monoxide (CO) poisoning of active sites [19-21]. However, studies have shown that the use of a

methanation catalyst in conjunction with the hydrogenation catalyst can be effective in reducing CO levels and allowing the desired reaction to proceed [21].

The objective of this research is to better understand the factors that govern the hydrogenation of PS in neat decahydronaphthalene (DHN) and in DHN expanded with $scCO_2$ in a slurry, batch reactor. One goal of this research is to determine the effect of using different palladium-based catalyst systems in PS hydrogenation. Another objective is to determine the effect of CO_2 as a co-solvent on gas-liquid, liquid-solid, and pore diffusion resistances for each catalyst in PS hydrogenation. In order to better understand the effect of CO_2 on mass transfer resistances, PS diffusion coefficients in CO_2-DHN were measured. The effect of polymer molecular weight on hydrogenation kinetics is quantified. This research also includes determination of the molecular-weight-distribution and glass transition temperatures of partially hydrogenated PS's.

1.2. Scope of Research

Chapter 2 is a review of the literature on hydrogenation, specifically polymer hydrogenation and hydrogenations in which dense-phase CO_2 is present. Information on homogeneous and heterogeneous polymer hydrogenations is presented, with emphasis on aromatic ring hydrogenation. The use of $scCO_2$ as a solvent and co-solvent in chemical reactions is also reviewed, with particular focus on hydrogenation processes.

In Chapter 3, the effect of various CO_2 concentrations on PS diffusion coefficients in DHN and polymer-solvent interactions are determined using high pressure dynamic

light scattering. The effect of temperature is measured, and hydrodynamic radii (R_H) are calculated at each of the experimental conditions.

Challenges associated with using mesoporous Pd catalysts for PS hydrogenation in CO_2-DHN are presented in Chapter 4. The use of physical mixtures of a Pd hydrogenation catalyst and a methanation catalyst for the reaction in CO_2-DHN is compared to the use of a bimetallic catalyst in which both metals are located on the same support. Carbon monoxide evolution from Pd-catalyzed PS hydrogenations was also studied, and a simple model was developed to describe CO formation and its effect on PS hydrogenation kinetics.

Chapter 5 focuses on the hydrogenation of a series of monodisperse PS in neat DHN and CO_2-DHN, using a bimetallic catalyst with a fairly narrow pore size distribution. By varying the polymer molecular weight and CO_2 concentration, the effect of polymer coil size on hydrogenation kinetics is studied. The influence of polymer diffusivity on heterogeneous PS hydrogenation is observed.

The influence of mass transfer resistances on PS hydrogenation and its products' physical properties is investigated in Chapter 6. The effects of temperature, catalyst concentration, and agitation rate on hydrogenation kinetics are determined. Possible causes for observed catalyst deactivation are investigated, and a model is developed to explain the decrease in catalyst concentration. Physical properties, e.g., molecular weight and glass transition temperatures, are measured. Deconvolution of the aromatic and cyclohexyl fractions are conducted using GPC equipped with UV and RI detection.

Chapter 7 summarizes the findings of this research and recommends some future avenues of work.

References

1. McManus, N.T., Rempel, G. L., *Chemical Modification of Polymers: Catalytic Hydrogenation and Related Reactions.* Polymer Reviews, 1995. **35**(2): p. 239-285.
2. McGrath, M.P., Sall, E. D., Tremont, S. J., *Functionalization of Polymers by Metal-Mediated Processes.* Chemical Reviews, 1995. **95**: p. 381-398.
3. Hucul, D.A., Hahn, S. F., *Catalytic Hydrogenation of Polystyrene.* Advanced Materials, 2000. **12**(23): p. 1855-1858.
4. Pendleton, J.F., Hoeg, D. F., Goldberg, E. P., *Novel Heat Resistant Platsics from Hydrogenation of Styrene Polymers*, in *Advances in Chemistry Series*. 1973: Washington, DC. p. 27-38.
5. Abe, A., Hama, T., *Structure and Properties of Poly(vinylcyclohexane).* Polymer Letters, 1969. **7**: p. 427-435.
6. Iio, A., Yoshinari, M., Komiya, Z., Goto, K. Optical Materials Based on Hydrogenated Alkenyl Aromatic Hydrocarbon Polymers. EP 317263 A2. 1988.
7. Wege, V., Bruder, F., Douzinas, K., Chen, Y. Vinylcyclohexane polymer, useful for the production of optical storage disks, has specified molecular weight, polydispersion index, and melt viscosity. DE 199 21 941 A1. 2000.

8. Helbig, M., Inoue, H., Vogl, O., *Preparation and Characterization of Head-to-Head Polymers. VIII. Head-to-Head Poly(vinylcyclohexane).* Journal of Polymer Science: Polymer Symposium, 1978. **63**: p. 329-342.

9. Elias, H.-G., Etter, O., *Glass Temperature of Hydrogenated Polystyrene.* Journal of Macromolecular Science, Part A, 1967. **5**: p. 943-953.

10. Nakatani, H., Nitta, K-h., Soga, K., *Effect of Hydrogenation on Dynamic Mechanical Relaxation 1. Atactic Polystyrene.* Polymer, 1998. **39**(18): p. 4273-4278.

11. Ruckenstein, E., Tsai, M. C., *Optimum Pore Size for the Catalytic Conversion of Large Molecules.* AIChE Journal, 1981. **27**(4): p. 697-699.

12. Shimura, M., Shiroto, Y., Takeuchi, C., *Effect of Catalyst Pore Structure on Hydrotreating of Heavy Oil.* Industrial and Engineering Chemistry Fundamentals, 1986. **25**: p. 330-337.

13. Chang, J.-R., Huang, S-M., *Pd/Al_2O_3 Catalysts for Selective Hydrogenation of Polystyrene-block-Polybutadiene-block-Polystyrene Thermoplastic Elastomers.* Industrial & Engineering Chemistry Research, 1998. **37**: p. 1220-1227.

14. Shirai, M., Suzuki, N., Nishiyama, Y., Torii, K., Arai, M., *Size-Selective Hydrogenation of NBR Polymers Catalyzed by Pore-Size Controlled Smectites Loaded with Palladium.* Applied Catalysis A: General, 1999. **171**: p. 219-225.

15. Baiker, A., *Supercritical Fluids in Heterogeneous Catalysis.* Chemical Reviews, 1999. **99**: p. 453-473.

16. Beckman, E.J., *Supercritical and Near-Critical CO_2 in Green Chemical Synthesis and Processing.* Journal of Supercritical Fluids, 2004. **28**: p. 121-191.

17. Subramaniam, B., Lyon, C. J., Arunajatesan, V., *Environmentally Benign Multiphase Catalysis with Dense Phase Carbon Dioxide.* Applied Catalysis B: Environmental, 2002. **37**: p. 279-292.

18. Jessop, P.G., Subramaniam, B., *Gas-Expanded Liquids.* Chemical Reviews, 2007. **107**: p. 2666-2694.

19. Ichikawa, S., Tada, M., Iwasawa, Y., Ikariya, T., *The Role of Carbon Dioxide in Chemoselective Hydrogenation of Halonitroaromatics Over Supported Noble Metal Catalysts in Supercritical Carbon Dioxide.* Chemical Communications, 2005(7): p. 924-926.

20. Minder, B., Mallat, T., Pickel, K. H., Steiner, K., Baiker, A., *Enantioselective Hydrogenation of Ethyl Pyruvate in Supercritical Fluids.* Catalysis Letters, 1995. **34**: p. 1-9.

21. Xu, D., Carbonell, R. G., Kiserow, D. J., Roberts, G. W., *Hydrogenation of Polystyrene in CO_2-Expanded Solvents: Catalyst Poisoning.* Industrial & Engineering Chemistry Research, 2005. **44**: p. 6164-6170.

CHAPTER 2 :

LITERATURE REVIEW

2.1. Introduction

By a conservative estimate, in 2002, the polymer industry accounted for one-fifth of the output of the U. S. organic chemical industry [1]. Polymer hydrogenation is a post-polymerization process that can be used to synthesize specialty polymers. Hydrogenated polymers exhibit improved thermal and oxidative stability and higher glass transition temperatures (T_g) than their unsaturated counterparts [2-4]. They can also exhibit better solvent resistance or attractive optical properties.

Homogeneous and heterogeneous catalysts can be used to hydrogenate polymers. Homogeneously-catalyzed hydrogenation offers the ability to target specific chemical moieties on a polymer at moderate reaction conditions. However, separation of the catalyst and polymer is often difficult and expensive. The separation is viewed as a necessary step to prevent polymer degradation by catalyst residuals.

The high solution viscosities and low polymer diffusivities make the reaction of polymer molecules difficult. The impact of transport properties in heterogeneous-catalyzed polymer reactions are encompassed in gas-liquid, liquid-solid, and internal mass transfer resistances. Ideally, since the relatively large polymers must diffuse through the catalyst pores and react, internal mass transfer limitations should be minimized or reduced.

The use of dense carbon dioxide (CO_2) as a reaction medium or as part of a CO_2-expanded liquid (CXL) has proved to be beneficial on reactant diffusivity and solution viscosity. As a result, increased reaction rates may be observed. These enhancements have been shown to be beneficial to small molecule and polymer hydrogenation using heterogeneous catalysts.

In this chapter, polymer hydrogenation using homogeneous and heterogeneous catalysts is reviewed. Focus is centered on aromatic ring hydrogenation and the resulting properties of the product polymer. The use of supercritical CO_2 ($scCO_2$) in chemical reactions is discussed, with focus on heterogeneous hydrogenation. Finally, the effect of $scCO_2$ on polymer solution transport properties, with focus on PS-CO_2-DHN, will be briefly reviewed.

2.2. Polymer Hydrogenation

Homogeneously and heterogeneously-catalyzed polymer hydrogenations have been reviewed by McManus et al. [5] and McGrath et al. [6]. As previously mentioned, the homogeneous catalyst route offers the ability to selectively saturate specific functional groups while the use of heterogeneous catalysts provides a facile way of separating the catalyst and polymer solution at the end of the reaction.

Polymers that have been hydrogenated are polyisoprene (PI), polybutadiene (PB), polystyrene (PS), styrene-isoprene block copolymer, styrene-butadiene-styrene (SBS)

block copolymer, and acrylonitrile-butadiene natural rubber (NBR). Commercial processes to hydrogenate the butadiene units of SBS and NBR exist [7-9].

As shown in Figure 2.1, the incomplete hydrogenation of the aromatic rings of polystyrene yields polystyrene-polyvinylcyclohexane (PVCH) copolymers. PVCH has a lower density and higher glass transition temperature than its parent polymer; the completely saturated product is also transparent and has a stress-optical coefficient that makes it appealing for use in digital media applications [10].

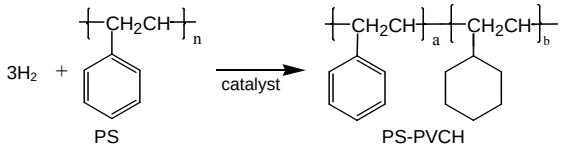

Figure 2.1. Polystyrene Hydrogenation

Depending on the configuration of the olefin link (1,4- or 1,2- microstructure), the hydrogenation of the butadiene links in SBS copolymers gives styrene-ethylene/propylene-styrene (SEPS) or styrene-ethylene/butylene-styrene (SEBS) copolymers. The components of the copolymer is shown in Figure 2.2.

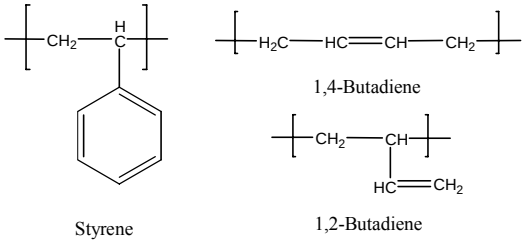

Figure 2.2. Components of Styrene-Butadiene Block Copolymers

Hydrogenated SBS has high temperature stability and has resistance to oxygen, ozone, and UV radiation [5]. Known commercially as the Kraton G family of polymers, SEPS and SEBS are used in handles, grips, and diapers; as impact modifiers for thermoplastics; and as an additive in polypropylene [7]. It can also be used as a viscosity index improver.

Zetpol and Therban are trade names for hydrogenated NBR (HNBR) [8, 9]. An oil-resistant elastomer, HNBR can be used at elevated temperature; is oxygen, ozone, and chemical resistant; and can retain its elastomeric properties after being exposed to high temperatures [5]. Seals, hoses, and belts in the automotive and chemical industries are often comprised of HNBR [11].

2.2.1. Homogeneous Polymer Hydrogenation

Homogeneous polymer hydrogenation catalysts can be classified as metal salts and complexes that consist of osmium, palladium, rhodium, or ruthenium. The reaction temperatures for homogeneously-catalyzed polymer hydrogenation are typically milder than those used in heterogeneously-catalyzed saturations. Therefore, most homogeneous polymer hydrogenations saturate olefinic double bonds.

The metal salts used in polymer hydrogenation are also referred to as Ziegler-type catalysts. These catalysts, which are relatively inexpensive, are typically used in high concentrations. A nickel-aluminum catalyst has been used to selectively saturate the olefinic portion of styrene-isoprene and styrene-butadiene block copolymers at 80^{o}C to

90°C [12]. Styrene-based copolymers were hydrogenated using a cobalt-aluminum based catalyst [13]. The second component in the copolymer was either PI or PB, which can also be hydrogenated to form ethylene-propylene or ethylene-butene polymers, respectively.

Osmium complexes have been used to selectively hydrogenate the olefinic portion of NBR polymers [14]. The use of palladium carboxylate or palladium acetate complexes has been reported. The rhodium complex that is typically used in the homogeneous hydrogenation of olefinic bonds in polymers is commonly known as Wilkinson's catalyst ($Rh(PPh_3)_3Cl$). Acrylonitrile-butadiene, styrene-butadiene latexes, and PBs have all been hydrogenated using the Wilkinson's catalyst.

Ruthenium complexes with a structure similar to Wilkinson's catalyst are sometimes preferred because they are more cost-effective than rhodium. Ruthenium complexes have been used to hydrogenate the olefinic portion of SBS copolymers at temperatures ranging form 120°C to 160°C [4] and in hydrogenating natural rubber (polyisoprene) [15]. Molecular weight reduction was insignificant in the latter case.

Skim natural rubber (SNR), which is mostly *cis*-1,4-polyisoprene, has been saturated at temperatures ranging from 60 to 80°C through the use of a diimide hydrogen donor that was formed by the copper-catalyzed reaction of hydrazine and hydrogen peroxide [16]. Skim natural rubber was hydrogenated in the latex form, which resulted in mass transfer limitations in the reaction process. The apparent activation energy was 9.5 kJ/mol, which is suggestive of a diffusion-limited reaction. Asymptotic degrees of

hydrogenation were reached after 6 hours of reaction at all temperatures studied. Differential scanning calorimetry (DSC) of a 64.5% hydrogenated SNR product revealed the existence of two T_g's, a novel feature. The authors attributed the two T_g's to non-hydrogenated and hydrogenated polymers that were formed as consequences of mass transfer limitations in the reaction.

2.2.2. Heterogeneous Polymer Hydrogenation

Heterogeneous hydrogenation has been used to saturate homopolymers and copolymers. Reaction temperature typically depends on the energy required to saturate the desired moiety. Typical moieties that are hydrogenated are olefinic double bonds and aromatic rings. As shown in Table 2.1, the aromatic ring hydrogenation requires more energy input than the saturation of the carbonyl or olefinic groups; thus aromatic ring hydrogenation typically occurs at higher temperatures (>100^{o}C).

Table 2.1. Enthalpies of Hydrogenation (adapted from Bartholomew and Farrauto[17])

Reactions	**$-\Delta H_r$, kJ/mol**
Carbonyl Group to Alcohol	65
C==C to C--C	125
Aromatic Ring Saturation	210
Nitro Group to Amine	550

2.2.2.1. Olefinic Polymer Hydrogenation

Polyisoprene was hydrogenated at room temperature and atmospheric pressure using a 5% Pd/$CaCO_3$ catalyst [18]. The major findings of Schulz and Worsfold's

research were (1) lower molecular weight PI had higher degrees of hydrogenation than the higher molecular weight polymer, (2) significant chain scission occurred during the hydrogenation of all of the studied polyisoprenes, and (3) phase separation of the product polymer solutions were suggestive of immiscibility of product polymers. The immiscibility was attributed to the existence of blocks of isoprene and hydrogenated isoprene.

Based on the analysis of the bimodal molecular weight distribution of partially hydrogenated PB, Rosedale and Bates proposed a blocky hydrogenation mechanism [19]. Solubility experiments revealed that one fraction of the product polymer was 85% hydrogenated while the other fraction was unreacted PB. Typical reaction parameters were 10 g PB/L cyclohexane solution with 5% $Pd/CaCO_3$ (0.5 to 1.8 g catalyst/g polymer), 70^{o}C, 500 psi H_2.

Cassano et al. studied the hydrogenation of PB using two different palladium catalysts (5% $Pd/CaCO_3$ and 5% $Pd/BaSO_4$) and two different solvents for the polymer (cyclohexane and heptane) [20]. These researchers found that one fraction of the product polymers had an average degree of hydrogenation of 89%, which was very similar to the results obtained by Rosedale and Bates. In the work of Cassano et al., when the reaction temperature was 75^{o}C, 0.5 grams of 5% $Pd/CaCO_3$ per gram of polymer was used to hydrogenate a 0.5 wt% PB-cyclohexane solution. Similarly, when the reaction temperature was 98^{o}C, 0.4 grams of 5% $Pd/BaSO_4$ per gram of polymer was used to hydrogenate a 0.5 wt% PB-heptane solution.

Costello et al. studied the hydrogenation of the olefinic units of PB, PI, and PS-PI using Pd/C catalysts [2]. An organic liquid such as cyclohexane, heptane, or toluene was used in conjunction with an alcohol such as ethanol, t-butyl alcohol, or 1-octadecanol as a solvent for the polymer hydrogenations. Formic acid served as the hydrogen source. Complete polyisoprene hydrogenation catalyzed by 5% $Pd/CaCO_3$ or 5% $Pd/BaSO_4$ was reported [21].

2.2.2.2. Aromatic Ring Hydrogenation

Polystyrene hydrogenation has been the most frequently studied aromatic ring-containing polymer hydrogenation. Studies of the partial hydrogenation of PS, as well as its complete hydrogenation to form PVCH, have been reported. Earlier research used supported nickel catalysts for aromatic ring hydrogenation. Recent efforts have employed supported palladium or platinum catalysts.

Table 2.2 summarizes the reaction conditions for PS hydrogenation that were found in the literature. Solvents for PS were fully saturated organic liquids. In a couple of studies, a small amount of THF was added to cyclohexane to improve polymer solubility [22, 23].

Table 2.2. Polystyrene Hydrogenation Conditions

Catalyst	Temp. (^oC)	H_2 Pressure (psig)	Catalyst: Polymer (w:w)	Polymer Conc. (%)	Solvent
Red. $NiCO_3$ [24]	200	2057	4:1	3	DHN
Raney Ni [24]	200-270	3087-3821	7:1, 9:1	3	DHN
Activated Ni [25]	170	2418	---	---	CH
10% Ni/SiO_2 [26]	185-190	1740	0.1:1 to 0.3:1	3.2	MCH
$Ni/SiO_2/Al_2O_3$ [27]	160-180	1450	0.125:1	---	CH/ MTBE
5% $Pd/BaSO_4$ [22]	140	500	5:1	1	CH/THF
5% $Pd/BaSO_4$ [21]	140	500	2.5:1	1	CH
5% $Pd/BaSO_4$ [28]	150	750	1:1	3	DHN
5% $Pd/CaCO_3$ [21]	140	500	2.5:1	1	CH
0.5% Pd/Al_2O_3 [23]	150-180	500	---	2, 10	CH/THF
5% Pt/SiO_2 [10]	150	975	0.07:1	---	CH
5% Pt/SiO_2 [29]	170	500	0.05:1	4	CH
10% Rh/C [30]	200	2000	0.15:1	1	DHN
5% Rh/C [31]	140	1422	1.8:1	9	THF

CH= cyclohexane, DHN = decahydronaphthalene, MCH=methylcyclohexane, MTBE = methyl-t-butyl ether, THF= tetrahydrofuran

Due to the low surface areas of the supports, a fair amount of PS hydrogenation research has been conducted with $Pd/BaSO_4$ and $Pd/CaCO_3$ catalysts. As the information in the table indicates, relatively high reaction temperatures and high catalyst to polymer ratios were used. The high cost of precious metals makes the use of high catalyst to polymer ratios undesirable.

Presently, it appears that the 5% Pt/SiO_2 catalyst is the most efficient in hydrogenating the aromatic rings of PS, as noted by the low catalyst to polymer ratio and the high degrees of hydrogenation reached in a short amount of time [3]. These results may be attributed to the ultra-wide pore support, which had an average pore diameter of

380 nm and a BET surface area of 16.5 m^2/g [10]. These catalyst characteristics should result in reduced pore diffusion limitations for the large polymer coils. Also an optimum balance between the surface area of the catalyst and the metal dispersion appears to have been reached in order to obtain such high reaction rates.

Some analysis of PS hydrogenation kinetics has been reported in the literature. At 150°C, the observed rate constant of 0.5% Pd/Al_2O_3-catalyzed PS hydrogenation (3.1 x 10^{-5} L/g Pd/s) [23] was comparable to the rate of 5% $Pd/BaSO_4$-catalyzed PS hydrogenation (3.2 x 10^{-5} L/g Pd/s) [28]. The initial rates of hydrogenation for monodisperse PS's, which were measured by Ness et al., were found to be dependent on the molecular weight of the polymer [29]. The initial rates of hydrogenation for the PS's with molecular weights 190,000 and 276,000 g/mol fell below the trend line for the lower molecular weight PS (1,500 to 102,000 g/mol) rate data.

Intrinsic viscosity, osmometry, and gel permeation chromatography have been used to measure the molecular weights of the starting PS and the PS hydrogenation products. Significant chain degradation occurred when nickel [24-26] or rhodium [30] was the catalyst of choice. No significant changes in molecular weight were observed when supported Pd or Pt was the catalyst [10, 21, 22, 29].

The hydrogenated polymers are typically recovered using a small chain alcohol, with methanol being the most popular choice. Sometimes a mixture of small chain alcohols have bee used to precipitate hydrogenated polymers. Elias and Etter used acetone to recover their partially hydrogenated PS's [24].

Differences in the glass transition temperatures of partially and fully hydrogenated PS exist in the literature. Elias and Etter reported the existence of two T_g's for partially hydrogenated PS's (42.8% and 75.8% hydrogenated) [24]. One T_g was approximately 75°C while the other was roughly 100°C. The lower T_g was associated with PVCH and the higher T_g with PS. These results contrast with other research, which indicates that PVCH has a higher T_g than PS.

Both Abe and Hama [25] and Nakatani et al. [26] saw monotonic increases in T_g with increasing degrees of hydrogenation. The differences in the reported data are less than 7°C; approximately 40°C existed between the T_g's measured for PS and PVCH. Abe and Hama used differential scanning calorimetry (DSC) and dilatometry to confirm the behavior of the T_g's of partially hydrogenated PS.

Nakatani et al. used dynamic mechanical analysis and DSC to obtain their T_g data for atactic PS. These researchers also used small angle light scattering and transmission electron microscopy to characterize partially hydrogenated PS. At the intermediate degrees of hydrogenation (56 and 62%), PS phases were dispersed in the hydrogenated phases. This phase separation was not observed with lower and highly hydrogenated polymers. Similarly, phase segregation was also observed with partially hydrogenated syndiotactic PS [32]. The phase separation was attributed to amorphous and crystalline phases in the product polymers.

For the fully saturated polymer, Gehlsen et al. reported a glass transition temperature of 137°C for high molecular weight PVCH [22]. These polymers were

created by 5% $Pd/BaSO_4$-catalyzed PS hydrogenation in a mixture of cyclohexane and THF solvent. Differential scanning calorimetry was used to measure T_g; a heating rate of 10^oC/min was used. The value measured by Gehlsen et al. is exactly the value reported by Iio et al. for their PVCH created using a 5% Rh/C catalyst [31].

A slightly higher T_g of 140^oC was reported by Xu et al. for a 48,000 g/mol PVCH that was created via PS hydrogenation in cyclohexane using a Pt/SiO_2-based catalyst [33]. A DSC heating rate of 10^oC/min was used in the work of Xu et al.

Zhao et al. reported a T_g of 145^oC for their 48,000 g/mol PVCH, which was created through Pt/SiO_2-catalyzed PS hydrogenation [34]. This report is surprising since one would expect that Zhao et al.'s DSC heating rate (3^oC/min) [34] would result in a lower T_g than what was observed with Nakatani et al.'s heating rate of 10^oC/min [26]. However, the T_g's (146-148^oC) for the high molecular weight PVCH's (molecular weights greater than 100,000 g/mol) are in good agreement with the value (146^oC) reported by Nakatani et al. for atactic PVCH [26].

One of the challenges associated with PVCH is its brittleness. To that end, some research has focused hydrogenating aromatic units in styrene-based polymers. Examples that have been researched include polymethylstyrenes [22], styrene-α-methylstyrene copolymers [33], styrene-butadiene [12, 13, 35, 36], and styrene-isoprene [12].

Gehlsen et al. reported incomplete hydrogenation of styrene-isoprene to vinylcyclohexane-ethylene/propylene when 5% $Pd/CaCO_3$ was the catalyst for a reaction at 105^oC [21]. The use of 5% $Pd/BaSO_4$ at the same reaction temperature yielded a

completely hydrogenated product. In the work of Adams et al., both the aromatic and olefinic portions of styrene-isoprene and styrene-butadiene block copolymers were hydrogenated when 5% $Pd/BaSO_4$ or 5% $Pd/CaCO_3$ was used as the catalyst [12]. Reaction temperature was between 90°C and 100°C; hydrogen pressure ranged from 400 to 800 psi. Hahnfeld et al. used the previously mentioned ultra-wide pore Pt/SiO_2 catalyst and an ultra-wide pore $Pt/Re/SiO_2$ catalyst to hydrogenate SBS at 150°C [35]. Maheshwari et al. used the wide-pore $Pt/Re/SiO_2$ catalyst to selectively hydrogenate the aromatic ring of styrene in PS-PDMS-PS block copolymer to form PVCH-PDMS-PVCH [37]. The PVCH adds stiffness and thermal stability to PDMS.

The effects of catalyst pore size and metal dispersion on polymer hydrogenation was illustrated by Chang and Huang [36]. There appeared to be a trade-off between pore size and metal dispersion that negated the effect of increasing pore diameter on the hydrogenation of the olefinic portion of SBS block copolymers. There was a distinct difference in the degree of aromatic ring hydrogenation when the smallest pore diameter catalyst was used; there was not a significant difference between the two larger pore diameter catalysts.

The role of pore size on NBR hydrogenation kinetics was observed by Shirai and co-workers [38]. For a NBR with a molecular weight of 3000 dissolved in carbon tetrachloride, the initial rate of hydrogenation increased significantly when pore size increased from 63 to 79 Å. When the same NBR was dissolved in acetone and hydrogenated, there was no dramatic increase in the olefinic saturation with increasing

pore size. This behavior was attributed the expansion of NBR in the good solvent acetone, which prevented the polymer from easily diffusing through the interior of the catalyst.

2.3. Supercritical Carbon Dioxide

Supercritical carbon dioxide is part of a larger category known as supercritical fluids (SCF). The critical properties of chemicals that have been used in SCF research are provided in Table 2.3. The critical temperatures of the chosen fluids range from near ambient to quite high, while in general, the differences in the critical pressures are not as large.

The attractive physical and transport properties of SCFs has led to their usage in reactions, separations processes, and particle formations. Supercritical fluids are unique in that they exhibit both gas- and liquid-like properties. Order-of-magnitude estimates of a few of these properties are provided in Table 2.4. The density of a SCF can be changed by varying the system pressure and temperature; this flexibility offers a way to tune the properties of a process to achieve a desired product. The decrease in viscosity and increase in diffusivity associated with a liquid-SCF mixture is attractive in areas where there is significant transport resistance; examples of research areas where mass transport limitations exist are heterogeneously-catalyzed reactions, polymer processing, and polymer reactions.

Table 2.3. Critical Properties of Selected Fluids [39]

Fluid	T_c (K)	P_c (atm)
Ethylene	282.4	49.7
Xenon	289.7	57.6
Trifluoromethane	299.1	48.1
Carbon dioxide	304.2	72.8
Ethane	305.4	48.2
Nitrous oxide	309.6	71.5
Sulfur hexafluoride	318.7	37.1
Propane	369.8	41.9
1,1-Difluoroethane	386.6	44.4
Ammonia	405.6	111.3
Methyl amine	430.0	73.6
1-Hexene	504.0	31.3
t-Butanol	506.2	39.2
n-Hexane	507.4	29.3
Acetone	508.1	46.4
i-Propanol	508.3	47.0
Methanol	512.6	79.9
Ethanol	516.2	63.0
Toluene	591.7	40.6
p-Xylene	616.2	34.7
Water	647.3	217.6
Tetralin	719.0	34.7

Table 2.4. Comparison of Typical SCF, Liquid, and Gas Properties [39]

	Liquid	SCF	Gas
Density (g/cm^3)	1	0.1-0.5	10^{-3}
Viscosity (Pa*s)	10^{-3}	10^{-4} to 10^{-5}	10^{-5}
Diffusivity (cm^2/s)	10^{-5}	10^{-3}	10^{-1}

Also, the increased solubility of gases in supercritical fluids versus neat organic solvents has made the use of SCFs in chemical reactions attractive. The enhanced heat capacity of SCF-organic liquids enables the mixtures to be used in reactions where temperature stability is an issue. The use of SCFs for extraction of coke deposits on heterogeneous catalysts in hydrogenation and Fischer-Tropsch syntheses has been reviewed [40]. The coke removal prevents the effective diffusivities of the reactant molecules from declining during the course of the reaction; therefore the effectiveness factors remain constant and pore diffusion limitations do not worsen.

An example of a commercialized supercritical fluid application is the decaffeination of coffee using water-supercritical CO_2. The technology to hydrogenate polymers in supercritical hexane-expanded solvents has been patented [41].

Supercritical carbon dioxide has been the focus of much research, due to its relative inertness, low toxicity, and non-flammability. It is sometimes viewed as a "green solvent" because its use can reduce the amount of organic solvent used in a process. Beckman reviewed the use of CO_2 as a green processing aid [42]. The miscibility of CO_2 with H_2, CO, and O_2 is viewed as an advantage in using CO_2 in chemical reactions. The positive effect of CO_2 on H_2 solubility in CO_2-unidentified organic feed can be seen in Figure 2.3. Points worth noting are the maxima in H_2 solubility at approximately 50 wt% CO_2 and the roughly three-fold increase in H_2 solubility in the organic liquid with the addition of CO_2.

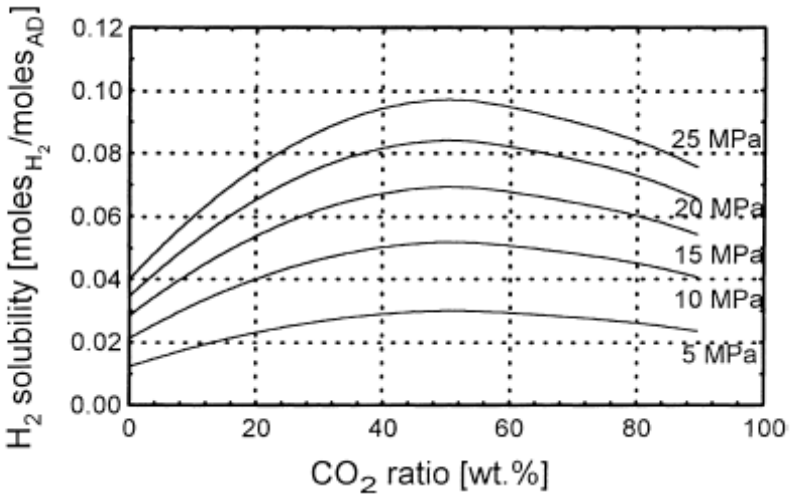

Figure 2.3. Calculated Liquid Hydrogen Solubility at Different CO_2 Feed Ratios at 100°C [43]

2.3.1. Reactions with the Aid of Dense Carbon Dioxide

Homogeneous and heterogeneously-catalyzed reactions conducted with the aid of dense CO_2 have been reviewed by Baiker [44], Beckman [42], Subramaniam et al. [45], Arai et al. [46], and Jessop and Subramaniam [47]. Homogeneous catalysts used in CO_2 environments typically contain fluorine-based ligands since fluorine compounds are CO_2-philic. Beckman provides examples of homogeneous hydrogenations and hydroformylations conducted in dense CO_2 [42].

Heterogeneously-catalyzed alkylations, aminations, disproportionation, esterifications, hydroformylations, hydrogenations, isomerizations, and oxidations in dense CO_2 have been reviewed [42, 44]. Kinetic data for heterogeneously-catalyzed reactions in CO_2 was compiled by Martinez et al. [48]. The use of dense CO_2 should

reduce the mass transfer resistance between the gas-liquid interface, promote the diffusion of reactant molecules through the solid catalyst particles, and reduce solution viscosity, all of which should be advantageous on reaction rates.

Reactions containing CO_2 can be conducted in a single phase or in multiple phases. One benefit to conducting the reaction in the multiphase domain is that the operating pressures are lower than those needed to obtain a single phase. Operating in the multiphase domain allows us to take advantage of the enhanced transport properties while requiring less strenuous equipment design and capital costs. Examples of the use of dense CO_2 in multiphase reactions are the use of CO_2 as a co-solvent, i. e., CO_2-expanded liquids (CXLs) or as the sole solvent in a heterogeneously-catalyzed chemical reaction.

The use of CXLs as particle formation, separation, polymer processing, or reaction media was reviewed by Jessop and Subramaniam [47]. The increases in the solubility of gases in CXL's have made the alternative reaction medium attractive in the oxidation, hydroformylation, and hydrogenation of small molecules. Also, the use of a CXL in polymer hydrogenation has been reported [49, 50]. Oftentimes, a heterogeneous catalyst is used in CXL-containing reactions.

Phenylacetylene was hydrogenated using a $Pd_{81}Si_{19}$ alloy in a fixed-bed reactor containing $scCO_2$. Tschan et al. found that operating in a single phase with low hydrogen excess was the best for obtaining the desired styrene product instead of complete hydrogenation to ethylbenzene [51]. These researchers found that operating in the

biphasic fluid region resulted in different selectivity than when the system was operated in a single phase.

Zhao et al. studied the 5% Pt/C-catalyzed hydrogenation of benzaldehyde and cinnamaldehyde in $scCO_2$ at 50°C [52]. They found that when CO_2 was present, benzaldehyde conversion was far less than when the reaction was conducted in the absence of CO_2 or with N_2. Contrastingly, when the reaction was conducted in biphasic fluid, slight improvements in cinnamaldehyde conversion were noted with increasing CO_2 pressure.

Bertucco et al. used an internal recycle reactor to successfully hydrogenate the olefinic bonds of a ketone in supercritical CO_2 [53]. An eggshell 1% Pd/Al_2O_3 catalyst was the catalyst for reactions run at 150°C or 200°C and a pressure between 12 and 17.5 MPa [53]. In subsequent studies, an eggshell 0.5% Pd/Al_2O_3 catalyst was used in the ketone hydrogenation, which was conducted at a temperature between 50°C and 180°C and a pressure of 20 MPa [43].

At 40°C, the turnover frequencies (TOF) for the hydrogenation of naphthalene in $scCO_2$ varied with the dispersions of the Rh/C catalysts [54]. At low metal dispersions, the TOF of the reaction conducted in $scCO_2$ was higher than the TOF for the reaction in n-heptane. However, for high metal dispersions, the TOFs in both solvents were comparable to one another. Hiyoshi and co-workers also studied the effect of rhodium dispersion on tetralin hydrogenation in $scCO_2$ and n-heptane. A maximum in TOF was observed at a metal dispersion of 20% for each solvent. The TOF's for tetralin

hydrogenation in $scCO_2$ were consistently higher than the TOF's for the reaction in n-heptane. The results for the $scCO_2$-containing reactions in Hiyoshi et al.'s research fail to obey the Madon criterion [55], which says that in the absence of external mass transfer effects the TOF for a given metal in a given chemical reaction should be the same. Therefore, there may have been some mass transfer resistances that were not commented upon in the paper.

Citral, which contains three types of unsaturated bonds, was hydrogenated at 40°C using 5% Pd/Al_2O_3 in hexane, dioxane, and supercritical CO_2 [56]. For studies conducted in a batch reactor, the turnover frequency for citral hydrogenation in supercritical CO_2 was approximately 50-fold higher than the TOFs for the saturation in hexane or dioxane. In the batch reactor, the conversion of citral increased when the reaction changed from a two-phase to one-phase system at an approximate pressure of 100 bar. The positive change in conversion with phase change contrasts with what was observed in the continuous reactor. For a reaction pressure of 130 bar in the continuous reactor, citral conversion decreased monotonically as CO_2/citral ratio increased; the transition from two-phase to one-phase occurred at a CO_2/citral ratio of 80 (molar). The selectivity of hydrogenating the olefinic bonds instead of the carbonyl bond was maintained in $scCO_2$.

Panpranot et al. found evidence of palladium sintering in cyclohexene hydrogenation in $scCO_2$ [57]. Several organic liquids (benzene, heptanol, and n-methylpyrrolidone) and $scCO_2$ were used as solvents to determine the effect of solvent

polarity on cyclohexene conversion and metal sintering. These researchers found that the reaction conducted in $scCO_2$ was faster than the reactions in organic solvents. The hydrogenation activity decreased with increasing solvent polarity. The spent catalysts were recovered and analyzed to determine if Pd leaching and crystallite growth occurred. Atomic absorption spectroscopy (AAS) measurements indicate that approximately 21% of the Pd was lost during the CO_2-containing reaction. With the exception of NMP, the amount of leached Pd in the CO_2-solvated reaction was larger than the values obtained for the hydrogenations in the organic solvents. Palladium dispersion, which was calculated from CO chemisorption and the AAS results, decreased from 44% to 14% when CO_2 was the solvent. The decrease in Pd dispersion due to CO_2 was not as drastic as the drops seen with the solvent-less, heptanol, or NMP reactions. These results illustrated that catalyst activity may change during hydrogenation in dense CO_2.

The effect of $scCO_2$ on the selectivity for 2-chloronitrobenzene hydrogenation to 2-chloroaniline was studied [58]. At reaction temperatures of 40 and 90^{o}C, the formation of 2-chloroaniline was preferred over dehalogenated product when the Pt/C-catalyzed reaction was conducted in $scCO_2$. Carbon monoxide formation was observed in IR studies where a mixture of CO_2 and H_2 (10:1) was passed over the Pt/C catalyst. Ichikawa and co-workers suggested that CO adsorbed to the steps and kinks of the Pt crystallites, which prevented the dehalogenation of 2-chloroaniline. It is believed that the CO is formed via the reverse water-gas shift (RWGS) reaction (Equation 2-1).

$$CO_2 + H_2 \leftrightarrow CO + H_2O \qquad (2\text{-}1)$$

In the aforementioned research, the formation of CO promoted the formation of the desired product. In other cases, CO can have a negative impact on the desired reaction.

Minder et al. studied the 5% Pt/Al_2O_3-catalyzed hydrogenation of ethyl pyruvate in organic solvents, $scCO_2$, and supercritical ethane in an autoclave [59]. Upon CO_2 addition (80 bar) to the reactor at 35°C, hydrogen consumption ceased, which is suggestive of catalyst deactivation. Subsequent IR studies indicated that linear and bridged CO adsorbed to 5% Pt/Al_2O_3 when a mixture of CO_2 and H_2 (1:4) was passed over the catalyst at 40°C. When supercritical ethane was used as a solvent, no catalyst deactivation was observed. These results support the hypothesis that CO poisons sites for ethyl pyruvate hydrogenation.

Cyclohexene was hydrogenated in a fixed-bed reactor with $scCO_2$ as the solvent using a 2% Pd/C catalyst [60]. No catalyst deactivation was observed even though CO formation was observed in IR studies of CO_2/H_2 over the same catalyst. The researchers attributed these observances to the relatively short residence time of CO on the Pd, which did not allow the CO molecules to strongly adsorb and poison hydrogenation sites. These results are consistent with the work of other researchers who did not observe catalyst deactivation when continuous reactors were used in hydrogenation processes. The authors suggested that the longer residence time of CO in a batch reactor results in catalyst poisoning that was reported by other researchers [49, 58, 59].

Reverse water-gas shift activities of different heterogeneous catalysts with $scCO_2$ were further investigated by Burgener et al. [61] and Arunajatesan et al. [62]. Burgener

et al. investigated the effect of catalyst composition on the RWGS reaction using a 1 mol% H_2/supercritical CO_2 mixture [61]. Their attenuated total reflection infrared spectroscopy (ATR-IR) results showed that more CO formed at 50^oC when a Pt/Al_2O_3 or Pd/Al_2O_3 film was used as the catalyst than when Ru/Al_2O_3 or Rh/Al_2O_3 were used.

Similar results were obtained by Arunajatesan and co-workers, who used Fourier transform infrared (FTIR) spectroscopy to study the RWGS reaction at a feed molar ratio of CO_2:H_2=19 and at 70^oC [62]. Carbon monoxide formation was noted when a Pd/Al_2O_3 catalyst was used. No CO formed when Ni/Al_2O_3 or Ru/Al_2O_3 was the catalyst. It is apparent that when compared to Pd and Pt catalysts, CO_2 and H_2 behave differently over supported Ni, Ru, and Rh catalysts.

The negative effect of CO_2 on polymer hydrogenation was observed by Li et al. [63] and Xu et al. [49]. In the work of Li et al., NBR that was impregnated with Wilkinson's catalyst was swollen with $scCO_2$ [63]. A negative effect on NBR conversion was observed when $scCO_2$ was present. The authors attributed these observances to the polymer swelling by CO_2, which facilitated catalyst removal from the polymer. Thus, there was less catalyst available to assist the hydrogenation process

In other work, at 150^oC, catalyst deactivation resulted in PS hydrogenation in CO_2-expanded DHN reached an asymptote when a 5% $Pd/BaSO_4$ catalyst was used [49]. Catalyst deactivation occurred CO, which formed via the RWGS reaction, poisoning of active sites. The use of a small amount of a 65% Ni/SiO_2-Al_2O_3 catalyst with the 5%

$Pd/BaSO_4$ for the polymer hydrogenation resulted in CO conversion to methane via the reaction shown in Equation 2-2.

$$CO + 3H_2 \leftrightarrow CH_4 + H_2O \quad (2\text{-}2)$$

When the physical mixture of Pd and Ni catalyst was used, PS hydrogenation was able to proceed in the CO_2-expanded solvent. The use of a bimetallic catalyst mixture in hydrogenation is a method to circumvent CO poisoning while taking advantage of the enhanced transport properties that occurs in the CO_2-expanded reaction medium.

2.3.2. Carbon Dioxide-Polymer Interactions

The interactions between CO_2 and polymer molecules have driven the use of dense CO_2 in polymer processes including polymerizations, separations, impregnations, property modifications, and processing applications such as molding and extrusion. These topics have been reviewed by Kiran [64]. While fluorinated polymers and PDMS are known to be soluble in CO_2, PS is not soluble. In order to benefit from the enhanced transport properties that occur in the presence of dense CO_2, an organic solvent for PS could be swollen with the CO_2. Properties that are relevant to heterogeneously catalyzed polymeric reactions are solution viscosity, polymer diffusivity, and polymer coil size.

Polymer diffusivities in SCF's have been studied. The diffusion coefficients of poly(ethylene-co-1-butene) in supercritical ethane, propane, n-butane, and n-pentane were measured [65]; the hydrodynamic radii of the polymer dissolved in the different solvents were calculated from the infinite dilution diffusion coefficients. More recently,

the diffusivities of PDMS and fluorinated alkyl methacrylates dissolved in CO_2 were determined [66, 67]. The hydrodynamic radii of the polymers were dependent on the CO_2 density.

None of the aforementioned studies were conducted in a CXL. Small angle x-ray scattering has been used to determine the effect of CO_2 on the solvent quality and radius of gyration of PS dissolved in cyclohexane [68], tetrahydrofuran (THF) [69], and toluene [70]. These researchers observed decreases in the osmotic second virial coefficient, an indicator of solvent quality, as CO_2 concentration increased. Concurrently, the radii of gyration of PS decreased in both CO_2-expanded solvent systems.

The viscosity of CO_2-expanded PS-toluene systems were studied by Yeo and Kiran [71] and Li and co-workers [70]. Both research groups observed decreasing polymer solution viscosity with increasing CO_2 concentration. The work of Yeo and Kiran was conducted at 320 K while varying CO_2 concentration and hydrostatic pressure [71]. The highest CO_2 concentration studied was 14.7 wt%. In the research of Li et al., PS solution viscosities were measured at pressures up to 4.2 MPa; this corresponded to a weight fraction of 0.25 for CO_2 in the liquid phase.

A minimum of one order-of-magnitude reduction in PS-DHN solution viscosity with a CO_2 pressure of approximately 14 MPa (corresponds to a CO_2 weight fraction of nearly 24%) was reported by Whittier et al. at a variety of temperatures [72]. The viscosity decreases appeared to be larger for the more concentrated polymer solutions.

Since CO_2 is an anti-solvent for PS, precipitation of the polymer must be avoided in order to conduct hydrogenation in the liquid phase. Phase behavior studies of PS-CO_2-DHN were conducted by Xu et al. [50]. Their results show that PS precipitates from a moderately concentrated polymer-CO_2-DHN solution at 3000 psig at 150^{o}C and 180^{o}C. The precipitation pressure of a 50% hydrogenated PS and a 99% hydrogenated PS from CO_2-DHN did not change from PS's precipitation pressure in the same mixed solvent.

2.4. Conclusions

Polymer hydrogenation is a post-polymerization process that can be used to create novel materials. When compared to their unsaturated parent polymer, hydrogenated polymers have improved materials properties. The use of homogeneous catalysts to hydrogenate the diene units in polymers is well-established. The hydrogenation of the aromatic rings in polymers requires more energy input, i.e., a higher reaction temperature. Heterogeneous catalysts are suitable for such a reaction since they are more thermally stable than homogeneous catalysts.

The kinetics of heterogeneously-catalyzed polymer hydrogenation are dependent on the mass transfer of reactant and product molecules in the reaction system. The relatively large size of a polymer molecule results in increased polymer solution viscosity, decreased polymer diffusivity, and depending on the pore diameter of the catalyst, preclusion of reactant molecules. Hindered diffusion of polymer molecules is also likely to occur in the catalyst. As a result, reaction rates should be impacted.

The use of a macroporous catalyst would be a first step in eliminating mass transfer resistances associated with heterogeneous polymer hydrogenation. A delicate balance between the average particle size of the catalytic element and the surface area of the support needs to be established in order to maximize hydrogenation rates.

The expansion of the organic solvent with dense CO_2 is an alternative method of reducing mass transfer resistances, namely decreased polymer solution viscosity and increased polymer diffusion, in polymer hydrogenation. Also, the increased hydrogen solubility in CO_2-expanded solvent should be beneficial. In general, the anti-solvent power of CO_2 decreases polymer coil size, which should allow more coils to access the catalyst interior. The CO_2 concentration should also be maintained below the precipitation pressure of the polymer if the reaction is occurring in the liquid phase.

The use of CO_2 in hydrogenations can result in an unwanted side reaction-the reverse water-gas shift reaction- that generates carbon monoxide (CO). Consequently, catalyst deactivation by CO poisoning of active sites can occur. The use of two catalysts- one for hydrogenation, the other for conversion of CO to methane- is required for batch hydrogenations to proceed in CO_2-expanded solvents.

References

[1] H.A. Wittcoff, Reuben, B. G., Plotkin, J. S., Industrial Organic Chemicals, 2nd ed., John Wiley & Sons, Hoboken, 2004.

[2] C.A. Costello, Wright, P. J., Schulz, D. N., Sissano, J. A., Exxon Research and Engineering, Co., US 5,399,632, 1995, p. 5.

[3] F.S. Bates, Fredrickson, G. H., Hucul, D., Hahn, S. F., AlChE J. 47 (2001) 762-765.

[4] Q. Pan, Rempel, G. L., Macromol. Rapid Commun. 25 (2004) 843-847.

[5] N.T. McManus, Rempel, G. L., Polymer Reviews. 35 (1995) 239-285.

[6] M.P. McGrath, Sall, E. D., Tremont, S. J., Chem. Rev. 95 (1995) 381-398.

[7] http://www.kraton.com

[8] http://www.zeonchemicals.com/hnbrzetpol.aspx

[9] http://www.therban.com

[10] D.A. Hucul, Hahn, S. F., Adv. Mater. 12 (2000) 1855-1858.

[11] C.M.R. Madhuranthakam, Pan, Q., Rempel, G. L., AlChE J. 55 (2009) 2934-2944.

[12] J.L. Adams, Quiram, D. J., Graessley, W. W., Register, R. A., Macromolecules. 31 (1998) 201-204.

[13] J.F. Pendleton, Hoeg, D. F., Goldberg, E. P., Adv. Chem. Ser., Washington, DC, 1973, pp. 27-38.

[14] J.S. Parent, McManus, N. T., Rempel, G. L., Industrial & Engineering Chemistry Research. 37 (1998) 4253-4261.

[15] R. Tangthongkul, Prasassarakich, P., Rempel, G. L., J. Appl. Polym. Sci. 97 (2005) 2399-2406.

[16] K. Simma, Rempel, G. L., Prasassarakich, P., Polym. Degrad. Stab. 94 (2009) 1914-1923.

[17] C.H. Bartholomew, Farrauto, R. J., Fundamentals of Industrial Catalytic Processes, 2nd ed., Wiley, Hoboken, 2006.

[18] G. Schulz, Worsfold, D. J., Polymer Communications. 25 (1984) 206-207.

[19] J.H. Rosedale, Bates, F. S., J. Am. Chem. Soc. 110 (1988) 3542-3545.

[20] G.A. Cassano, Valles, E. M., Quinzani, L. M., Polymer. 39 (1998) 5573-5577.

[21] M.D. Gehlsen, Bates, F. S., Macromolecules. 26 (1993) 4122-4127.

[22] M.D. Gehlsen, Weimann, P. A., Bates, F. S., Harville, S., Mays, J. W., Wignall, G. D., Journal of Applied Polymer Science, Part B: Polymer Physics. 33 (1995) 1527-1536.

[23] A. Bussard, Dooley, K. M., AlChE J. 54 (2008) 1064-1072.

[24] H.-G. Elias, Etter, O., Journal of Macromolecular Science, Part A. 5 (1967) 943-953.

[25] A. Abe, Hama, T., Polymer Letters. 7 (1969) 427-435.

[26] H. Nakatani, Nitta, K-h., Soga, K., Polymer. 39 (1998) 4273-4278.

[27] V. Wege, Bruder, F., Douzinas, K., Chen, Y., Bayer AG, DE 19921941, 2000.

[28] D. Xu, Carbonell, R. G., Kiserow, D. J., Roberts, G. W., Industrial & Engineering Chemistry Research. 42 (2003) 3509-3515.

[29] J.S. Ness, Brodil, J. C., Bates, F. S., Hahn, S. F., Hucul, D. A., Hillmyer, M. A., Macromolecules. 35 (2002) 602-609.

[30] M. Helbig, Inoue, H., Vogl, O., Journal of Polymer Science: Polymer Symposium. 63 (1978) 329-342.

[31] A. Iio, Yoshinari, M., Komiya, Z., Goto, K., Japan Synthetic Rubber Co., LTD., EP 317263, 1988.

[32] H. Nakatani, Nitta, K-h., Soga, K., Polymer. 40 (1999) 1547-1552.

[33] J.J. Xu, Nguyen, B. T., Bates, F. S., Hahn, S. F., Hudack, M. L., Journal of Polymer Science Part B: Polymer Physics. 41 (2003) 725-735.

[34] J. Zhao, Hahn, S. F., Hucul, D. A., Meunier, D. M., Macromolecules. 34 (2001) 1737-1741.

[35] J.L. Hahnfeld, Newman, T. H., Patel, A. M., Dow Global Technologies, Inc., US 6455656, 2002, p. 6.

[36] J.-R. Chang, Huang, S-M., Industrial & Engineering Chemistry Research. 37 (1998) 1220-1227.

[37] S. Maheshwari, Tsapatsis, M., Bates, F. S., Macromolecules. 40 (2007) 6638-6646.

[38] M. Shirai, Suzuki, N., Nishiyama, Y., Torii, K., Arai, M., Applied Catalysis A: General. 171 (1999) 219-225.

[39] P.E. Savage, Gopalan, S., Mizan, T. I., Martino, C. J., Brock, E. E., AlChE J. 41 (1995) 1723-1778.

[40] B. Subramaniam, Applied Catalysis A: General. 212 (2001) 199-213.

[41] W. Cole, Bridgestone/Firestone Americas, US 0250912, 2005.

[42] E.J. Beckman, J. Supercrit. Fluids. 28 (2004) 121-191.

[43] L. Devetta, Giovanzana, A., Canu, P., Bertucco, A., Minder, B. J., Catal. Today. 48 (1999) 337-345.

[44] A. Baiker, Chem. Rev. 99 (1999) 453-473.

[45] B. Subramaniam, Lyon, C. J., Arunajatesan, V., Applied Catalysis B: Environmental. 37 (2002) 279-292.

[46] M. Arai, Fujita, S-I., Shirai, M., J. Supercrit. Fluids. 47 (2009) 351-356.

[47] P.G. Jessop, Subramaniam, B., Chem. Rev. 107 (2007) 2666-2694.

[48] E. Ramirez, Zgarni, S., Larrayoz, M. A., Recasens, F., Eng. Life. Sci. 2 (2002) 257-264.

[49] D. Xu, Carbonell, R. G., Kiserow, D. J., Roberts, G. W., Industrial & Engineering Chemistry Research. 44 (2005) 6164-6170.

[50] D. Xu, Carbonell, R. G., Roberts, G. W., Kiserow, D. J., The Journal of Supercritical Fluids. 34 (2005) 1-9.

[51] R. Tschan, Wandeler, R., Schneider, M. S., Schubert, M. M., Baiker, A., J. Catal. 204 (2001) 219-229.

[52] F. Zhao, Fujita, S., Akihara, S., Arai, M., J. Phys. Chem. A. 109 (2005) 4419-4424.

[53] A. Bertucco, Canu, P., Devetta, L., Zwahlen, A. G., Industrial & Engineering Chemistry Research. 36 (1997) 2626-2633.

[54] N. Hiyoshi, Rode, C. V., Sato, O., Masuda, Y., Yamaguchi, A., Shirai, M., Chem. Lett. 37 (2008) 734-735.

[55] R.J. Madon, Boudart, M., Ind. Eng. Chem. Fundam. 21 (1982) 438-447.

[56] M. Burgener, Furrer, R., Mallat, T., Baiker, A., Applied Catalysis A: General. 268 (2004) 1-8.

[57] J. Panpranot, Phandinthong, K., Praserthdam, P., Hasegawa, M., Fujita, S., Arai, M., Journal of Molecular Catalysis A: Chemical. 253 (2006) 20-24.

[58] S. Ichikawa, Tada, M., Iwasawa, Y., Ikariya, T., Chem. Commun. (2005) 924-926.

[59] B. Minder, Mallat, T., Pickel, K. H., Steiner, K., Baiker, A., Catal. Lett. 34 (1995) 1-9.

[60] V. Arunajatesan, Subramaniam, B., Hutchenson, K. W., Herkes, F. E., in: D.G. Morrel (Ed.), Catalysis of Organic Reactions, Marcel Dekker, New York, 2003, pp. 461-475.

[61] M. Burgener, Ferri, D., Grunwaldt, J-D., Mallat, T., Baiker, A., J. Phys. Chem. B. 109 (2005) 16794-16800.

[62] V. Arunajatesan, Subramaniam, B., Hutchenson, K. W., Herkes, F. E., Chem. Eng. Sci. 62 (2007) 5062-5069.

[63] G. Li, Pan, Q., Rempel, G. L., Ng, F. T. T., Macromolecular Symposia. 204 (2003) 141-149.

[64] E. Kiran, J. Supercrit. Fluids. 47 (2009) 466-483.

[65] T.W. Kermis, Li, D., Guney-Altay, O., Park, I-H., van Zanten, J. H., McHugh, M. A., Macromolecules. 37 (2004) 9123-9131.

[66] A.F. Kostko, McHugh, M. A., van Zanten, J. H., Macromolecules. 39 (2006) 1657-1659.

[67] J. Guo, Andre, P., Adam, M., Panyukov, S., Rubinstein, M., DeSimone, J. M., Macromolecules. 39 (2006) 3427-3434.

[68] D. Li, Liu, Z., Han, B., Yang, G., Song, L., Wang, J., Dong, B., Macromolecules. 35 (2002) 10114-10118.

[69] D. Li, Liu, Z., Han, B., Yang, G., Wu, Z., Liu, Y., Dong, B., Macromolecules. 33 (2000) 7990-7993.

[70] D. Li, Han, B., Liu, Z., Liu, J., Zhang, X., Wang, S., Zhang, X., Macromolecules. 34 (2001) 2195-2201.

[71] S.D. Yeo, Kiran, E., J. Appl. Polym. Sci. 75 (2000) 306-315.

[72] R.E. Whittier, Xu, D., van Zanten, J. H., Kiserow, D. J., Roberts, G. W., J. Appl. Polym. Sci. 99 (2006) 540-549.

CHAPTER 3 :

DETERMINATION OF POLYSTYRENE-CARBON DIOXIDE-DECAHYDRONAPHTHALENE SOLUTION PROPERTIES BY HIGH PRESSURE DYNAMIC LIGHT SCATTERING

Chapter 3 is a manuscript published in Polymer.

Dong, L. B., Carbonell, R. G., Roberts, G. W., Kiserow, D. J. *Polymer* 2009, 50(24) 5728-5732.

Determination of Polystyrene-Carbon Dioxide-Decahydronaphthalene Solution Properties by High Pressure Dynamic Light Scattering

Laura Beth Dong, Ruben G. Carbonell, George W. Roberts*, Douglas J. Kiserow[1]

Department of Chemical and Biomolecular Engineering, North Carolina State University, Campus Box 7905, Raleigh, NC 27695-7905, USA

[1] Also: U. S. Army Research Office, P. O. Box 12211, Research Triangel Park, NC 27709-2211, USA

* To whom correspondence should be addressed: Email: groberts@eos.ncsu.edu, Fax: 919-515-3465, Phone: 919-515-7328

Abstract

The diffusion coefficients of polystyrene (PS) in decahydronaphthalene (DHN) and in solutions of carbon dioxide (CO_2) and DHN were measured for dilute PS solutions over a range of temperatures and CO_2-DHN ratios using high pressure dynamic light scattering. Infinite dilution diffusion coefficients (D_0) of PS and dynamic second virial coefficients (k_D) were determined for essentially monodisperse 308 kDa PS. At a system pressure of 20.7 MPa, PS diffusion coefficients increased by a factor of 2.5, and the activation energy of diffusion decreased by approximately 16 percent when DHN was "expanded" with 44 mol% CO_2. However, the hydrodynamic radius of PS at a given temperature was not particularly sensitive to the CO_2 concentration. Solvent quality, as measured by k_D, decreased at higher CO_2 concentrations. The addition of CO_2 to

polymer solutions may offer a way to "tune" the properties of the solution to facilitate the heterogeneous catalytic hydrogenation of polymers.

Keywords: polystyrene, diffusion, dynamic light scattering

3.1. Introduction

Catalytic polymer hydrogenation can provide an efficient means to synthesize novel polymers and can offer advantages over the polymerization of the corresponding monomers [1-3]. Since catalyst residuals in the product polymer can result in product degradation and high cost, complete catalyst removal is usually required. In this case, heterogeneous (solid) catalysts are more attractive than their homogeneous counterparts because the solid catalyst is easier to recover from the polymer solution.

The kinetics of polymer hydrogenation are often hindered by mass transport limitations associated with the high viscosity of the polymer solution and the low diffusivity of the polymer molecules. These transport difficulties can be particularly troublesome in reactions catalyzed by porous solids. With porous catalysts, the unhydrogenated polymer must diffuse through the catalyst pores and adsorb to active catalytic sites in the interior of the particle. The hydrogenated polymer must then diffuse out of the particle through these pores.

Conducting heterogeneously-catalyzed polymer reactions in organic solvents expanded with carbon dioxide (CO_2) is a way to both reduce transport limitations and approach chemical processing in an environmentally-friendly manner. Carbon dioxide-

expanded liquids (CXLs), a class of solvents in which CO_2 is dissolved in organic liquids, have been used as reaction media for small-molecule reactions. The amount of organic solvent required for a chemical reaction can be significantly reduced with the use of a CO_2-expanded solvent. For example, the volumes of organic solvent required for 2,6-di-tert-butylphenol oxidation, cyclohexene oxidation, or 1-octene hydroformylation were reduced by as much as 80 percent when the CO_2-expanded analogs were used [4-6].

While the addition of CO_2 to an organic solution can result in a significant decrease of solution viscosity and an increase in solute diffusion coefficient, solvent quality may also decrease as CO_2 concentration increases. Solvent quality is particularly important in polymeric systems since it affects the structure of polymer chains. Moreover, at some CO_2 concentration, the polymer chain will collapse and precipitate. Quantifying the effect of CO_2 on polymer chain dynamics will help to understand transport properties, to define the conditions that need to be maintained for polymer solubility, and may lead to a better understanding of how the polymer adsorbs to catalytic sites.

The focus of this research is the polystyrene (PS)-CO_2-decahydronaphthalene (DHN) system. Hydrogenation of the aromatic rings of PS produces polymers with improved thermal and oxidative resistance [3] and higher glass transition temperatures [7-8]. Supported nickel, palladium, and platinum catalysts have been used to saturate the aromatic rings of PS dissolved in various solvents [7, 9-11], including DHN. The high boiling point of DHN relative to other solvent candidates makes it quite suitable for aromatic ring hydrogenation. Moreover, DHN can dissolve approximately 60 mole

percent CO_2 before PS precipitation occurs [12]. Finally, the hydrogenation rate of PS in CO_2-expanded DHN was shown to be one and a half times faster than the same reaction in DHN [12].

While these outcomes are favorable, the behavior of PS in CO_2-expanded DHN is not well understood. A more complete understanding of this behavior should lead to the design of improved catalysts and allow reaction conditions to be tuned for high reaction rates and selectivities. In this research, high pressure dynamic light scattering (DLS) was used to measure the effect of CO_2 on the PS diffusion coefficient in DHN. The effects of CO_2 concentration on solvent quality and PS hydrodynamic radii were also quantified. Dynamic light scattering has been used to probe polymer solution properties for over 40 years. The use of high pressure DLS to understand polymer-supercritical fluid solution properties emerged in the late 1990s. Kermis et al. used high pressure DLS to measure poly(ethylene-co-1-butene) diffusion in various alkanes under supercritical conditions [13]. More recently, the high pressure technique has been used to study CO_2-poly(dimethylsiloxane) (PDMS) [14] and CO_2-fluorinated alkyl methacrylate [15] systems. The solvating power of CO_2 was found to be dependent on CO_2 density for both systems. The hydrodynamic radius of PDMS did not vary significantly with increasing CO_2 density. However, the hydrodynamic radius of the fluorinated alkyl methacrylate increased about 10 percent with CO_2 density increasing from 0.85 to 1.05 g/mL. The present research on the PS-CO_2-DHN system is the first known use of high pressure DLS to study solutions of a polymer dissolved in a CO_2-expanded liquid.

3.2. Experimental

3.2.1. Materials

Essentially monodisperse PS was purchased from Polymer Source, Incorporated (Montreal, Canada) and used as received. The number-average molecular weight (M_n) was 308 kDa, and the polydispersity index (PDI) was 1.04, both determined by gel permeation chromatography (GPC). The corresponding values reported by the supplier were 412 kDa and 1.05. Anhydrous DHN (24% *cis*, 76% *trans*) was purchased from Sigma Aldrich (St. Louis, MO). Carbon dioxide (≥99.99%) was purchased from National Welders (Charlotte, NC).

3.2.2. Polystyrene Solution Preparation

DHN was filtered through a 0.2 μm Millex polytetrafluoroethylene (PTFE) syringe filter (Millipore Corporation, Billerica, MA) before it was used to dissolve PS. The polymer solution was filtered through a 5 μm Millex PTFE syringe filter (Millipore, Corporation, Billerica, MA) before it was loaded into the DLS cell.

3.2.3. Molecular Weight Measurement

Gel permeation chromatography was used to measure the molecular weight of polystyrene. A Waters Alliance GPC system (Waters Corporation, Milford, MA) equipped with Styragel HR3, HR4, and HR4E columns (Waters Corporation, Milford, MA) was used. A miniDAWN Tristar light scattering detector (Wyatt Technology, Santa Barbara, CA) in combination with a refractive index detector (Optilab® rEX, Wyatt

Technology, Santa Barbara, CA) were used to measure polymer molecular weight and polydispersity index. Tetrahydrofuran (HPLC grade, Fisher Scientific, Pittsburgh, PA) was the mobile phase.

A Waters 150-CV GPC system (Waters Corporation, Milford, MA) equipped with Styragel HR5, HR4, HR2, and HR 0.5 columns (Waters Corporation, Milford, MA) and a refractive index detector was used to confirm the results provided by the Alliance system. The mobile phase was THF (Fisher Scientific, Pittsburgh, PA), and polystyrene standards were used for calibration. The averages of M_n and PDI obtained from three independent measurements on the two GPC systems are reported. The averaged M_n values ranged from 301 to 312 kDa while PDI values were between 1.03 and 1.04.

3.2.4. Dynamic Light Scattering

A 532 nm-solid state laser (Crystalaser, Reno, NV) was used as the light source. The high-pressure DLS sample cell was custom-built. Scattered light intensities were measured at 90^o from the light source. The cell temperature was maintained by circulating silicone fluid through a custom-made heating jacket.

For the diffusion coefficient measurements in CO_2-expanded DHN, a known amount of CO_2 was loaded into the cell via one of two methods. For the lowest CO_2 concentration, the amount of delivered CO_2 was determined gravimetrically. For the higher CO_2 concentrations, a known volume of CO_2 was delivered by an ISCO syringe pump (Teledyne ISCO, Lincoln, NE). A manual high pressure generator (High Pressure Equipment Company, Erie, PA) was used to pressurize the system to 20.7 MPa. At all of

the experimental temperatures, the CO_2-containing solutions are in a single liquid phase at this pressure.

A photomultiplier tube and TurboCorr digital autocorrelator card (both Brookhaven Instruments, Holtsville, NY) were used to measure the normalized, intensity-intensity correlation function, $g_2(t)$. The scattered intensity is related to the electric field autocorrelation function, $g_1(t)$, through Equation 3-1.

$$g_2(t) = B\left(1 + \beta\left|g_1(t)\right|^2\right) \qquad \textbf{(3-1)}$$

In Equation 3-1, B is the measured baseline and β accounts for non-ideal factors such as the area of the detector. For monodisperse, dilute polymer solutions, the electric field autocorrelation function is exponentially dependent on the characteristic decay rate, Γ, through Equation 3-2.

$$g_1(t) = \exp(-\Gamma t) \qquad \textbf{(3-2)}$$

Combining Equations 3-1 and 3-2,

$$g_2(t) = B\left(1 + \beta\left|exp(-\Gamma t)\right|^2\right) \qquad \textbf{(3-3)}$$

The characteristic decay rate is a function of the translational diffusion coefficient, D, and the square of the scattering vector, q, as shown in Equation 3-4.

$$\Gamma = q^2 D \qquad \textbf{(3-4)}$$

The scattering vector is a function of the scattering angle (θ), the solvent's refractive index (n_{mix}), and the incident wavelength of light (λ), as shown below.

$$q = \frac{4\pi n_{mix}}{\lambda} sin\left(\frac{\theta}{2}\right) \qquad \textbf{(3-5)}$$

The Lorenz-Lorentz equation was used to calculate the refractive indices of the CO_2-expanded DHN mixtures. As shown in Equation 3-6, the refractive index of the mixture (n_{mix}) is dependent on the mass fractions of the components (w_i), the component refractive indices (n_i), the component densities (ρ_i), and the mixture density (ρ_{mix}).

$$\frac{n_{mix}^2 - 1}{n_{mix}^2 + 2} = \rho_{mix}\left[\frac{w_1}{\rho_1}\frac{n_1^2 - 1}{n_1^2 + 2} + \frac{w_2}{\rho_2}\frac{n_2^2 - 1}{n_2^2 + 2}\right] \qquad \textbf{(3-6)}$$

In order to use the Lorenz-Lorentz equation, Hammel et al.'s refractive index data for DHN [16] and Michels et al.'s CO_2 data [17] were extrapolated. The densities of CO_2 were calculated from the NIST Thermophysical Properties database [18] and DHN densities were determined from the DIPPR database [19]. The densities of the CO_2-DHN mixtures were obtained from Cain [20]. The calculated values of n_{mix} were used to calculate values of q for each experiment using Equation 3-5.

The diffusion coefficients of PS (D) were obtained by minimizing the sum of the squares of the deviations between the measured values of $g_2(t)$ and Equation 3-3, to find the "best" values of Γ, B, and β. Once q was calculated from Equation 3-5, Equation 3-4 was used to calculate D.

In the dilute solution regime, the measured diffusion coefficients of PS should exhibit a linear dependence on polymer concentration (C) as shown in Equation 3-7, where D_0 is the infinite dilution diffusion coefficient and k_D is the dynamic second virial coefficient:

$$D = D_0\left(1 + k_D C\right) \qquad \textbf{(3-7)}$$

The infinite dilution diffusion coefficient can be used to calculate the hydrodynamic radius (R_H) of the dissolved polymer via the Stokes-Einstein equation, Equation 3-8.

$$R_H = \frac{k_B T}{6\pi\eta D_0} \quad \textbf{(3-8)}$$

Here, k_B is the Boltzmann constant, and T is the absolute temperature. Viscosities (η) for the *cis/trans*-DHN mixture were interpolated from data by Cain [20], while CO_2-DHN viscosities at 20.7 MPa were measured by Cain [20]. Since the form factor, i.e., the product of q and R_g (the radius of gyration of the polymer coil), was less than one for all experiments, the angular dependence of D should be weak and was neglected. Values of R_g were estimated as $R_H\sqrt{3/5}$.

3.3. Results and Discussion

3.3.1. PS Diffusion in Pure DHN

As shown in Figure 3.1, the diffusion coefficients of PS in DHN were found to be linearly dependent on polymer concentration between 0.111 and 0.50 wt% PS, for temperatures ranging from 297 K to 392 K. The infinite dilution diffusion coefficients were determined by extrapolating to zero polymer concentration. The dynamic second virial coefficients were calculated from the slopes of the straight lines and the D_0's. These two values, along with the hydrodynamic radii calculated from Equation 3-8, are provided in Table 3.1.

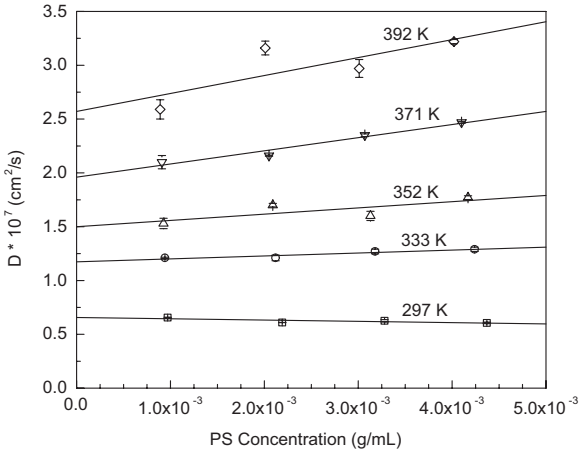

Figure 3.1. Dependence of PS Diffusion Coefficients on PS Concentration and Temperature (PS M_n = 308 kDa, PDI = 1.04) The error bars represent the standard deviations of three diffusion coefficient measurements.

Table 3.1. PS Diffusion in DHN

T (K)	$D_0 * 10^7$ (cm^2/s)	k_D (mL/g)	R_H (nm)
297	0.656	-18.0	14.2 ± 0.6
333	1.17	23.3	16.4 ± 0.7
352	1.50	38.7	17.7 ± 1.7
371	1.96	62.2	17.8 ± 1.1
392	2.57	65.0	18.0 ± 2.6

(PS M_n = 308 kDa, PDI = 1.04) The errors for R_H were calculated as described in the supporting information.

Infinite dilution diffusion coefficients increased roughly fourfold as temperature was increased from 297 K to 392 K. The D_0's at 333 K and 352 K were compared to Kotera et al.'s data for a 450 kDa PS in *trans*-DHN. These investigators used a modified electrophoretic apparatus to measure diffusion coefficients. The values obtained in this research ($1.17 * 10^{-7}$ and $1.50 * 10^{-7}$ cm^2/s, respectively) are in good agreement with the previously reported values ($1.1 * 10^{-7}$ and $1.45 * 10^{-7}$ cm^2/s) [21]. When the present

results are scaled to a molecular weight of 450 kDa using $\boldsymbol{D} \propto (\text{Molecular Weight})^{-0.5}$, the comparison becomes 0.968 * $10^{-7}$and 1.24 * 10^{-7} cm^2/s, respectively.

The dynamic second virial coefficient, an indicator of solvent quality, is related to the osmotic second virial coefficient (A_2), the polymer molecular weight (M), the first order friction coefficient (k_F), and the polymer specific molar volume (v_2) as shown in Equation 3-9 [22].

$$\boldsymbol{k_D = 2A_2M - k_F - v_2} \qquad \textbf{(3-9)}$$

Tsunashima and co-workers reported negative k_D values at a theta temperature of 293.4 K for a series of high molecular weight PS's dissolved in *trans*-DHN [23]. These negative k_D values are reasonable since A_2= 0 at the theta temperature of a polymer-solvent system. The negative k_D at 297 K that was obtained in this research is consistent with this analysis and the data of Tsunashima et al.

At temperatures greater than the theta temperature, A_2 is positive, and it increases as solvent quality improves [24], e.g. k_D values are expected to become more positive as the temperature increases. The k_D values reported in Table 3.1 are consistent with the normal behavior of A_2, as k_D transitions from negative to increasingly positive values over the temperature range studied.

The increase in R_H with temperature shown in Table 3.1 indicates that the PS coil relaxes as the solvent quality of DHN changes from a borderline theta condition at 297 K to the good solvent regime at higher temperatures. However, the change in R_H is not statistically significant once the solvent quality is relatively high, i.e., above about 350 K.

In the good solvent regime, the observed increases in the PS infinite dilution diffusion coefficients with temperature are almost exactly compensated by decreases in viscosity.

Nose and Chu measured R_H for a monodisperse, 179 kDa (M_w) PS in *trans*-DHN at 293 K [25]. If their value (9.11 nm) is scaled to the PS molecular weight used in this research (M_w = 320 kDa) using the relationship $R_H \propto \sqrt{\text{MolecularWeight}}$, the result is 12.7 nm. This value falls slightly below the R_H obtained at 297 K in this study (14.2 nm). Since this research was conducted above the θ-temperature of PS in *trans*-DHN, Nose and Chu's R_H was also scaled with (Molecular Weight)$^{0.6}$. The R_H marginally increased to 12.9 nm.

A slight difference in R_H can be expected since the present research used a 24% *cis*: 76% *trans* mixture of DHN as the solvent for PS. Other researchers have shown that the theta temperature of a PS-DHN solution is dependent on the *cis*/*trans* ratio [26-27]. Since the *cis* isomer is a better solvent for PS than the *trans* isomer, PS should be more relaxed, i.e., it should be larger in size, in a mixture of DHN isomers than in *trans*-DHN.

3.3.2. PS Diffusion in CO_2-Expanded DHN

The presence of CO_2 in polymer solutions is known to induce changes in solvent quality, polymer coil size, and solution viscosity [28-29]. The impact of CO_2 on PS diffusion coefficient, hydrodynamic radius, and solvent quality was determined over the same range of PS concentrations studied in the first part of this research. Previous research on the phase behavior of a moderately-concentrated PS-CO_2-DHN solution

indicated that PS precipitates at a CO_2 mole fraction of approximately 60 percent for temperatures ranging from 313 K to 423 K [12]. In order to avoid PS precipitation, CO_2 concentrations of 14, 26, and 44 mole percent were used in this research. System pressure was maintained at 20.7 MPa to ensure a single liquid phase at each experimental temperature. No PS diffusion coefficient measurements were made with CO_2-expanded DHN at 297 K and 20.7 MPa because there is evidence that CO_2 and DHN form a biphasic liquid mixture at this temperature and pressure [30].

3.3.2.1. PS Diffusion Coefficients in CO_2-DHN

The addition of almost 60 mole percent CO_2 to a moderately-concentrated PS-DHN solution can reduce polymer solution viscosity by nearly two orders of magnitude [31]. Such reductions in solution viscosity should increase PS diffusion coefficients in CO_2-expanded DHN.

The D_0's for the CO_2-containing polymer solutions were obtained in the manner described in Section 3.3.1. The effects of temperature and CO_2 concentration on D_0 are shown in Figure 3.2. At each temperature, the infinite dilution diffusion coefficients of PS increased with CO_2 concentration. In fact, D_0 increased by roughly a factor of 2.5 when the polymer solutions were expanded with 44 mole percent CO_2.

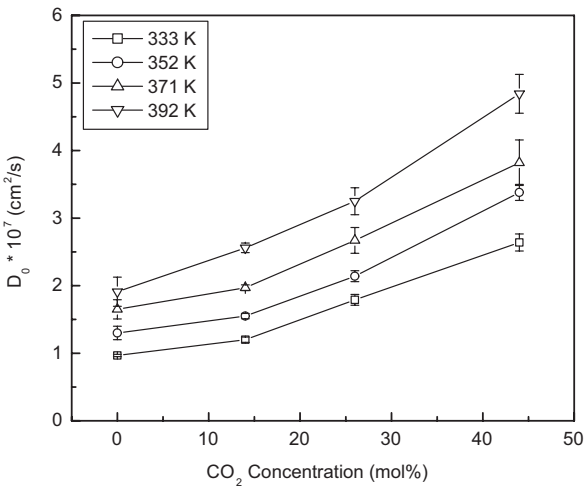

Figure 3.2. Effect of CO_2 and Temperature on PS Infinite Dilution Diffusion Coefficients at 20.7 MPa (PS M_n = 308 kDa, PDI = 1.04) The error bars represent the standard errors of the intercepts of the diffusion coefficient versus PS concentration plots.

The activation energies of diffusion (E) at each CO_2 concentration were calculated from the plots of the natural logarithm of the infinite dilution diffusion coefficient versus inverse absolute temperature. The values in Table 3.2 show that E decreases by roughly 16 percent as CO_2 concentration increases from 0 to 44 mole percent. The decrease in E with increasing CO_2 concentration is reasonable since CO_2 reduces polymer solution viscosity and therefore the drag forces on the polymer coils.

Table 3.2. Effect of CO_2 Concentration on the Activation Energy of PS Diffusion

CO_2 Concentration (mole %)	E (kJ/mol)
0	12.7 ± 0.9
14	13.8 ± 0.5
26	11.1 ± 0.5
44	10.7 ± 1.0

20.7 MPa (PS M_n = 308 kDa, PDI =1.04) The errors were defined as the standard errors of the slope in the ln (D_0) v. 1/T plots.

3.3.2.2. Solvent Quality and PS Coil Size

Dynamic second virial coefficients, calculated by the method described in Section 3.3.1, are shown as a function of temperature and CO_2 concentration in Figure 3.3. Errors for these measurements are provided in the supporting information. The addition of 14 mole percent CO_2 to PS-DHN appears to improve the solvent quality at temperatures of 372 K and lower since the k_D values for DHN containing 14 mole percent CO_2 are larger than the k_D's for PS-neat DHN. At the highest temperature, the k_D for 14 mole percent CO_2 in DHN is lower than that for neat DHN. However, the difference is not statistically significant. The addition of more CO_2 (beyond 14 mole percent) decreases solvent quality, as indicated by k_D values that are below those of DHN-14 mole percent CO_2.

The increase of solvent quality that was observed when low concentrations of CO_2 were added to DHN at low temperatures has little or no precedent in the literature. It is generally believed that adding any amount of CO_2 to an organic liquid reduces solvent

quality. The optimum k_D with CO_2 concentration that was observed in this study may be specific to the CO_2-DHN system.

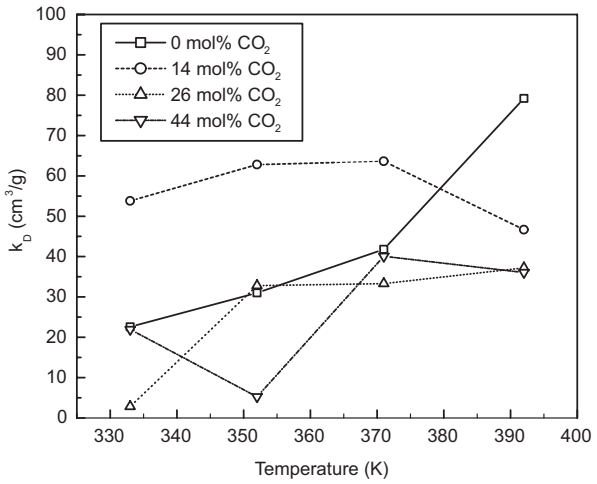

Figure 3.3. Effect of Temperature and CO_2 Concentration on Dynamic Second Virial Coefficient at 20.7 MPa (PS M_n = 308 kDa, PDI = 1.04)

Li and co-workers used small-angle X-ray scatterings (SAXS) to monitor changes in solvent quality and radii of gyration of PS in CO_2-tetrahydrofuran (THF) and CO_2-toluene mixtures at 308.15 K [28, 32]. The osmotic second virial coefficient (A_2) changed from positive to negative and decreased monotonically as CO_2 pressure increased from 0 to 2.7 MPa in PS (78 kDa)-THF. The change of sign for A_2 is indicative of decreasing solvent quality. Concurrently, the radius of gyration decreased from 14.0 nm to 10.5 nm [28].

The same 78 kDa PS dissolved in toluene exhibited similar behavior when CO_2 was added. The radius of gyration decreased from 9.55 to 7.13 nm as CO_2 pressure was

increased from 0 to 4.2 MPa. Li et al. indicate that the latter pressure corresponds to approximately 40 mole percent CO_2 dissolved in toluene. Over the same CO_2 concentration range, a 40 percent decrease in the second virial coefficient, A_2, was observed; this is indicative of the anti-solvent power of CO_2 [32].

Figure 3.4 shows the effect of CO_2 concentration on the hydrodynamic radii of PS in DHN at several temperatures. When the errors of these measurements are considered, the R_H for PS in CO_2-expanded DHN remains essentially constant as CO_2 concentration increases at each of the four temperatures. The errors in R_H are provided in the supporting information.

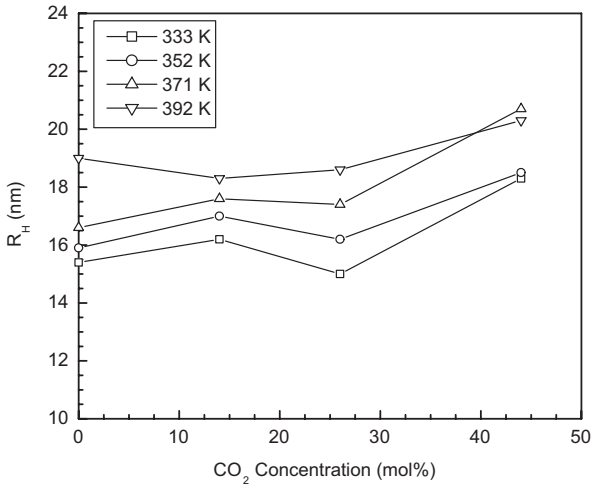

Figure 3.4. Effect of CO_2 and Temperature on PS Hydrodynamic Radii at 20.7 MPa
(PS M_n = 308 kDa, PDI = 1.04)

These results contrast with the SAXS results in which the R_g of PS in THF or toluene decreased with increasing CO_2 concentration. The manner in which R_g and R_H

are obtained differs. In SAXS, static polymer properties such as A_2 and R_g can be obtained directly from scattering data. However, with DLS, R_H must be calculated form values of D_0 and η, which are subject to some error. Finally the present experiments were conducted at constant hydrostatic pressure, whereas the hydrostatic pressure increased with CO_2 pressure in the studies of Li and coworkers [28, 32].

3.4. Conclusions

Polystyrene diffusion coefficients in DHN and CO_2-expanded DHN were measured using high pressure dynamic light scattering between 333 and 392 K. At each temperature, the infinite dilution diffusion coefficient of PS increased as the concentration of CO_2 in DHN increased. At 44 mole percent CO_2/56 mole percent DHN, the diffusion coefficients were about 2.5 times greater than in pure DHN, over the range of temperatures studied. A small (14 mole percent) addition of CO_2 resulted in a slight improvement of solvent quality, but further addition of CO_2 resulted in decreased solvent quality, as indicated by decreases in the dynamic second virial coefficients. These results demonstrate how the tunability of CO_2-expanded solutions can be used to increase polymer diffusion coefficients and to control solvent quality, which may be of practical use, particularly when working with catalytic polymer reaction systems.

3.5. Acknowledgements

The authors would like to thank Dr. John H. van Zanten of North Carolina State University for the helpful discussions. This research was supported by Contract

W911NF-04-D-0003 from the United States Army Research Office, Research Triangle Park, NC. Partial support was also provided by the STC Program of the National Science Foundation under Agreement No. CHE-9876674. This material is also based upon work supported under a National Science Foundation Graduate Research Fellowship (LBD).

References

1. Gehlsen M, Bates FS. Macromolecules 1993; 26(16): 4122-4127.
2. McManus NT, Rempel GL. Polymer Reviews 1995; 35(2): 239-285.
3. Hahn SF. Hydrogenated polystyrene: preparation and properties. In: Scheirs J, Priddy DB, editors. Modern styrenic polymers: polystyrenes and styrenic copolymers. Hoboken, NJ: John Wiley and Sons, 2003. pp. 533-555.
4. Wei M, Musie GT, Busch DH, Subramaniam B. J Am Chem Soc 2002; 124(11): 2513- 2517
5. Kerler B, Robinson RE, Borovik AS, Subramaniam, B. Appl Catal B 2004; 49(2): 91-98.
6. Jin H, Subramaniam B, Ghosh A, Tunge J. AIChE J 2006; 52(7): 2575-2581.
7. Nakatani H, Nitta K, Soga K. Polymer 1998; 39(18): 4273-4278.
8. Zhao J, Hahn SF, Hucul DA, Meunier DM. Macromolecules 2001; 34(6): 1737-1741.
9. Ness JS, Brodil JC, Bates FS, Hahn SF, Hucul DA, Hillmyer MA. Macromolecules 2002; 35(3): 602-609.

10. Xu D, Carbonell RG, Kiserow DJ, Roberts GW. Ind Eng Chem Res 2003; 42(15): 3509-3515.
11. Bussard A, Dooley KM. AIChE J 2008; 54(4): 1064-1072.
12. Xu D, Carbonell RG, Roberts GW, Kiserow DJ. J Supercritical Fluids 2005; 34(1): 1-9.
13. Kermis TW, Li D, Guney-Altay O, Park I-H, van Zanten JH, McHugh MA. Macromolecules 2004; 37(24): 9123-9131.
14. Kostko AF, McHugh MA, van Zanten JH. Macromolecules 2006; 39(4): 1657-1659.
15. Guo J, Andre P, Adam M, Panyukov S, Rubinstein M, DeSimone JM. Macromolecules 2006; 39(9): 3427-3434.
16. Hammel GL, Schulz GV, Lechner MD. Makromol Chem 1981; 182(6): 1829-1834.
17. Michels A, Hamers J. Physica 1937; 4(10): 995-1006.
18. Lemmon EW, McLinden MO, Friend DG. In *NIST Chemistry WebBook: NIST Standard Reference Database Number 69*; Linstrom PJ, Mallard WG, Ed.; National Institute of Standards and Technology: Gaithersburg, MD, June 2005.
19. DIPPR Data Ser 1998.
20. Cain NA, personal communication.
21. Kotera A, Matsuda H, Konishi K, Takemura K. J Polym Sci Part C 1968; 23(2): 619-627.
22. Yamakawa H. Modern theory of polymer solutions. New York: Harper & Row, 1971 (chapter 6).

23. Tsunashima Y, Nemoto N, Kurata M. Macromolecules 1983; 16(7): 1184-1188.

24. Rubinstein M, Colby RH. Polymer physics. Oxford: Oxford University Press, 2003 (chapter 1).

25. Nose T, Chu B. Macromolecules 1979; 12(4): 590-599.

26. Okada R, Toyoshima Y, Fujita H. Makromolekulare Chemie 1963; 59(1): 137-149.

27. Berry GC. J Chem Phys 1966; 44(12): 4550-4564.

28. Li D, Liu Z, Han B, Yang G, Wu Z, Liu Y, Dong B. Macromolecules 2000; 33(21): 7990-7993.

29. Jessop PG, Subramaniam B. Chem Rev 2007; 107(6): 2666-2694.

30. Tiffin DL, DeVera AL, Luks KD, Kohn JP. J Chem. Eng. Data 1978; 23(1): 45-47.

31. Whittier RE, Xu D, van Zanten JH, Kiserow DJ, Roberts GW. J Appl Polym Sci 2006; 99(2) 540-549.

32. Li D, Han B, Liu Z, Liu J, Zhang X, Wang S, Zhang X, Wang J, Dong B. Macromolecules 2001; 34(7) 2195-2201.

Supplemental Information

Using Equation 3-S-1, the errors associated with the concentration-dependent dynamic second virial coefficient were calculated from the standard errors of the slope and intercept of the diffusion coefficient versus concentration curves ($d(k_D*D_0)$ and $d(D_0)$, respectively). The resulting values are shown in Table 3.S.1.

$$d(k_D) = \frac{|d(k_D D_0)| + k_D * |d(D_0)|}{D_0} \qquad (3\text{-S-}1)$$

Table 3.S.1. Error Values for Dynamic Second Virial Coefficients (cm^3/g)

		CO_2 Concentration, 20.7 MPa			
T (K)	**0 mol% CO_2**	**0 mol%**	**14 mol%**	**26 mol%**	**44 mol%**
333	6.78	6.49	13.1	16.6	20.9
352	25.9	10.5	10.5	15.4	14.9
371	10.8	34.2	9.05	29.4	41.5
392	42.4	50.4	11.5	25.9	28.2

The errors associated with the hydrodynamic radii [$d(R_H)$] were calculated using Equation 3-S-2.

$$d(R_H) = \frac{k_B}{6\pi}\left[\frac{|d(T)|}{\eta D_0} + T\frac{|d(D_0)|}{\eta D_0^2} + T\frac{|d(\eta)|}{D_0 \eta^2}\right] \qquad (3\text{-S-}2)$$

The error in the infinite dilution diffusion coefficient [$d(D_0)$] was defined as the standard error of the intercept of the diffusion coefficient versus concentration curve. The error in the solvent viscosity [$d(\eta)$] were provided by Cain [20]. The errors in temperature [d(T)]

were the standard deviations from the average experimental temperature values. The errors in R_H associated with the data shown in Figure 3.4 are provided in Table 3.S.2.

Table 3.S.2. Error Values for Hydrodynamic Radii of 308 kDa PS in CO_2-DHN (nm)

		CO_2 Concentration, 20.7 MPa			
T (K)	**0 mol% CO_2**	**0 mol%**	**14 mol%**	**26 mol%**	**44 mol%**
333	0.678	0.744	0.894	1.37	1.50
352	1.69	1.07	1.34	1.54	1.01
371	1.13	2.26	1.40	2.72	2.63
392	2.63	3.33	2.17	2.92	1.85

CHAPTER 4 :

HYDROGENATION OF POLYSTYRENE IN CO_2-EXPANDED LIQUIDS: THE EFFECT OF CATALYST DECOMPOSITION ON DEACTIVATION

Chapter 4 is a manuscript that has been submitted for publication in **Applied Catalysis A: General.**

Hydrogenation of Polystyrene in CO_2-Expanded Liquids: The Effect of Catalyst Composition on Deactivation

Laura Beth Dong[a], Gary B. McVicker[a], Douglas J. Kiserow[a,b], George W. Roberts[a,*]

[a] Department of Chemical and Biomolecular Engineering, North Carolina State University, Campus Box 7905, Raleigh, NC 27695-7905, USA

[b] United States Army Research Office, P. O. Box 12211, Research Triangle Park, NC 27709-2211, USA

[*]Corresponding author: Tel: 919-515-7328; Fax: 919-515-3465. Email: groberts@eos.ncsu.edu

Abstract

The effect of catalyst composition on the hydrogenation of the aromatic rings of polystyrene dissolved in carbon dioxide-expanded decahydronaphthalene (CO_2-DHN) was studied using a slurry reactor at 150°C. Catalyst deactivation occurred within 15 minutes of the addition of CO_2 to the reactor when 5% Pd/SiO_2 or 5% Pd/Al_2O_3 was used as the catalyst. The deactivation is believed to be a consequence of CO formation via the reverse water-gas shift reaction, as CO was observed at the end of each hydrogenation reaction. The use of a physical mixture of either 5% Pd/SiO_2 or 5% Pd/Al_2O_3 with a methanation catalyst such as 5% Ru/Al_2O_3 or 65% Ni/SiO_2-Al_2O_3 resulted in decreased CO concentrations but no significant improvements in aromatic ring hydrogenation. When a catalyst containing both a hydrogenation and methanation function in a single

catalyst particle (1.6% Ru/4.2% Pd/SiO_2) was used, the degrees of hydrogenation in CO_2-DHN matched those obtained when neat DHN was the solvent. Furthermore, no CO was detected when the reaction was catalyzed by the bimetallic catalyst. These results suggest that the methanation function must be proximate to the hydrogenation (reverse water-gas shift) function in order for aromatic ring hydrogenation to proceed as rapidly in a CO_2-expanded solvent as in the unexpanded solvent.

Keywords: polystyrene, carbon dioxide-expanded liquid, reverse water-gas shift reaction, hydrogenation, catalyst deactivation

4.1. Introduction

Polymer hydrogenation is a post-polymerization process that yields polymers with greater thermal and chemical resistance than their unsaturated counterparts [1-3]. For example, the complete hydrogenation of polystyrene (PS) produces poly(vinylcyclohexane), a polymer that has a glass transition temperature (T_g) that is 41^{o}C higher than its parent polymer (T_g=147^{o}C versus T_g=105^{o}C for PS) [4]. This may enable the use of hydrogenated PS at higher temperatures than PS.

Polymer hydrogenation has been carried out with both homogeneous and heterogeneous catalysts, as reviewed by McManus et al. [2] and McGrath et al. [5]. The heterogeneous route offers the advantage of facile separation of catalyst and polymer, which is frequently necessary for economic reasons and for avoiding accelerated product degradation by residual catalyst.

The influence of mass transport on heterogeneously-catalyzed small molecule hydrogenations has been extensively discussed [6, 7]. Mass transport in polymeric reaction systems may be more challenging due to the high solution viscosities and low polymer diffusivities. In particular, macromolecules must be able to diffuse into and out of catalyst pores in order to access active sites in the catalyst interior.

This research explores the use of a carbon dioxide (CO_2)-expanded liquid (CXL), to aid mass transfer in the heterogeneous hydrogenation of PS using mesoporous catalysts. Carbon dioxide-expanded liquids, which are organic solvents in which CO_2 is dissolved, have been successfully used as reaction media for oxidations, hydrogenations, and polymerizations [8-11]. Increased reaction rates have been observed in CXLs and have been attributed to increases in solute diffusion coefficients and decreases in solution viscosities. In previous studies, it was determined that PS diffusivity increases and solution viscosity decreases as the concentration of CO_2 in a solution of PS/CO_2/decahydronaphthalene (DHN) is increased [12, 13].

The use of CO_2 as an aid in heterogeneously-catalyzed, small-molecule hydrogenations [14-17] and polymer hydrogenation [18] has been reported. However, catalyst deactivation was observed when CO_2 was used as a reaction medium in palladium and platinum-catalyzed hydrogenations [14, 18, 19]. Catalyst deactivation is believed to be a consequence of carbon monoxide (CO) formation. As shown in Equation 4-1, CO_2 and H_2 can react to form CO and H_2O in the reverse water gas shift (RWGS) reaction,

$$CO_2 + H_2 \leftrightarrow CO + H_2O \quad (4\text{-}1)$$

which is catalyzed by metals such as palladium and platinum.

Burgener et al. investigated the effect of catalyst composition on the RWGS reaction using a 1 mol% H_2/supercritical CO_2 mixture [20]. Their attenuated total reflection infrared spectroscopy (ATR-IR) results showed that more CO formed at 50°C when a Pt/Al_2O_3 or Pd/Al_2O_3 film was used as the catalyst than when Ru/Al_2O_3 or Rh/Al_2O_3 was used.

Similar results were obtained by Arunajatesan and co-workers, who used Fourier transform infrared (FTIR) spectroscopy to study the RWGS reaction at 70°C with a feed molar ratio of CO_2:H_2=19 [21]. Carbon monoxide formation was noted when a Pd/Al_2O_3 catalyst was used. No CO formed when Ni/Al_2O_3 or Ru/Al_2O_3 was the catalyst.

Solymosi and Erdohelyi studied the reaction of CO_2 and H_2 (CO_2:H_2=1:4) over Al_2O_3-supported palladium, rhodium, iridium, and ruthenium at temperatures ranging from 170 to 320°C [22]. They found that methane (CH_4) selectivity increased, while CO formation decreased, with increasing temperature. Furthermore, ruthenium and rhodium catalysts generated more CH_4 than their platinum, iridium, or palladium counterparts. The 5% Pd/Al_2O_3 was found to be the least active for CH_4 formation.

One plausible pathway for rhodium, nickel, and ruthenium catalysts to convert CO to CH_4, the methanation reaction, is shown in Equation 4-2.

$$CO + 3H_2 \leftrightarrow CH_4 + H_2O \qquad (4\text{-}2)$$

At 150°C, thermodynamic calculations indicate that CO methanation is preferred over the direct methanation of CO_2. Furthermore, Mills and Steffgen noted that CH_4 formation

by the direct hydrogenation of CO_2 does not occur when there are significant levels of CO present [23].

Xu et al. demonstrated that the hydrogenation of the aromatic rings in PS could proceed in CO_2-expanded DHN at 150°C when a small amount of 65% Ni/SiO_2-Al_2O_3 particles were mixed with non-porous 5% $Pd/BaSO_4$ particles [18]. The use of this "salt and pepper" catalyst system reduced CO concentrations significantly by converting it to CH_4. As a result, catalyst deactivation was circumvented, and higher PS hydrogenation rates were observed in CO_2-DHN than in neat DHN.

This research has focused on hydrogenating the aromatic rings of PS in CO_2-DHN using mesoporous palladium catalysts in a batch slurry reactor. Supported palladium, nickel, and platinum catalysts have been used to hydrogenate PS [1, 24-29]. The use of a palladium catalyst balances good hydrogenation activity with relatively low activity for polymer backbone scission. The effect of catalyst composition and structure, i.e., supported palladium, physical mixtures of supported palladium and a supported methanation catalyst, or a supported bimetallic catalyst, on the rate of PS hydrogenation in CO_2-DHN is demonstrated.

4.2. Experimental

4.2.1. Materials

Polystyrene was obtained from Sigma-Aldrich (St. Louis, MO) and used as received. Information provided by the supplier gave an approximate weight-average molecular weight (M_w) of 350,000 g/mol and an approximate number-average molecular

weight (M_n) of 170,000 g/mol. The average of four independent gel permeation chromatography measurements resulted in M_w = 233,000 g/mol and M_n = 130,000 g/mol for the PS. The reason for the discrepancy between internal measurements and supplier measurements is unknown, except possibly for the use of different experimental techniques. In any event, the ratio M_w/M_n (ca. 2) indicates that the PS had a wide range of molecular sizes.

Anhydrous decahydronaphthalene, a 26/74 mixture of *cis* and *trans* isomers, was purchased from Sigma-Aldrich (St. Louis, MO) and used as received. Carbon dioxide (≥99.99%) and hydrogen (≥99.999%) were purchased from Airgas National Welders (Charlotte, NC).

The 5% Pd/Al_2O_3, 65% Ni/SiO_2-Al_2O_3, and 5% Ru/Al_2O_3 catalysts were purchased from Sigma-Aldrich (St. Louis, MO) and used as received. The 5% Pd/SiO_2 catalyst was purchased from Strem Chemicals (Newburyport, MA) and used as received.

4.2.2. Catalyst Characterization

The Brunauer-Emmett-Teller (BET) surface areas and metal dispersions of the 5% Pd/Al_2O_3, 5% Pd/SiO_2, and 5% Ru/Al_2O_3 catalysts were measured using an Autosorb 1-C (Quantachrome Instruments, Boynton Beach, FL). The data is provided in Table 1. The samples were outgassed at 300°C for at least 1 hour before nitrogen physisorption measurements were conducted. For H_2 chemisorption measurements, the catalysts were dried at 120°C and reduced with hydrogen at 400°C. Dual H_2 isotherms were measured; the reported dispersion values are based on the chemisorbed species, assuming a Pd/H

ratio of 1. Average pore diameters, as determined from mercury intrusion volume and BET surface areas, are also provided in Table 4.1. Information regarding the 65% Ni/SiO_2-Al_2O_3 and 5% $Pd/BaSO_4$ was previously detailed in Xu et al. [18].

The average particle size was determined to be 122 μm for the 5% Pd/Al_2O_3 by optical microscopy. Scanning electron microscopy was used to measure an average particle size of 26 μm for the 5% Pd/SiO_2 catalyst.

Table 4.1. Catalysts Used in PS Hydrogenation

Catalyst	BET Surface Area (m^2/g)	Metal Dispersion (%)	Average Pore Diameter (nm)
5% Pd/Al_2O_3[a]	108	26[b]	10
5% Pd/SiO_2[a]	222	5.5[b]	16
5% $Pd/BaSO_4$	4.6[c]	0.3	1300[c]
5% Ru/Al_2O_3	86	14.8[b]	10
65% Ni/SiO_2-Al_2O_3[c]	142	7.7	33
1.6% Ru/4.2% Pd/SiO_2	222	n/a[d]	16[e]

[a] Palladium loadings were determined to be 4.7 wt% by ICP analyses; [b] Dispersion values measured by H_2 chemisorption assuming a Pd/H ratio of 1; [c] Xu et al. [18]; [d] Dispersion measurements by H_2 chemisorption are not valid because the technique does not differentiate between metals; [e] Average pore diameter before ruthenium impregnation

With the exception of the $Pd/BaSO_4$ catalyst, the average pore diameters of the Pd-containing catalysts probably fall within the range of polymer molecular sizes, so that some of the larger molecules may have great difficulty entering the pores of these catalysts.

4.2.3. Bimetallic Catalyst Preparation

The 1.6% Ru/4.2% Pd/SiO_2 catalyst was prepared by incipient wetness impregnation. Ruthenium (III) chloride hydrate (Strem Chemicals, Newburyport, MA) was dissolved in deionized ultra-filtered water (Fisher Chemical, Pittsburgh, PA) with the addition of a few drops of hydrochloric acid (99.999%, Alfa Aesar, Ward Hill, MA). The aqueous ruthenium chloride solution was then mixed with the purchased 5% Pd/SiO_2 (Strem Chemicals, Newburyport, MA) that had been dried overnight at 115^oC. The impregnated catalyst was then dried in air at 115^oC overnight before being calcined in air at 500^oC for 3 hours. It was then reduced with hydrogen for 2 hours at 327^oC. X-ray fluorescence (XRF) of the 1.6% Ru/4.2% Pd/SiO_2 confirmed the metal loadings.

Properties of the bimetallic catalyst are given in Table 4.1. The Scherrer equation was used to calculate average palladium and ruthenium particle sizes from x-ray diffraction (XRD) data for the bimetallic catalyst. The most abundant palladium phase in the bimetallic catalyst was determined to be Pd(111). This phase had an average diameter of 30 nm while the Ru(101) crystallites were 5.6 nm in diameter. For another point of comparison, the combined monolayer H_2 uptakes (both chemisorbed and physisorbed H_2) were measured. The uptake for 1.6% Ru/4.2% Pd/SiO_2 was 115 μmol/g while the corresponding value for the parent 5% Pd/SiO_2 was 177 μmol/g. The smaller H_2 uptake of the bimetallic catalyst suggests that the metals are more poorly dispersed than Pd was on the parent catalyst; this theory is supported by the findings of XRD.

4.2.4. Hydrogenation in a Slurry Reactor

A 50 mL batch slurry reactor equipped with 4 vertical baffles was used to hydrogenate PS. The catalyst (0.75 g) and polymer solution (25 mL) were loaded into the reactor. The reactor was sealed, purged with nitrogen to remove air, and then purged with H_2. Nitrogen and H_2 passed through moisture, oxygen, and CO_2 traps (all Alltech Associates, Deerfield, IL) before they were delivered to the bottom of the reactor via a dip tube. The agitation rate was set to 2500 rpm for all experiments. After being heated to the desired temperature, the reactor was pressurized with 5.6 MPa H_2. Unless noted, CO_2 was then added to the reactor via an ISCO syringe pump (Teledyne ISCO, Lincoln, NE). The time for the reaction was initialized when the reactor was pressurized, and the system was run for the desired time at 150^{o}C. For the reaction in neat DHN, H_2 was periodically fed to the reactor to maintain a constant pressure. Since the pressure drop in the CO_2-containing reactions was small, no additional H_2 was charged during the reaction. Once the desired time was reached, the agitation was stopped, and the reactor was cooled to ambient temperature before it was vented.

The hydrogenated polymer solution was then filtered using a 0.45 μm PTFE syringe filter (Millipore Corporation, Billerica, MA) to remove the catalyst before the solution was diluted with DHN. An ultraviolet visible spectrophotometer (JASCO V-550, JASCO Incorporated, Easton, MD) was used to measure the change in the aromatic ring absorbance at 261.5 nm. The degree of aromatic ring hydrogenation (x_A) was determined from $x_A = 1- (C_A/C_{A0})$, where C_A is the aromatic ring concentration at the end of the reaction and C_{A0} is initial aromatic ring concentration.

The gas from the CO_2-containing reactions was collected in a gas sampling bag. An accuro bellows pump (Draeger Safety, Pittsburgh, PA) was used to draw the gas through a carbon pre-tube and CO detection tube (10/b, Draeger Safety, Pittsburgh, PA). The length of the colored portion of the detection tube was correlated to CO concentration, providing semi-quantitative CO measurements.

4.3. Results and Discussion

4.3.1. PS Hydrogenation in CO_2-DHN Using Pd Catalysts

The 5% Pd/Al_2O_3 and 5% Pd/SiO_2 were used to hydrogenate PS in DHN and in DHN expanded with 8.4 MPa CO_2. The Peng-Robinson equation of state was used to estimate a liquid-phase mole fraction of 0.37 for CO_2 in the H_2-CO_2-*trans*-DHN system at 150^{o}C.

As shown in Figure 4.1, relatively high degrees of hydrogenation were obtained for the 5% Pd/SiO_2 and 5% Pd/Al_2O_3-catalyzed reactions in neat DHN. Despite its lower dispersion, the 5% Pd/SiO_2 catalyst is more active in hydrogenating the aromatic rings of PS than the 5% Pd/Al_2O_3 catalyst. This behavior may be explained by the difference in the catalyst particle sizes (122 μm for 5% Pd/Al_2O_3 versus 26 μm for the 5% Pd/SiO_2), and perhaps by the average pore diameters (10 nm for 5% Pd/Al_2O_3 versus 16 nm for the 5% Pd/SiO_2). As a result, both the external and internal transport resistances were smaller for the Pd/SiO_2 catalyst. Calculations of external surface area per unit of weight, which is based on particle density and particle diameter, showed that 5% Pd/SiO_2 has an order of magnitude larger external surface area per unit of weight than 5% Pd/Al_2O_3.

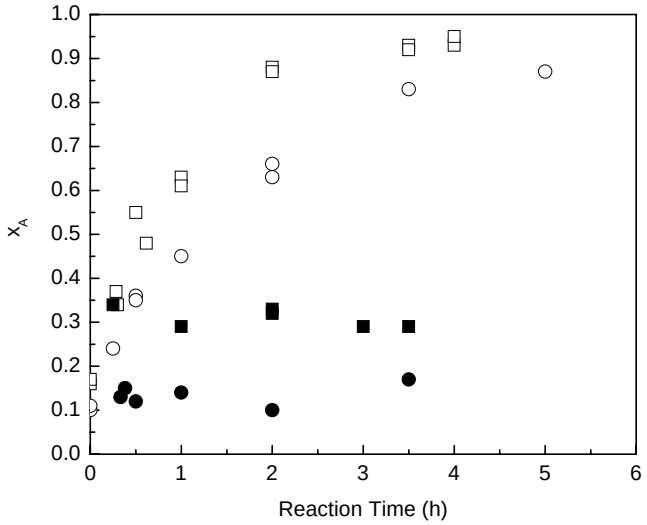

Figure 4.1. Effect of CO_2 on PS Hydrogenation Using Porous Palladium Catalysts. "Neat" DHN (0 MPa CO_2)- □: 5% Pd/SiO_2, ○: 5% Pd/Al_2O_3; 8.4 MPa CO_2- ■: 5% Pd/SiO_2, ●: 5% Pd/Al_2O_3. T=150°C, 3 wt% PS (M_w=233,000 g/mol, M_n=130,000 g/mol)-DHN, 5.6 MPa H_2, 1 g catalyst/g polymer, 2500 rpm.

The influence of external and internal mass transfer resistances on PS hydrogenation can also be seen by comparison of the initial turnover frequencies (TOF) of hydrogen for the two catalysts. The TOF for the 5% Pd/SiO_2 catalyst is 0.28 s^{-1} while the TOF of 5% Pd/Al_2O_3 is an order-of-magnitude smaller at 0.03 s^{-1}. Both of the TOF values are far less than the 0.95 s^{-1} reported by Xu et al. for 5% $Pd/BaSO_4$-catalyzed PS hydrogenation under comparable reaction conditions [30]. The failure of the TOF's obtained in the present research to obey the Madon-Boudart criterion suggests that mass transfer resistances significantly influence the current work.

When CO_2 was present, asymptotic degrees of hydrogenation were reached when either palladium catalyst was used. The plateaus, which fell far below the values that were obtained for the ring hydrogenation in neat DHN, were reached within about 15

minutes after the start of the reaction. The asymptotic degrees of hydrogenation, which were approximately 0.30 for 5% Pd/SiO_2 and 0.16 for 5% Pd/Al_2O_3, suggest catalyst deactivation.

The CO concentrations measured at the end of each CO_2-containing reaction are represented by the squares in Figures 4.2a and 4.2b. Note that these figures show measured CO concentrations for two types of experiments: 1) polymer is present (squares); 2) polymer is not present (circles). Agreement between the CO concentrations for the two types of experiment is reasonable, especially in the early stages of the reactions. Since the CO concentrations in this research are far from the reported equilibrium CO values at 150^{o}C [18], the apparent plateaus in the CO concentrations that occur with each catalyst suggest that the RWGS reaction is "self-poisoning." When 5% Pd/Al_2O_3 was used as the catalyst, concentrations of CO were higher than when 5% Pd/SiO_2 was used. This difference is believed to be a consequence of the lower metal dispersion of 5% Pd/SiO_2.

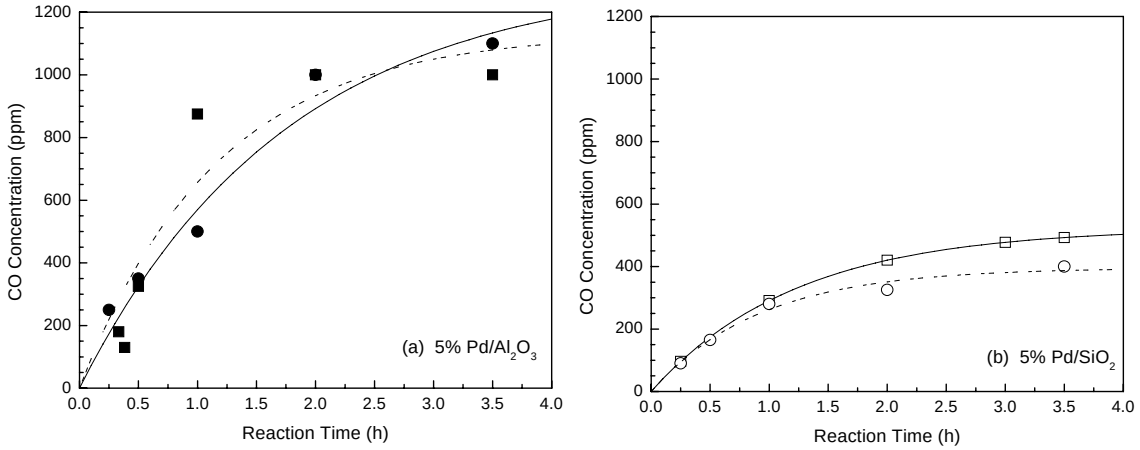

Figure 4.2. Carbon Monoxide Concentrations in PS Hydrogenation in CO_2-DHN. (a) 5% Pd/Al_2O_3-Catalyzed Reaction, (b) 5% Pd/SiO_2-Catalyzed Reaction. Both figures: ■, □: Polymer Present; ●, ○: No Polymer Present. Solid lines represent theoretical CO concentrations when polymer is present; dashed lines represent theoretical CO concentration with no polymer present. T=150°C, 3 wt% PS (M_w=233,000 g/mol, M_n=130,000 g/mol)-DHN or DHN, 5.6 MPa H_2 + 8.4 MPa CO_2, 1 g catalyst/g polymer, 2500 rpm.

To test this theory, the initial TOFs for RWGS activity of 5% Pd/SiO_2 and 5% Pd/Al_2O_3 were calculated using Equation 4-3

$$TOF = \frac{k_{CO} MW_{Pd}}{D \times L} \qquad (4\text{-}3)$$

where k_{CO} is the rate constant for CO formation, MW_{Pd} is the molecular weight of palladium, D is the palladium dispersion, and L is the Pd loading of the catalyst (wt Pd/wt catalyst). The rate constants for CO formation (k_{CO}) and catalyst deactivation (k_d) were determined by fitting the data shown in Figures 4.2a and 4.2b to the expression

$$C_{CO} = \frac{k_{CO}}{k_d} C_{cat,0} \left[1 - \exp(-k_d t)\right] \qquad (4\text{-}4)$$

Equation 4-4 is obtained by assuming that the rate of catalyst deactivation is first order in catalyst concentration (C_{cat}), i.e., $\frac{dC_{cat}}{dt} = -k_d C_{cat}$, and that the change in CO concentration is zero order in CO_2 and H_2 concentration $\left(\frac{dC_{CO}}{dt} = k_{CO} C_{cat} \right)$.

For the polymer-containing reactions, the initial TOFs for CO formation were about 8 s^{-1} for the 5% Pd/SiO_2 and 4 s^{-1} for the 5% Pd/Al_2O_3. There is some scatter in the CO concentration data, but the initial TOFs for CO formation in the absence of polymer were comparable to the initial TOFs when polymer was present (8 s^{-1} for the 5% Pd/SiO_2 and 3 s^{-1} for the 5% Pd/Al_2O_3). In accordance with the Madon-Boudart criterion [31], since the TOFs are reasonably close for the same catalytic metal, there appears to be essentially no mass transfer resistance to CO formation, and the variation in CO concentrations between the two palladium catalysts can be attributed to differences in their metal dispersions.

To further test the hypothesis that CO formation via the RWGS reaction is the source of catalyst deactivation, a series of reactions were run in which CO_2 was added to neat DHN after 1 hour of reaction. As shown by the filled points in Figure 4.3, within 15 minutes of the addition of CO_2, aromatic ring hydrogenation slowed and then ceased. However, the asymptotic aromatic ring conversions in these experiments are higher than those in Figure 4.1, consistent with the later addition of CO_2. Post-reaction analyses found that CO was also present in the gas phases of these reactions. These results support the contention that CO poisons sites for aromatic ring hydrogenation.

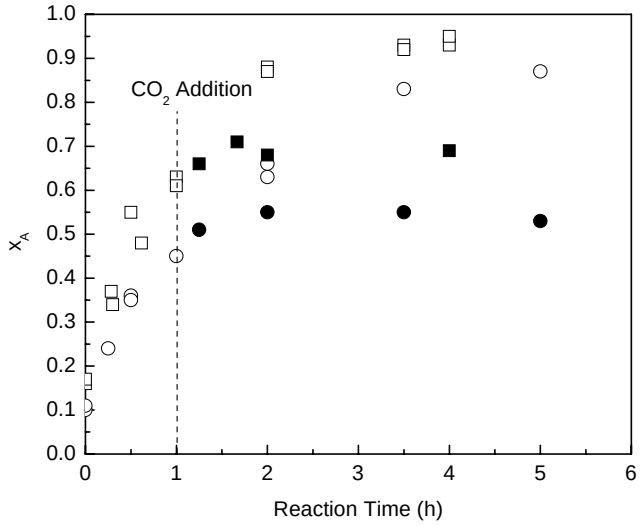

Figure 4.3. Late Addition of CO_2 to PS Hydrogenation. "Neat" DHN (0 MPa CO_2)-□: 5% Pd/SiO_2, ○: 5% Pd/Al_2O_3; 8.4 MPa CO_2 at t= 1 h- ■: 5% Pd/SiO_2, ●: 5% Pd/Al_2O_3. T=150°C, 3 wt% PS (M_w=233,000 g/mol, M_n=130,000 g/mol)-DHN, 5.6 MPa H_2, 1 g catalyst/g polymer, 2500 rpm.

4.3.2. PS Hydrogenation in CO_2-DHN Using Physical Mixtures of Catalysts

In an effort to negate the effect of CO poisoning, a physical mixture of a hydrogenation catalyst and a methanation catalyst were combined in a ratio of 2.5 grams palladium per gram methanation metal. This approach, with this catalytic metal ratio, was previously found to be effective in circumventing CO poisoning in PS hydrogenation in CO_2-DHN [18]. In that research, the hydrogenation catalyst was 5% $Pd/BaSO_4$ and the methanation catalyst was 65% Ni/SiO_2-Al_2O_3. Two-hour reactions at 150°C served as metrics for determining the effectiveness of the different catalyst combinations. Two different methanation catalysts (65% Ni/SiO_2-Al_2O_3 and 5% Ru/Al_2O_3) were used with each hydrogenation catalyst (5% Pd/Al_2O_3 and 5% Pd/SiO_2).

Table 4.2 shows that adding the methanation catalyst was generally effective in reducing the CO concentrations after 2 hours of reaction. However, the extents of ring hydrogenation in the presence of CO_2 did not improve significantly relative to the cases of the hydrogenation catalyst alone. Ruthenium was more effective than nickel in reducing CO levels.

Table 4.2. PS Hydrogenation in CO_2-DHN Using Physical Mixture of Catalysts

Catalyst	CO_2 (MPa)	x_A	CO (ppm)
5% Pd/Al_2O_3	0	0.66	---
	8.4	0.16	1000
5% Pd/Al_2O_3 + 65% Ni/SiO_2-Al_2O_3	8.4	0.21	90
5% Pd/Al_2O_3 + 5% Ru/Al_2O_3	8.4	0.43	4
5% Pd/SiO_2	0	0.88	---
	8.4	0.32	500
5% Pd/SiO_2 + 65% Ni/SiO_2-Al_2O_3	8.4	0.29	500
5% Pd/SiO_2 + 5% Ru/Al_2O_3	8.4	0.36	14

T=150°C, 2 hr., 3 wt% PS (M_w=233,000 g/mol, M_n=130,000 g/mol)-DHN, 5.6 MPa H_2, 2500 rpm, 1 g catalyst (total)/g PS, Pd/(Ni or Ru)=2.5 g/g

These results differ from those obtained for PS hydrogenation catalyzed by a physical mixture of 5% $Pd/BaSO_4$ and 65% Ni/SiO_2-Al_2O_3. In the previous work, degrees of aromatic ring hydrogenation in CO_2-DHN matched those obtained in neat DHN when the salt and pepper catalyst system was used [32]. One major difference between the previously-studied system and the current systems is the structure of the palladium hydrogenation catalysts. The dispersions of the 5% Pd/SiO_2 and 5% Pd/Al_2O_3 catalysts (5.5% and 26%, respectively) are one and two orders of magnitude larger than the dispersion of Xu et al.'s 5% $Pd/BaSO_4$ catalyst (0.3%). As demonstrated in Section

4.3.1, the RWGS activity is nearly proportional to the palladium dispersion. Therefore, the balance between RWGS activity and methanation activity is different in those catalyst mixtures containing the 65% Ni/SiO_2-Al_2O_3 catalyst since this catalyst was the same in the present studies and those of Xu et al. [18]. Thus, the methanation activity in the three catalyst mixtures should be the same, but the RWGS activity should be much higher for the present catalysts because of their much higher Pd dispersions.

In addition, BET surface area measurements indicate that the 5% $Pd/BaSO_4$ is essentially non-porous (5 m^2/g) while the 5% Pd/Al_2O_3 and 5% Pd/SiO_2 are quite porous (>100 m^2/g). Since the palladium is located on the exterior of the $BaSO_4$ particle, aromatic ring hydrogenation occurs on the exterior of the catalyst, and there are essentially no internal diffusion limitations for $Pd/BaSO_4$. However, both the Al_2O_3 and SiO_2-supported Pd catalysts are mesoporous, with active sites located in the interior of the catalyst particle. Based on the average pore diameters of these two catalysts, some of the PS molecules should experience hindered diffusion in the catalyst pores because the average pore diameter and the average molecular diameter are comparable in magnitude [12]. This leads to a polymer concentration gradient from the exterior to the interior of the catalyst particle and to significant internal diffusion limitations, consistent with the previously noted failure to obey the Madon-Boudart criterion.

The much smaller CO_2 and H_2 molecules (hard sphere diameters = 0.453 nm and 0.271 nm, respectively [33]) can diffuse in and out of the porous catalyst particles (Pd/Al_2O_3 and Pd/SiO_2) much faster than the large polymer molecules (hydrodynamic diameter ca. 25 nm). The slow RWGS reaction is not subject to any significant transport

limitation, in contrast to the aromatic ring hydrogenation reaction. The CO molecules formed by the RWGS reaction eventually contact the methanation catalyst in the physical mixture, but they have already poisoned catalytic hydrogenation sites.

4.3.3. PS Hydrogenation in CO_2-DHN Using a Bimetallic Catalyst

In an effort to create an environment in which CO could be methanated before hydrogenation sites were poisoned, a catalyst with both metals in the same particle was synthesized and used to hydrogenate PS in CO_2-DHN. Since ruthenium appeared to be more effective than nickel in reducing CO levels when the salt and pepper catalyst systems were used, a $Pd/Ru/SiO_2$, prepared as described in Section 4.2.3, was used to hydrogenate PS. As shown in Figure 4.4, with the 1.6% Ru/4.2% Pd/SiO_2 catalyst, the degrees of aromatic ring hydrogenation were essentially the same in both pure DHN and CO_2-expanded DHN. Furthermore, no CO was detected with the Draeger detection tubes.

Xu et al. [28] and Bussard et al. [29] found that the rate of disappearance of aromatic rings in PS hydrogenation is first order in aromatic ring concentration and zero order in hydrogen concentration when the hydrogen pressure is sufficiently high. The data obtained in the present research was analyzed using the approach of Xu et al. and Bussard et al. Observed rate constants (k_{obs}), which were obtained from the slopes of the $-\ln(1-x_A)$ versus $C_{cat}*t$ plots, are provided in Table 4.3.

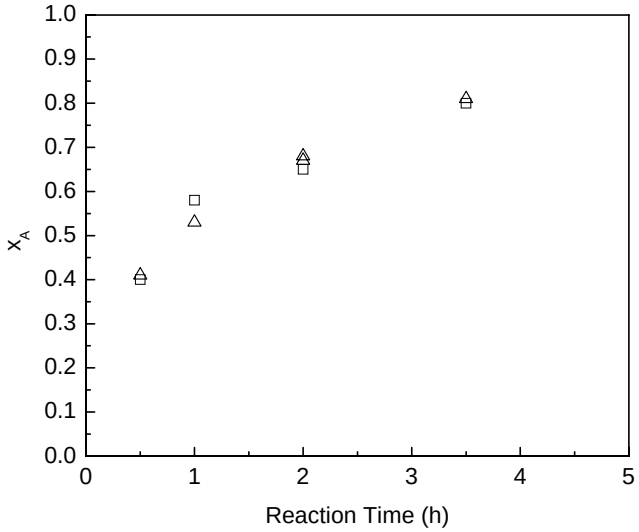

Figure 4.4. 1.6% Ru/4.2% Pd/SiO_2-Catalyzed PS Hydrogenation in CO_2-DHN. □: 0 MPa CO_2; Δ: 8.4 MPa CO_2. T=150°C, 3 wt% PS (M_w=233,000 g/mol, M_n=130,000 g/mol)-DHN, 5.6 MPa H_2, 1 g catalyst/g polymer, 2500 rpm

Table 4.3. Comparison of Observed Rate Constants for PS Hydrogenation

Catalyst	Pressure (MPa)	k_{obs} (L/g metal/s)
1.6% Ru/4.2% Pd/SiO_2	5.6	6.28 E-05
	5.6 MPa H_2 + 8.4 MPa CO_2	7.93 E-05
5% Pd/SiO_2	5.6	2.00 E-04
5% Pd/Al_2O_3	5.6	9.88 E-05
5% Pd/$BaSO_4$ [a]	5.3	3.20 E-05

T=150°C. All experiments at 2500 rpm, 3 wt% PS (M_w=233,000 g/mol, M_n=130,000 g/mol)-DHN, 5.6 MPa H_2, 1 g catalyst/g PS. [a] Data from Xu et al. [28]

For the bimetallic catalyst, the presence of 8.4 MPa CO_2 resulted in a modest increase in k_{obs}. The improvement is believed to be due to some combination of the lower viscosity of the polymer solution, the increased polymer diffusivity, and the decrease in the polymer coil diameters that occur when CO_2 is present. The diameter of a PS with M_n=154,000 g/mol (which is similar to the M_n of the PS used in this research)

decreases by about 20% when 8.4 MPa CO_2 is used to expand DHN [34]. The decrease in polymer sizes should allow more PS to access catalytic sites located in the catalyst pores.

The rate constants for PS hydrogenation for the three catalysts used in this study and for the $Pd/BaSO_4$ catalyst of Xu et al. [28] are compared in Table 4.3. In pure DHN, the bimetallic catalyst is about twice as active as the 5% $Pd/BaSO_4$. However, it is significantly less active than either the 5% Pd/SiO_2 or the 5% Pd/Al_2O_3 catalyst.

The lower hydrogenation activity of the bimetallic catalyst may be due to the effect of crystallite size on PS hydrogenation. As noted in Section 4.2.3, for the 1.6% Ru/4.2% Pd/SiO_2 catalyst, the average Pd(111) crystallite size is 30 nm. There is a discrepancy between the crystallite sizes for 5% Pd/SiO_2 determined by XRD (Pd(111) crystallite size = 9.7 nm), hydrogen chemisorption (21 nm), and scanning transmission electron microscopy (15 nm). Nevertheless, it is apparent that the palladium crystallites on the 1.6% Ru/4.2% Pd/SiO_2 are larger than those on the parent 5% Pd/SiO_2. During the preparation of the bimetallic catalyst, agglomeration of palladium atoms could have occurred during the ruthenium impregnation step (since an acidic precursor solution was used) or during the calcination step after ruthenium addition.

The 5% Pd/Al_2O_3 catalyst, which is one and a half times more active than the bimetallic catalyst, has a much smaller palladium crystallite size (4.4 nm by H_2 chemisorption versus 30 nm). The 5% $Pd/BaSO_4$ used by Xu et al. has a much larger crystallite size (250 nm by H_2 chemisorption) and is only about half as active as the bimetallic catalyst.

Nevertheless, the successful hydrogenation of PS in CO_2-DHN using 1.6% Ru/4.2% Pd/SiO_2 demonstrates the importance of the location of the methanation metal when the reaction is catalyzed by a mesoporous catalyst. The use of a bimetallic catalyst for PS hydrogenation in CO_2-expanded DHN may make it feasible to take advantage of the increased polymer diffusion coefficient and decreased polymer solution viscosity that results from the presence of CO_2 dissolved in the organic solvent.

4.4. Conclusions

In a slurry reactor at 150°C, hydrogenation of the aromatic rings of polystyrene dissolved in CO_2-expanded decahydronaphthalene is severely retarded when a mesoporous 5% Pd/Al_2O_3 or 5% Pd/SiO_2 catalyst is used. The low asymptotic degrees of hydrogenation that are observed are a consequence of carbon monoxide poisoning of catalytic sites. In contrast with an essentially non-porous Pd catalyst (Pd/$BaSO_4$), the use of a small amount of a methanation catalyst such as 5% Ru/Al_2O_3 or 65% Ni/SiO_2-Al_2O_3 physically mixed with either mesoporous palladium catalyst resulted in decreased CO levels but no dramatic improvements in the degrees of ring hydrogenation. However, with a 1.6% Ru/4.2% Pd/SiO_2 catalyst, PS hydrogenation was able to proceed to the same extent in CO_2-DHN as in neat DHN, and no CO formation was observed. In order for PS hydrogenation to proceed in CO_2-DHN on a mesoporous catalyst, it appears that the hydrogenation metal and the methanation metal must be located in close proximity on the same support. This prevents CO from poisoning the catalytic sites for hydrogenation.

4.5. Acknowledgements

This research was supported by Contract W911NF-04-D-0003 from the United States Army Research Office, Research Triangle Park, NC. Partial support was also provided by the STC Program of the National Science Foundation under Agreement No. CHE-9876674. This material is also based upon work supported under a National Science Foundation Graduate Research Fellowship (LBD). The authors also thank Dr. Wayne P. Robarge (Department of Soil Science, North Carolina State University) for the ICP measurements.

References

[1] M.D. Gehlsen, Bates, F. S., Macromolecules. 26 (1993) 4122-4127.

[2] N.T. McManus, Rempel, G. L., Polymer Reviews. 35 (1995) 239-285.

[3] S.F. Hahn, in: J. Scheirs, Priddy, D. B. (Ed.), Modern Styrenic Polymers: Polystyrenes and Styrenic Copolymers, John Wiley & Sons, Hoboken, NJ, 2003, pp. 533-555.

[4] F.S. Bates, Fredrickson, G. H., Hucul, D., Hahn, S. F., AlChE J. 47 (2001) 762-765.

[5] M.P. McGrath, Sall, E. D., Tremont, S. J., Chem. Rev. 95 (1995) 381-398.

[6] C.N. Satterfield, Mass Transfer in Heterogeneous Catalysis, MIT Press, Cambridge, MA, 1970.

[7] G.W. Roberts, in: P.N. Rylander, Greenfield, H. (Ed.), Catalysis in Organic Synthesis, Academic Press, New York, 1976.

[8] P.G. Jessop, Subramaniam, B., Chem. Rev. 107 (2007) 2666-2694.

[9] P.E. Savage, Gopalan, S., Mizan, T. I., Martino, C. J., Brock, E. E., AlChE J. 41 (1995) 1723-1778.

[10] M. Arai, Fujita, S-I., Shirai, M., J. Supercrit. Fluids. 47 (2009) 351-356.

[11] A. Baiker, Chem. Rev. 99 (1999) 453-473.

[12] L.B. Dong, Carbonell, R. G., Roberts, G. W., Kiserow, D. J., Polymer. 50 (2009) 5728-5732.

[13] R.E. Whittier, Xu, D., van Zanten, J. H., Kiserow, D. J., Roberts, G. W., J. Appl. Polym. Sci. 99 (2006) 540-549.

[14] A. Bertucco, Canu, P., Devetta, L., Zwahlen, A. G., Industrial & Engineering Chemistry Research. 36 (1997) 2626-2633.

[15] V. Arunajatesan, Subramaniam, B., Hutchenson, K. W., Herkes, F. E., in: D.G. Morrel (Ed.), Catalysis of Organic Reactions, Marcel Dekker, New York, 2003, pp. 461-475.

[16] S. Ichikawa, Tada, M., Iwasawa, Y., Ikariya, T., Chem. Commun. (2005) 924-926.

[17] N. Hiyoshi, Rode, C. V., Sato, O., Masuda, Y., Yamaguchi, A., Shirai, M., Chem. Lett. 37 (2008) 734-735.

[18] D. Xu, Carbonell, R. G., Kiserow, D. J., Roberts, G. W., Industrial & Engineering Chemistry Research. 44 (2005) 6164-6170.

[19] B. Minder, Mallat, T., Pickel, K. H., Steiner, K., Baiker, A., Catal. Lett. 34 (1995) 1-9.

[20] M. Burgener, Ferri, D., Grunwaldt, J-D., Mallat, T., Baiker, A., J. Phys. Chem. B. 109 (2005) 16794-16800.

[21] V. Arunajatesan, Subramaniam, B., Hutchenson, K. W., Herkes, F. E., Chem. Eng. Sci. 62 (2007) 5062-5069.

[22] F. Solymosi, Erdohelyi, A., Journal of Molecular Catalysis B. 8 (1980) 471-474.

[23] G. Mills, Steffgen, F.W., Catalysis Reviews. 8 (1974) 159-210.

[24] H.-G. Elias, Etter, O., Journal of Macromolecular Science, Part A. 5 (1967) 943-953.

[25] A. Abe, Hama, T., Polymer Letters. 7 (1969) 427-435.

[26] H. Nakatani, Nitta, K-h., Soga, K., Polymer. 39 (1998) 4273-4278.

[27] J.S. Ness, Brodil, J. C., Bates, F. S., Hahn, S. F., Hucul, D. A., Hillmyer, M. A., Macromolecules. 35 (2002) 602-609.

[28] D. Xu, Carbonell, R. G., Kiserow, D. J., Roberts, G. W., Industrial & Engineering Chemistry Research. 42 (2003) 3509-3515.

[29] A. Bussard, Dooley, K. M., AlChE J. 54 (2008) 1064-1072.

[30] D. Xu, PhD thesis, Department of Chemical and Biomolecular Engineering, North Carolina State University (2005).

[31] R.J. Madon, Boudart, M., Ind. Eng. Chem. Fundam. 21 (1982) 438-447.

[32] D. Xu, Carbonell, R. G., Roberts, G. W., Kiserow, D. J., The Journal of Supercritical Fluids. 34 (2005) 1-9.

[33] CRC Handbook of Chemistry and Physics, 87th ed., Taylor and Francis, Boca Raton, 2006.

[34] L.B. Dong, Kiserow, D. J., Roberts, G. W., In Preparation (2010).

CHAPTER 5 :

EFFECT OF POLYMER SIZE ON POLYSTYRENE HYDROGENATION

Chapter 5 is a manuscript that will be submitted for publication.

Effect of Polymer Size on Heterogeneous Polystyrene Hydrogenation

Laura Beth Dong[a], Douglas J. Kiserow[a,b], George W. Roberts[a,*]

[a]Department of Chemical and Biomolecular Engineering, North Carolina State University, Campus Box 7905, Raleigh, NC 27695-7905 USA

[b]United States Army Research Office, P. O. Box 12211, Research Triangle Park, NC 27709-2211, USA

*Corresponding author. Tel.: 919-515-7328; Fax: 919-515-3465. Email: groberts@eos.ncsu.edu

Abstract

The effect of polymer coil size on the rate of polystyrene (PS) hydrogenation was studied in a slurry reactor with mixtures of decahydronaphthalene (DHN) and carbon dioxide (CO_2) as the solvent for the polymer. The PS coil size was changed by varying the polymer molecular weight from 9,300 g/mol to 160,000 g/mol and by varying the CO_2 concentration. Using a 5% Pd/5% Ru/SiO_2 catalyst, the rate of aromatic ring hydrogenation at 150^{o}C was found to be strongly dependent on the size of a polymer coil relative to the average pore diameter of the catalyst. Significant pore diffusion limitations, as indicated by the Weisz modulus, were observed with increasing polymer molecular weight. Increasing the concentration of CO_2 resulted in increased reaction rates, with an order-of-magnitude improvement at the highest PS molecular weight.

5.1. Introduction

The influence of mass transfer in heterogeneous catalytic reactions has been discussed in much detail [1, 2], generally for situations where the diameter of the reactant molecules is small compared to the diameter of the catalyst pores. However, when the sizes of reactant molecules and catalyst pores are comparable, analysis of internal mass transport (pore diffusion) can be more challenging. For example, catalyst pore size was found to affect the rates of hydrotreatment of petroleum molecules, which can be comparable to the size of the pores in typical hydrotreating catalysts [3, 4]. Similarly, Chang and Huang [5] and Shirai et al. [6] demonstrated that copolymer hydrogenation rates and selectivity depended on catalyst pore size.

Chang and Huang found that the catalyst pore size and metal dispersion affected the extent to which the olefinic portion of polystyrene-*b*-polybutadiene-*b*-polystyrene was hydrogenated [5]. To study the effect of pore size on polymer hydrogenation, Chang and Huang prepared three 0.5% Pd/Al_2O_3 catalysts with average pore diameters of 17.1 nm, 38.9 nm, and 64.6 nm; the corresponding dispersions, as measured by CO chemisorption, were 58%, 36%, and 28%. The authors hypothesized that a trade-off between pore size and metal dispersion negated the effect of increasing pore diameter on the hydrogenation of olefinic microstructures. When catalyst pore diameter increased from 38.9 nm to 64.6 nm, Pd dispersion decreased from 36% to 28%, which is nearly a 25% reduction in exposed Pd atoms. The pore size-dispersion balance appeared to influence the hydrogenation of the olefinic microstructures as illustrated by the 38.9 nm-

Pd/Al_2O_3 catalyst yielding a higher percentage of saturated olefinic microstructures than the 64.6 nm or 17.1 nm-Pd/Al_2O_3 catalysts.

The 25% reduction in catalytic surface area that is associated with the 38.9 nm and 64.6 nm catalysts did not appear to affect the rate of aromatic ring hydrogenation in the same manner. The rate of 64.6 nm-Pd/Al_2O_3-catalyzed aromatic ring hydrogenation was slightly higher than the value for the 38.9 nm-Pd/Al_2O_3 catalyst. The reaction rates of the two larger pore catalysts were significantly faster than the rate for 17.1 nm-Pd/Al_2O_3-catalyzed hydrogenation. The authors suggested that the larger Pd particle size may promote the hydrogenation of aromatic rings.

Shirai and co-workers found that the hydrogenation kinetics of acrylonitrile-butadiene rubber (NBR) depended on the pore size of the palladium catalysts [6]. A "breakthrough" curve for the hydrogenation of an NBR (molecular weight of 3000) dissolved in carbon tetrachloride (CCl_4) showed that the initial rate of hydrogenation increased significantly when pore size increased from 42 to 63 Å. When the same NBR was dissolved in acetone and hydrogenated for 15 hours, the olefinic conversion increased almost linearly from 5% to 30% with increasing pore size. At a reaction time of 15 hours and a pore size of 63 Å, which is slightly above the onset of the breakthrough for NBR hydrogenation in CCl_4, NBR conversion is nearly 90% for the reaction in CCl_4; the corresponding value for the reaction in acetone is roughly 15%.

The differences in the observed behaviors of NBR hydrogenation in CCl_4 and acetone, namely the higher conversions in CCl_4 and the breakthrough curve with

increasing pore size for the reaction in CCl_4, were attributed to the relaxation of NBR in the good solvent, acetone. The effect of coil size on hydrogenation was effectively shown for the hydrogenation in CCl_4. The results of dynamic light scattering experiments indicated that the NBR had a slight molecular weight distribution and an average coil size of 42 Å. Therefore, the breakthrough in NBR hydrogenation that occurred between 42 Å and 63 Å is reasonable since most of the polymer coils could not diffuse inside the catalyst with pore diameters smaller than their size. The authors hypothesized that NBR coil relaxation in acetone prevented the polymer from easily diffusing through the interior of the catalyst and reacting, but they did not provide information on the size of NBR in acetone for comparison. Another possibility for explaining the differences in NBR hydrogenation in CCl_4 and acetone is that the solvent quality may affect polymer adsorption to catalytic sites, and thus, affect reaction rates.

The role of solute diffusivity on internal mass transport in an irreversible, heterogeneously-catalyzed reaction can be analyzed through the Weisz modulus (Φ):

$$\Phi = \frac{(n+1)^2 l_c^2 \left(-R_{A,v}\right)}{2 D_{A,eff} C_{A,s}} \qquad (5\text{-}1)$$

As shown in Equation 5-1, Φ is a function of the order of the reaction with respect to species A (n), the characteristic length of the catalyst particle (l_c), the measured reaction rate of species A per geometric catalyst volume ($-R_{A,v}$), the effective diffusion coefficient of species A ($D_{A,eff}$) and the surface concentration of species A ($C_{A,s}$). The characteristic length is a function of the particle geometry; for a sphere, $l_c = \frac{R}{3}$, where R is the radius

of the catalyst particle. The Weisz modulus can then be used to estimate an effectiveness factor (η); plots of η versus Φ can be found in many references [7].

In order to calculate a value of Φ, a value of $D_{A,eff}$ must be estimated for the system comprising the polymer being hydrogenated and the hydrogenation catalyst. Satterfield et al. [8] suggested that, at steady state, the $D_{A,eff}$ of species A diffusing through a porous membrane could be described by

$$D_{A,eff} = D_0 \frac{\theta K_p K_r}{\tau} \qquad (5\text{-}2)$$

where D_0 is the infinite dilution diffusion coefficient of species A in the bulk fluid, θ is the catalyst porosity, τ is the catalyst tortuosity, K_p is the equilibrium partition coefficient, and K_r is the reduction of diffusivity that occurs when the solute and pore size are similar in size. The equilibrium partition coefficient, as described by Ferry [9], is

$$K_p = (1-\lambda)^2 \qquad (5\text{-}3)$$

where λ is ratio of the solute diameter to the pore diameter.

The product of the D_0, K_p and K_r in Equation 5-2 describes the steric and frictional resistances of a hard sphere in a pore and is the diffusion coefficient, D, of the solute in the pores of the catalyst. This reduces Equation 5-2 to

$$D_{eff} = \frac{D\theta}{\tau} \qquad (5\text{-}4)$$

which is commonly used to calculate effective diffusion coefficients for heterogeneously-catalyzed small molecule reactions. For $\lambda<0.5$, a value of D can be predicted using the Renkin equation (Equation 5-5) [10]:

$$D = D_0(1-\lambda)^2\left[1 - 2.1044\lambda + 2.0888\lambda^3 - 0.948\lambda^5\right] \quad (5\text{-}5)$$

For $\lambda>0.5$, D can be estimated using Equation 3 and K_r values from Paine and Scherr [11].

Colton et al. measured the D_{eff}'s of monodisperse polystyrenes (PS) in porous borosilicate glass cubes with different average pore diameters [12]. The pore size distributions of the cubes were narrow, generally with greater than 90% of the pore volume being within 10% of the average pore diameter. The D_{eff}'s were used to compute D_{eff}/D_0 for PS in 1,2-dichloroethane and chloroform, and it was found that the ratio was higher in 1,2-dichloroethane than in chloroform. This finding suggests that solvent quality plays a role in polymer diffusion in pores. While the radii of gyration of PS in the bulk solvents were comparable at each molecular weight, 1,2-dichloroethane is a poorer solvent for PS than chloroform (based on the scaling relationships used by Colton et al.); therefore, the polymer molecules may be less likely to reconfigure themselves in the poorer solvent, 1,2-dichloroethane, than in the good solvent, chloroform.

Kathawalla and co-workers studied the effect of coil relaxation on PS diffusion coefficients through a membrane immersed in tetrahydrofuran (THF), a good solvent for PS [13]. They compared their data to predictions from the Renkin equation and found that for small λ, the Renkin equation overpredicted D_{eff}/D_0. For larger λ, the converse

was true. These authors attributed the underprediction of D_{eff}/D_o to overestimation of the reduction in polymer mobility, i.e., too large of a reduction calculated for the K_r term in Equation 2. The error may be due to the fact that the Renkin equation was developed for the diffusion of hard spheres in porous media; it does not take into the account the ability of a polymer to reconform itself to fit inside pores.

This research explores the effect of λ and polymer diffusion coefficient on PS hydrogenation kinetics in a batch, slurry reactor. Solvent quality was varied by dissolving various concentrations of carbon dioxide (CO_2) into the main solvent for the polymer (decahydronaphthalene, DHN) and by using monodisperse PS's ranging from 9,300 g/mol to 160,000 g/mol in molecular weight (which corresponds to average coil diameters ranging from 5 to 22 nm). Previous research demonstrated that the expansion of PS-DHN solutions with CO_2 reduces polymer solution viscosity [14], increases PS diffusivity [15], and leads to higher PS hydrogenation rates in CO_2-DHN than in neat DHN when a bimetallic catalyst is used [16, 17].

5.2. Experimental

5.2.1. Materials

The 5% Pd/5% Ru/SiO_2 catalyst was donated by BASF Catalysts, LLC. The BET surface area was 94 m^2/g. An average pore diameter of 30 nm was determined by mercury intrusion; the pore size distribution was narrow with nearly 90% of the pore volume within 20% of the average pore diameter. The catalyst porosity was 0.48 and the

particle density was 1.39 g/mL, both determined by mercury porosimetry. An average particle size of 102 μm was measured by electron microscopy.

Polystyrene standards were purchased from Pressure Chemical (Pittsburgh, PA) and Polymer Source, Incorporated (Montreal, Canada) and used as received. Molecular weights of the PS standards were measured by gel permeation chromatography (GPC) with tetrahydrofuran (THF) as the mobile phase. An Optilab rEX refractometer (Wyatt Technology, Santa Barbara, CA) was used in conjunction with a minDAWN Tristar light scattering detector (Model WTR-02, Wyatt Technology, Santa Barbara, CA). ASTRA software (Version 5.3.2.20, Wyatt Technology, Santa Barbara, CA) was used to correlate the polymer concentrations and intensities of scattered light to obtain the number-average and weight-average molecular weights (M_n and M_w, respectively). The resulting molecular weights of the PS standards are provided in Table 5.1. The PS are labeled according to the M_n (in kilodaltons, 1 kDa= 1,000 g/mol) that were provided by the suppliers. In some cases, the supplied M_n did not match the M_n measured by GPC.

Table 5.1. Characteristics of Polystyrene Standards

Sample	M_w (g/mol)	M_n (g/mol)
PS-9.3	9,580	9,290
PS-24	22,400	22,300
PS-46	43,100	42,600
PS-100	102,000	100,000
PS-131	146,000	143,000
PS-160	158,000	154,000

Commercial PS (Sigma-Aldrich, St. Louis, MO) was used as received. Information provided by the supplier gave an approximate average M_w of 350,000 g/mol and an approximate average M_n of 170,000 g/mol. The average of four independent GPC measurements resulted in M_w= 230,000 g/mol and M_n=130,000 g/mol for the commercial PS. The mass fraction distribution of one of the GPC measurements is shown in Figure 5.1.

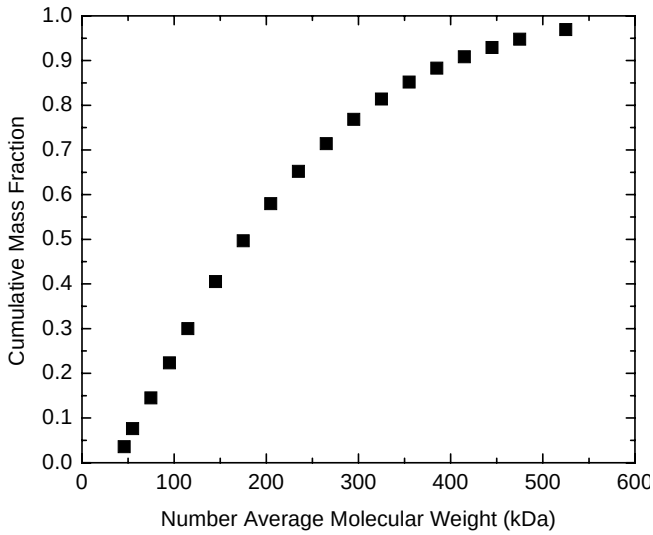

Figure 5.1. Cumulative Molecular Weight Distribution of Commercial Polystyrene

Anhydrous DHN, a 24/76 mixture of *cis* and *trans* isomers, was purchased from Sigma-Aldrich (St. Louis, MO) and used as received. Carbon dioxide (≥99.99%) and hydrogen (≥99.999%) were purchased from National Welders (Charlotte, NC).

5.2.2. High Pressure Dynamic Light Scattering

High pressure dynamic light scattering (DLS) was used to determine PS diffusion coefficients at 150°C. Details of the experimental technique may be found in Dong et al. [15]. The diffusion coefficients of PS-160 were measured at a scattering angle of 90° for polymer solutions containing 1, 2, and 3 wt% PS (concentration before the addition of CO_2). As discussed in detail later in this document, at reaction pressures of 2000 psig and 3000 psig, the mole fractions of CO_2 in the liquid phase are 0.37 and 0.54. Neglecting the concentration of the polymer, volumes of CO_2 were added to the DLS cell to obtain CO_2 mole fractions of 0.37 and 0.54. The pressure was then increased to the total pressure of the CO_2-containing reaction system- 2000 psig or 3000 psig.

5.2.3. Hydrogenation Experiments

Polystyrene was hydrogenated using a slurry reactor at 150°C and an agitation rate of 2500 rpm. Hydrogen pressure was maintained at 800 psig. For the CO_2-containing reactions, the CO_2 pressure was either 1200 psig or 2200 psig. The concentration of aromatic rings was monitored at 261.5 nm using UV-VIS spectroscopy and used to calculate the degrees of aromatic ring hydrogenation (x_A) . Further details of the reaction procedure and the subsequent analysis can be found in Dong et al. [17].

5.3. Results and Discussion

5.3.1. Polystyrene Diffusion Coefficients

The H_2-CO_2-DHN liquid phase compositions were estimated using the Peng-Robinson equation of state (PR-EOS). Since the DHN used in this research is 76 mol% *trans* isomer, the calculations were based on *trans*-DHN. Binary interaction parameters of -0.162, 0, and 0.125 were used for H_2-CO_2, H_2-*trans*-DHN, and CO_2-*trans*-DHN. As shown in Table 5.2, CO_2 solubility in *trans*-DHN increased when CO_2 pressure was increased from 1200 psig to 2200 psig.

Table 5.2. Liquid Phase Compositions in PS Hydrogenation Reactor at 150°C

Gas Feed	x_{H2}	x_{CO2}	x_{DHN}
800 psig H_2	0.04	---	0.96
800 psig H_2 + 1200 psig CO_2	0.02	0.37	0.61
800 psig H_2 + 2200 psig CO_2	0.03	0.54	0.43

The bulk diffusion coefficients of PS (D_{bulk}), which were measured at the reaction conditions (T=150°C, total pressure=2000 or 3000 psig and CO_2 concentration = 37 or 54 mol% CO_2), were found to be linearly dependent on polymer concentration (c_{PS}). The y-intercepts of D_{bulk} versus c_{PS} curves yielded PS infinite dilution diffusion coefficients (D_0) while the dynamic second virial coefficients (k_D), estimators of solvent quality, were obtained from the slopes of the best-fit lines.

The Stokes-Einstein equation (Equation 5-6) was used to determine hydrodynamic radii (R_H) of the polymer coils from the values of D_0.

$$R_H = \frac{k_B T}{6\pi\eta D_0} \quad (5\text{-}6)$$

In Equation 5-6, k_B is Boltzmann's constant, T is the absolute temperature, and η is the solvent viscosity. Carbon dioxide-DHN viscosities were obtained from Cain [18].

As shown in Table 5.3, D_0 increased by a factor of 3.5 as the CO_2 concentration increased from 0 to 54 mol%. The mixture of CO_2 and DHN is a poorer solvent for PS than neat DHN, as indicated by the decrease in k_D as CO_2 concentration increased. Also note that, R_H decreased 40% as CO_2 concentration increased. When no CO_2 is present, one coil can fit inside the catalyst. At the higher CO_2 concentration, two can enter the pore at the same time. The decrease in R_H suggests that more polymer coils can fit inside catalyst pores as CO_2 concentration increases, and that the diffusion coefficient of PS in the catalyst pores, D, should increase because the value of λ decreases with increasing CO_2 concentration. The decreasing values of k_D, i.e. decreasing solvent quality, suggest that polymer adsorption to catalytic sites may be enhanced. The decrease in solvent quality results in the polymer-solvent interactions becoming less favorable; as a result, polymer-polymer or polymer-catalyst interactions become more favorable.

Table 5.3. Effect of CO_2 on Properties of 160 kDa PS-DHN (T=150°C)

[CO_2] (mol%)	**Pressure (psig)**	**k_D (cm^3/g)**	**D_0*10^6 (cm^2/s)**	**R_H (nm)**
0	0	16 +/- 1.0	0.609 +/- 0.0139	11.1
37	2000	3.5 +/- 0.40	1.10 +/- 0.00236	8.9
54	3000	12 +/- 0.82	2.12 +/- 0.0242	6.8

The effect of solvent quality on polymer adsorption was demonstrated in the works of Kawaguchi et al. [19, 20]. These researchers found that more PS adsorbed onto a chrome substrate when the θ-solvent cyclohexane was used instead of the good solvents CCl_4 or toluene [20]. In subsequent studies, they found that the equilibrium concentration of 355 kDa-PS on a SiO_2 with an average pore diameter of 30 nm was 0.3 * 10^{-4} g/m^2 when CCl_4 was the solvent [19]. When cyclohexane, was used, the equilibrium concentration was approximately 1 * 10^{-4} g/m^2 for the same PS-SiO_2 combination. These results indicated that less polymer adsorbs onto porous SiO_2 from a good solvent than from a poor solvent. Similarly, in this research, the use of CO_2-DHN, which is a poorer solvent for PS than neat DHN, may promote polymer adsorption to active catalytic sites and result in increased polymer hydrogenation.

The D_0's of the PS's used in this research were scaled from the value measured for PS-160 using the relationship $D_2 \propto D_1\sqrt{MW_1/MW_2}$. After calculating R_H's from the scaled D_0's, the hydrodynamic radii for the polymer dissolved in neat DHN and average pore diameter were used to determine λ's at each polymer molecular weight. The λ values, which are provided in Table 5.4, spanned from 0.19 to 0.75.

Table 5.4. Ratios of PS Diameter to Average Pore Diameter in Neat DHN (T=150°C)

Sample	
PS-9.3	0.19
PS-24	0.29
PS-46	0.40
PS-100	0.51
PS-131	0.72
PS-160	0.75

5.3.2. Effect of Molecular Weight on PS Hydrogenation

To illustrate the effect of molecular weight on PS hydrogenation, a series of monodisperse PS's (ranging from M_n=9,300 g/mol to M_n=154,000 g/mol) were hydrogenated using 5% Pd/5% Ru/SiO_2 for two hours at 150°C. The resulting degrees of hydrogenation, which are shown in Figure 5.2, illustrate that hydrogenation of the polymer becomes progressively slower as its molecular weight increases. For molecular weights below approximately 22,000 g/mol (λ ca. 0.3), conversion of the aromatic rings is essentially complete at the specified conditions. However, for the polymer with M_n=154,000 g/mol, the conversion of aromatic rings was only about 15% at the same conditions. The degree of hydrogenation starts to decrease below 1 rather precipitously when λ exceeds about 0.35. In the region of λ=0.8, the decrease in the degree of hydrogenation appears to abate somewhat. The importance of the ratio of polymer size to support pore diameter corresponds to the findings of Kawaguchi et al. for PS adsorption on porous silicas. They hypothesized that at λ>0.4 the polymer molecule had to deform to fit inside the SiO_2 pores; the need for deformation resulted in lower equilibrium

polymer concentration [19, 21]. A critical λ was also observed by Shirai and co-workers, who saw a dramatic increase in NBR hydrogenation when λ was roughly 0.6 [6].

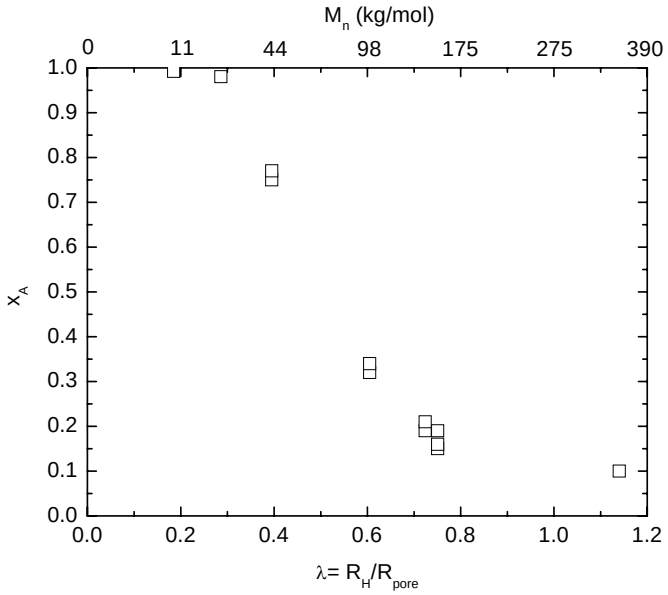

Figure 5.2. Effect of Polymer Molecular Weight on Polystyrene Hydrogenation
(T=150°C, t=2h, 3 wt% PS-DHN, 800 psig H_2, 1 g catalyst/g PS, 2500 rpm)

The potential effect of diffusion limitations on polymer hydrogenation was noted by Ness and co-workers when they hydrogenated PS using an ultra-wide pore Pt/SiO_2 catalyst with an average pore diameter of 380 nm [22, 23]. They saw a drastic decrease in the initial rate of hydrogenation when the PS molecular weight reached 200,000 g/mol and attributed the behavior to pore diffusion resistances and differences in the adsorption of the polymer molecules to the catalyst surface. The results shown in Figure 5.2 are

similar to the works of Ness et al. since the diffusivity of the polymer molecule decreases as its molecular weight increases.

The effect of molecular weight, which influences λ, on PS diffusivity is more clearly shown in Figure 5.3. Infinite dilution diffusion coefficients for the various PS's were obtained by scaling as described in Section 5.3.1. A tortuosity (τ) of 6 for the catalyst particle was assumed, and effective PS diffusion coefficients were calculated using Equation 5-4. As illustrated in Figure 5.3, PS diffusion coefficients begin to significantly increase when the value of λ falls below about 0.7. This behavior is not unlike that of x_A shown in Figure 5.2. The increase in polymer diffusivity below approximate λ = 0.7 appears to positively influence the PS hydrogenation process.

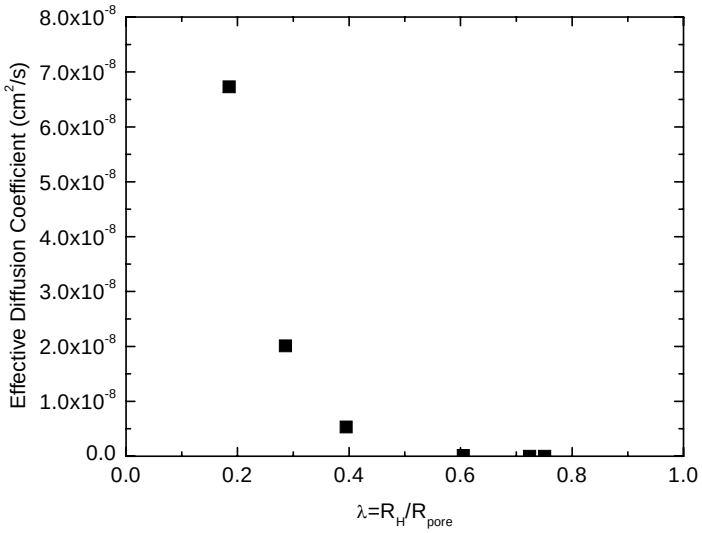

Figure 5.3. Effective Polystyrene Diffusion Coefficients in DHN (T=150°C)

5.3.3. Effect of CO_2 on Monodisperse PS Hydrogenation

The effect of 1200 psig CO_2, which corresponds to roughly 37 mole percent CO_2 in the liquid phase, on 5% Pd/5% Ru/SiO_2-catalyzed PS hydrogenation in DHN was determined at several different polymer molecular weights. A second CO_2 concentration (54 mole percent CO_2 in the liquid phase) was used in the hydrogenation of PS-160. At low to moderate degrees of hydrogenation, the rates of disappearance of aromatic rings was first order in aromatic ring concentration, first order in catalyst concentration (C_{cat}), and zero order in hydrogen concentration. Observed rate constants (k_{obs}) were obtained from the slopes of the best-fit lines to $-\ln(1-x_A)$ versus $C_{cat}*t$.

As shown in Table 5.5, the addition of CO_2 increases the rate of hydrogenation, as described by k_{obs}, for each of the polymers studied. Furthermore, when compared to the reaction conducted in neat DHN (0 psig CO_2), the presence of 2200 psig CO_2 results in an order of magnitude increase in the rate constant.

Table 5.5. Observed Rate Constants[a] for Aromatic Ring Hydrogenation

Polymer	0 psig CO_2	1200 psig CO_2	2200 psig CO_2
PS-24	2.15 E-05		
PS-46	6.74 E-06	1.21 E-05	
PS-100	1.63 E-06	5.93 E-06	
PS-131	9.29 E-07		
PS-160	7.14 E-07	2.70 E-06	8.31 E-06

(T=150°C, 3 wt% PS-DHN, 800 psig H_2, 1 g catalyst/g PS, 2500 rpm)

[a] Units for the observed rate constant are L/g cat/s

The order-of-magnitude increase in k_{obs} for PS-160 with the addition of 2200 psig CO_2 cannot be solely explained by the 3.5-fold increase in polymer diffusion coefficient, as described in Section 5.3.1. The decrease in polymer coil size that is accompanied by the decreasing solvent power/increasing CO_2 concentration should facilitate faster polymer diffusion into the catalyst interior. As a result, more catalytic surface area is available for hydrogenation, and higher rates of hydrogenation should be observed.

The rate constants in Table 5.5 for the reactions in neat DHN and the PS-160 were plotted as a function of the ratio of polymer size to pore size (λ). As shown in Figure 5.4, the addition of CO_2 to the reaction system results in the λ of PS-160 decreasing from 0.75 in neat DHN to 0.60 for the reaction with 1200 psig CO_2 to 0.46 for the 2200 psig CO_2-containing reaction. As a result, the observed rate constants for PS-160 with 1200 and 2200 psi CO_2 are comparable to those observed for lower molecular weight PS's with similar λ's. These results illustrate how pore diffusion restrictions strongly influence the kinetics of PS hydrogenation. This research also demonstrates how the utility of an anti-solvent such as CO_2 in heterogeneous polymer hydrogenation can create an environment that allows more polymer molecules to access the active sites in the catalyst interior; thus increased reaction rates are observed.

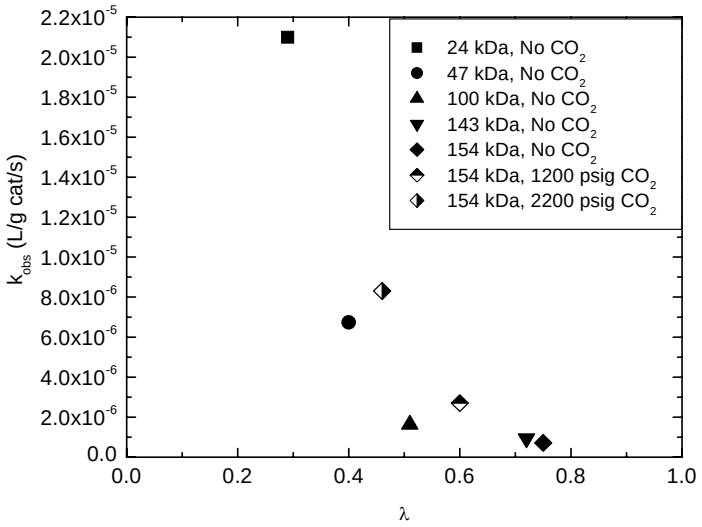

Figure 5.4. Dependence of Observed Rate Constants for PS Hydrogenation on $\lambda=R_H/r_{pore}$ (T=150°C, 3 wt% PS-DHN, 800 psig H_2, 1 g cat/g PS, 2500 rpm)

5.3.4. Analysis of Mass Transport

The rate of reaction of aromatic rings is expressed as

$$-R_A = \eta W k' C_{A,s} \qquad (5\text{-}7)$$

where η is the effectiveness factor, W is the mass of catalyst, k' is the intrinsic rate constant, and $C_{A,s}$ is the aromatic ring concentration at the surface of the catalyst. The rate of liquid-solid mass transport of aromatic rings is described by

$$-R_A = k_{LS} A_{LS} \left(C_{A,b} - C_{A,s} \right) \qquad (5\text{-}8)$$

where k_{LS} is the liquid-solid mass transfer coefficient, A_{LS} is the liquid-solid interfacial area, and $C_{A,b}$ is the aromatic ring concentration in the bulk liquid. In order to obtain an expression for $C_{A,s}$ in terms of $C_{A,b}$, Equations 5-7 and 5-8 can be set equal to one another and solved. Equation 5-7 then becomes

$$-R_A = \frac{1}{\frac{1}{k_{LS}A_{LS}} + \frac{1}{\eta W k'}} C_{A,b} = k_{obs} C_{A,b} \qquad (5\text{-}9)$$

$$\text{where } k_{obs} = \frac{1}{\frac{1}{k_{LS}A_{LS}} + \frac{1}{\eta W k'}} \qquad (5\text{-}10)$$

The observed rate constant can be a function of the liquid-solid mass transfer coefficient if the two terms in the denominator of Equation 5-10 are comparable in magnitude. Liquid-solid mass transfer coefficients were calculated using Equation 5-11, which was derived from the work of Brian and Hales [24].

$$k_{LS} = \frac{D}{d_p}\left\{16 + 4.84\left[\frac{g d_p^3 (\rho_a - \rho_l)}{18 \mu D}\right]^{2/3}\right\}^{1/2} \qquad (5\text{-}11)$$

In Equation 5-11, D is the diffusion coefficient of the reactant of interest, d_p is the catalyst particle diameter, g is the gravitational constant, μ is the liquid viscosity, ρ_a is the apparent density of the catalyst particle, ρ_l is the liquid density. The apparent density can be calculated from the skeletal density (ρ_s) of the catalyst and the porosity (ε) by

$$\rho_a = \varepsilon \rho_l + (1 - \varepsilon)\rho_s \qquad (5\text{-}12)$$

Liquid-solid mass transfer coefficients for the aromatic rings in each PS-DHN solution were calculated using Equation 5-11. The product of the number of monomers in a given polymer and the scaled infinite dilution diffusion coefficient that was used to calculate the D_{eff}'s in Section 5.3.2 was used as the D. The solution viscosities were scaled to the 0.7 power using the Mark-Houwink-Sakurada equation and DHN and

polymer solution viscosities reported by Whittier [25]. The ratio of the measured volume-based reaction rate to the calculated rate of liquid-solid mass transfer ($\eta k_v l_c/k_{LS}$) is analogous to the first term in the denominator of Equation 5-10 if the denominator is multiplied by the quantity ($\eta Wk'$). If $\eta k_v l_c/k_{LS}$ is far less than 1, then the reaction is not significantly influenced by liquid-solid mass transfer. As shown by the small values of $\eta k_v l_c/k_{LS}$ in Table 5.6, liquid-solid mass transport is not a signficant resistance in 5% Pd/5% Ru/SiO_2-catalyzed PS hydrogenation. Therefore, Equation 5-9 is reduced to Equation 5-7.

Table 5.6. Liquid-Solid Mass Transfer Coefficients for Aromatic Ring Hydrogenation

	k_{LS} (m/s)	$k_v l_c/k_{LS}$
PS-24	2.68 E-03	1.85 E-04
PS-46	3.37 E-03	4.73 E-05
PS-100	4.55 E-03	8.47 E-06
PS-131	5.17 E-03	4.25 E-06
PS-160	5.31 E-03	3.18 E-06

T=150^{o}C, 3 wt% PS-DHN

Weisz moduli were calculated for the aromatic rings of each PS and are provided in Table 5.7. The corresponding η's, which were obtained from a plot of η versus Φ, are also given in Table 5.7. As indicated by the decreasing values of η, pore diffusion resistance increases with polymer molecular weight when no CO_2 is present. The addition of 1200 psig CO_2 results in η increasing from 0.88 to 0.90. As expected, the addition of a higher concentration of CO_2 (2200 psig) increases η to 0.92. These results

demonstrate that the use of CO_2 can reduce the internal mass transfer resistance in high molecular weight PS hydrogenation.

Table 5.7. Internal Mass Transfer Parameters for PS Hydrogenation

Polymer		
PS-24, 0 psig CO_2	0.014	0.99
PS-46, 0 psig CO_2	0.007	0.995
PS-100, 0 psig CO_2	0.03	0.98
PS-131, 0 psig CO_2	0.16	0.80
PS-160, 0 psig CO_2	0.36	0.47
PS-160, 1200 psig CO_2	0.30	0.81
PS-160, 2200 psig CO_2	0.25	0.88

T=150^{o}C, 3 wt% PS-DHN

5.3.5. Commercial PS Hydrogenation Catalyzed by 5% Pd/5% Ru/SiO_2

Figure 5.5 shows that the hydrogenation of commercial grade PS using the 5% Pd/5% Ru/SiO_2 catalyst is a first-order process with an observed rate constant of 1.43 E-06 L/g cat/s. The kinetic behavior of commercial PS hydrogenation agrees with the findings for monodisperse PS hydrogenation, which were detailed in previous sections.

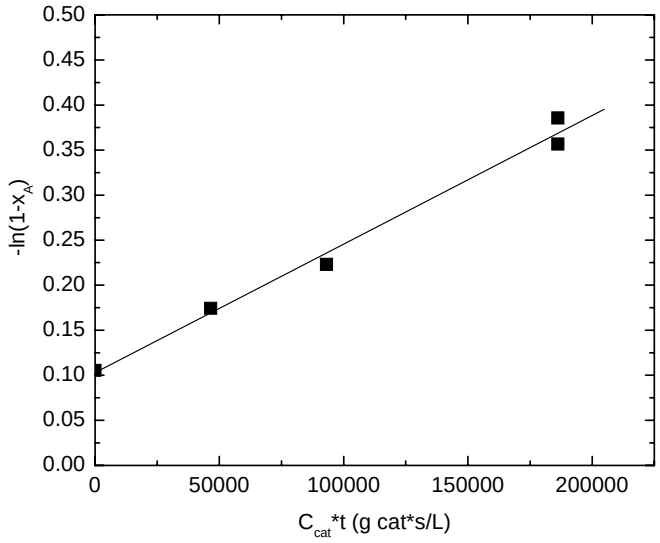

Figure 5.5. Commercial PS Hydrogenation Using 5% Pd/5% Ru/SiO_2
(T=150°C, 3 wt% PS-DHN, 800 psig H_2, 1 g catalyst/g PS, 2500 rpm)

The material balance for the hydrogenation of a polymer with molecular weight M_i should be

$$\frac{dC_i}{dt} = k_i C_{cat} C_i \qquad (5\text{-}13)$$

where C_i is the concentration of species *i* and k_i is the rate constant for species *i*. The concentration of species *i* can be expressed in terms of the aromatic ring concentration C_A by the relationship $C_i=x_iC_A$, where x_i is the fractional contribution of species *i* to the total aromatic ring concentration. For the monodisperse polymers discussed in previous sections, $x_i=1$. However, for a polymer with a molecular weight distribution, x_i will be less than 1. The summation of the material balances for each polymer of molecular weight M_i yields

$$\frac{dC_A}{dt} = -\left[k_\alpha w_\alpha + k_\beta w_\beta + k_\delta w_\delta + \ldots\right] C_{cat} C_A \qquad (5\text{-}14)$$

In Equation 5-14, k_α is the rate constant for polymer of molecular weight M_α, w_α is the fraction of aromatic rings in polymers with a molecular weight α .

Gel permeation chromatography and the ASTRA software program were used to measure the molecular weight distribution of the commercial grade PS (refer to Figure 5.1). The molecular weight distribution was divided into 18 increments to determine the weight fraction that each increment contributed to the overall polymer composition. The observed rate constants, which were provided in Table 5.5, and weight fractions of each increment of polymer were used in the calculations. For $M_n \leq 154$ kDa, the rate constants were interpolated from the data in Table 5.5. For $M_n \geq 154$ kDa, the rate constants were calculated from extrapolation of the data in Figure 5.4. An overall rate constant of 1.36 E-06 L/g cat/s for commercial grade PS hydrogenation using 5% Pd/5% Ru/SiO_2 was obtained from the calculation. This value is in very good agreement with the value that was obtained from the slope of the data shown in Figure 5.5 (1.43 E-06 L/g cat/s). It appears that Equation 14 can provide a first-pass approach in describing the hydrogenation of commercial grade PS.

5.4. Conclusions

At 150^{o}C, the heterogeneous hydrogenation of polystyrene is influenced by significant pore diffusion resistances when using a 5% Pd/5% Ru/SiO_2 catalyst. The

observed rate of aromatic ring hydrogenation is dependent on polymer molecular weight and size. The addition of CO_2 reduces polymer coil size by 40 percent, which enables faster diffusion of the polymer molecules in the catalyst and higher observed reaction rates. As a first approach, the summation of weighted rates of hydrogenation of monodisperse PS can be used to describe the hydrogenation of a commercial grade PS.

5.5. Acknowledgements

The authors would like to thank BASF Catalysts, LLC for supplying the 5% Pd/5% Ru/SiO_2 catalyst used in this work. This research was supported by Contract W911NF-04-D-0003 from the United States Army Research Office, Research Triangle Park, NC. Partial support was also provided by the STC Program of the National Science Foundation under Agreement No. CHE-9876674.

References

[1] G.W. Roberts, in: P.N. Rylander, Greenfield, H. (Ed.), Catalysis in Organic Synthesis, Academic Press, New York, 1976.

[2] C.N. Satterfield, Mass Transfer in Heterogeneous Catalysis, MIT Press, Cambridge, MA, 1970.

[3] E. Ruckenstein, Tsai, M. C., AlChE J. 27 (1981) 697-699.

[4] M. Shimura, Shiroto, Y., Takeuchi, C., Ind. Eng. Chem. Fundam. 25 (1986) 330-337.

[5] J.-R. Chang, Huang, S-M., Industrial & Engineering Chemistry Research. 37 (1998) 1220-1227.

[6] M. Shirai, Suzuki, N., Nishiyama, Y., Torii, K., Arai, M., Applied Catalysis A: General. 171 (1999) 219-225.

[7] G.W. Roberts, Chemical Reactions and Chemical Reactors, John Wiley & Sons, Hoboken, 2009.

[8] C.N. Satterfield, Colton, C. K., Pitcher Jr., W. H., AlChE J. 19 (1973) 628-635.

[9] J.D. Ferry, Journal of General Physiology. 20 (1936) 95-104.

[10] E.M. Renkin, The Journal of General Physiology. 38 (1954) 225-243.

[11] P.L. Paine, Scherr, P., Biophys. J. 15 (1975) 1087-1091.

[12] C.K. Colton, Satterfield, C. N., Lai, C-J, AlChE J. 21 (1975) 289-298.

[13] I.A. Kathawalla, Anderson, J. L., Industrial & Engineering Chemistry Research. 27 (1988) 866-871.

[14] R.E. Whittier, Xu, D., van Zanten, J. H., Kiserow, D. J., Roberts, G. W., J. Appl. Polym. Sci. 99 (2006) 540-549.

[15] L.B. Dong, Carbonell, R. G., Roberts, G. W., Kiserow, D. J., Polymer. 50 (2009) 5728-5732.

[16] D. Xu, Carbonell, R. G., Roberts, G. W., Kiserow, D. J., The Journal of Supercritical Fluids. 34 (2005) 1-9.

[17] L.B. Dong, McVicker, G. B., Roberts, G. W., Kiserow, D. J., In Preparation (2010).

[18] N.A. Cain, Roberts, G. W., 5th International Symposium in Chemical Engineering and High Pressure Processes, Segovia, Spain, 2007.

[19] M. Kawaguchi, Anada, S., Nishikawa, K., Kurata, N., Macromolecules. 25 (1992) 1588-1593.

[20] M. Kawaguchi, Hayakawa, K., Takahashi, A., Macromolecules. 16 (1983) 631-635.

[21] M. Kawaguchi, Sakata, Y., Anada, S., Kato, T., Takahashi, A., Langmuir. 10 (1994) 538-541.

[22] J.S. Ness, Brodil, J. C., Bates, F. S., Hahn, S. F., Hucul, D. A., Hillmyer, M. A., Macromolecules. 35 (2002) 602-609.

[23] D.A. Hucul, Hahn, S. F., Adv. Mater. 12 (2000) 1855-1858.

[24] P.L.T. Brian, Hales, H. B., AlChE J. 15 (1969) 419-425.

[25] R.E. Whittier, Chemical Engineering, North Carolina State University, Raleigh, 2004.

CHAPTER 6 :

SYNTHESIS AND CHARACTERIZATION OF STYRENE-VINYLCYCLOHEXANE COPOLYMERS

Chapter 6 is a manuscript that will be submitted for publication in two parts.

Synthesis and Characterization of Styrene-Vinylcyclohexane Copolymers

Laura Beth Dong[a], Salomon Turgman[a], Steven K. Burgess[a], Douglas J. Kiserow[a,b], George W. Roberts[a, *]

[a]Department of Chemical and Biomolecular Engineering, North Carolina State University, Campus Box 7905, Raleigh, NC 27695-7905 USA

[b]United States Army Research Office, P. O. Box 12211, Research Triangle Park, NC 27709-2211, USA

* To whom correspondence should be addressed: Email: groberts@eos.ncsu.edu, Fax: 919-515-3465, Phone: 919-515-7328

Abstract

Styrene-vinylcyclohexane (S-VCH) copolymers were synthesized by the partial hydrogenation of commercial grade polystyrene (PS) in a slurry batch reactor. Decahydronaphthalene (DHN) was used as the solvent for the polymer while either 5% Pd/Al_2O_3 or 5% Pd/SiO_2 was used as catalysts. The rate of hydrogenation was found to be linearly dependent on catalyst concentration. Polystyrene hydrogenation kinetics were found to deviate from a first-order kinetic model. The surface areas of used catalysts were measured and were found to be well below those of unused, fresh catalyst. This suggested that the observed catalyst deactivation may be due to polymer fouling of the catalyst.

Gel permeation chromatography (GPC) with refractive index and ultraviolet (UV) detection results showed that lower molecular weight fractions of the polymer were more highly hydrogenated than the high molecular weight fractions. Differential scanning calorimetry (DSC) measurements showed that S-VCH copolymers formed from 5% Pd/Al_2O_3-catalyzed PS hydrogenation had two glass transition temperatures (T_g) while the polymers made with the 5% Pd/SiO_2-catalyst possessed a single T_g. The polymer produced in each reaction was then separated into hexane-soluble and hexane-insoluble fractions. Based on the UV and DSC analyses of the hexane-soluble fractions, it is believed that PS hydrogenation proceeds via a blocky mechanism, which was first proposed for polybutadiene hydrogenation.

Keywords: polystyrene, hydrogenation, glass transition temperature

6.1. Introduction

Polymer hydrogenation is a means to create saturated polymers with improved physical properties. For example, completely hydrogenated polystyrene (PS) possesses lower density, lower water absorption, higher transparency, and a higher glass transition temperature (T_g) than PS itself [1]. The improved transparency, as measured by the stress-optical coefficient, may make the use of hydrogenated PS attractive for optical storage media applications [2, 3]. There is some discrepancy in the exact value of the T_g

of fully hydrogenated PS, but the previously reported T_g values of hydrogenated PS are consistently higher than the T_g of the parent polymer [1, 2, 4-7].

The partial hydrogenation of PS yields styrene-vinylcyclohexane (S-VCH) copolymers (Scheme 6-1). Partial hydrogenation provides a means for the product polymer to possess physical properties that are characteristic of the component polymers. Block copolymers are often designed so that they have properties of each component. The T_g's of partially hydrogenated PS's depend on the degree of aromatic ring hydrogenation [6, 7].

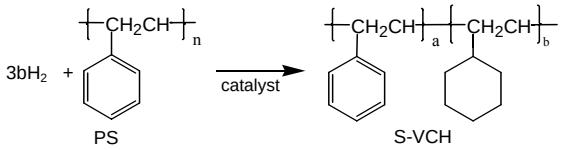

Scheme 6-1. Polystyrene Hydrogenation

Previous research on heterogeneously-catalyzed polybutadiene and polyisoprene hydrogenation suggests that the saturation occurs in a blocky fashion [8-10]. In the blocky hydrogenation mechanism, multiple monomer units of a single polymer coil adsorb to catalytic sites in a single catalyst particle and react. The saturated units desorb, and other unsaturated moieties adsorb and undergo hydrogenation. This process repeats itself until a certain fraction of each coil is hydrogenated. Based on the analyses of polybutadiene hydrogenation products, the critical fraction was 85% for Rosedale and Bates' polymers [9] and 89% for the products of Cassano et al. [8]. Ness et al. suggested

that the blocky hydrogenation mechanism may apply to heterogeneous PS hydrogenation [11], while Nakatani et al. suggested that the phase separation in their PS hydrogenation products may be due to the blocky character of the polymers [7].

If heterogeneous PS hydrogenation does proceed in a blocky fashion, then the metal crystallite size of the catalyst, polymer-support interactions, and polymer-catalytic metal interactions should influence the reaction kinetics and the physical properties of the polymer product. This research identifies catalysts with activity for hydrogenating the aromatic rings of PS dissolved in decahydronaphthalene (DHN). The effects of temperature, catalyst concentration, and agitation rate on PS hydrogenation kinetics were quantified. The effects of catalyst composition on the molecular weight distributions and T_g's of the S-VCH products were determined.

6.2. Experimental

6.2.1. Materials

Commercial grade PS was purchased from Sigma-Aldrich (St. Louis, MO) and used as received. Information provided by the supplier gave an approximate average M_w of 350,000 g/mol and an approximate average M_n of 170,000 g/mol. The average of four independent gel permeation (GPC) measurements resulted in M_w= 230,000 g/mol and M_n=130,000 g/mol for the commercial PS.

Anhydrous DHN, a 24/76 mixture of *cis* and *trans* isomers, and anhydrous hexane were purchased from Sigma-Aldrich (St. Louis, MO) and used as received.

Tetrahydrofuran (HPLC grade, Fisher Chemical, Pittsburgh, PA) and methylene chloride (Fisher Chemical, Pittsburgh, PA) were used as received. Hydrogen (≥99.999%) was purchased from National Welders (Charlotte, NC).

The 5% Pd/Al_2O_3 (also denoted 5% Pd/Al_2O_3-A),10% Pd/Al_2O_3, and 5% Ru/Al_2O_3 catalysts were purchased from Sigma-Aldrich (St. Louis, MO) and used as received. The 5% Pd/Al_2O_3-E, 5% Pt/Al_2O_3-E, 5% Pd/Al_2O_3-S, 5% Pt/Al_2O_3-S, and 5% Pd/SiO_2 catalysts were purchased from Strem Chemicals (Newburyport, MA) and used as received. The BET surface areas of the aforementioned catalysts are given in Table 6.1. Hydrogen chemisorption was used to measure the palladium dispersions, assuming a Pd/H ratio of 1; the dispersion values are also provided in Table 6.1. Selected bulk densities; skeletal densities; porosities; and average pore diameters, which were calculated from the mercury intrusion volumes and BET surface areas, are also tabulated.

Table 6.1. Properties of Catalysts Used for PS Hydrogenation

Catalyst	BET Surface Area (m^2/g)	Dispersion[a]	d_{pore} (nm)	ρ_b (g/mL)	ρ_s (g/mL)	ε
5% Pd/Al_2O_3-A	108	26%	10	1.2	4.7	0.33
5% Pd/Al_2O_3-E	114	13%				
5% Pd/Al_2O_3-S	1	0.21%				
10% Pd/Al_2O_3-A	100	21%	10	0.61	0.99	0.40
5% Pd/SiO_2	222	5.5%	16	0.40	2.3	0.42
5% Ru/Al_2O_3	86	14.8%	10	0.92	2.7	0.31
5% Pt/Al_2O_3-E	115	19%				
5% Pt/Al_2O_3-S	1	0.84%				

[a] Dispersion values measured by H_2 chemisorption assuming a Pd/H ratio of 1

X-ray diffraction (XRD) was used to identify that the support in the 5% Pd/Al_2O_3-A as the δ-phase while α-phase was used in the 5% Pd/Al_2O_3-S. The 5% Pd/Al_2O_3 has an average particle size of 122 μm. The average particle size of the 5% Pd/SiO_2 catalyst is 26.0 μm.

6.2.2. Polystyrene Hydrogenation

Polystyrene hydrogenation was carried out in a 50 mL slurry batch reactor. The reaction temperature ranged from 90°C to 180°C. Agitation rate was varied between 2500 and 4000 rpm. Unless otherwise noted, hydrogen pressure was maintained at 800 psig. Details of the hydrogenation procedure may be found in Dong et al. [12].

The concentration of aromatic rings (C_A) was measured at 261.5 nm using UV-VIS spectroscopy. The degree of aromatic ring hydrogenation (x_A) was calculated from $x_A=1-C_A/C_{A0}$ where C_{A0} is the aromatic ring concentration at t=0.

Polymers were recovered by precipitation in methanol. The polymer samples were dried at 80°C under 25 in. Hg for at least 24 hours. An additional drying step- 150°C, 25 in Hg, 3 days- was used to ensure complete solvent removal from the polymer.

6.2.3. Catalyst Deactivation Studies

The BET surface areas and metal dispersions of recovered 5% Pd/Al_2O_3 and 5% Pd/SiO_2 catalysts were measured using an Autosorb 1C (Quantachrome Instruments, Boynton Beach, FL). In order to remove excess polymer, the spent catalysts were

agitated in methylene chloride for 12 days at ambient temperature and pressure. The catalysts were then separated from the solvent using vacuum filtration. The recovered catalysts were dried overnight in a vacuum oven at 115^{o}C.

Two outgassing procedures were used. In one procedure, residual moisture and volatile components were removed from recovered catalysts by outgassing at 115^{o}C for at least 2 hours. This outgassing temperature is far below the decomposition temperature of PS (~280^{o}C, determined by thermal gravimetric analysis (TGA)) or PVCH (~250^{o}C by TGA). The BET surface areas of these catalysts were then measured using nitrogen physisorption. Recovered catalyst was also outgassed at 300^{o}C, which is above the decomposition temperatures of the polymers. Residue was found on the wall of the sample tubes when outgassing was conducted at the elevated temperature.

6.2.4. Gel Permeation Chromatography

Polymer molecular weights were measured by gel permeation chromatography (GPC) with THF as the mobile phase. The GPC is equipped with an Optilab rEX refractometer (Wyatt Technology, Santa Barbara, CA), a UV detector, and a miniDAWN Tristar light scattering detector (Model WTR-02, Wyatt Technology, Santa Barbara, CA).

The refractive index (RI) detector was used in conjunction with the UV detector to determine the aromatic and cyclohexane fractions present in the product polymers. Individual component fractions of styrene-butadiene copolymers [13], styrene-isobutylene copolymers [14], and PS-poly(methylmethacrylate) blends [15] have been

determined using GPC equipped with RI and UV detectors . The aromatic ring, which is found in styrene, is UV-active while the cyclohexyl ring is not UV-active. The product of the volumetric flow rate of the eluent (r) and the area under the UV detector's response (A_{UV}) is purely a function of the mass of aromatic rings (m_A) that pass through the detector. In Equation 6-1, a_A is a constant for the UV response; this value was measured by passing solutions of known aromatic ring concentrations through the UV detector and taking the slope of the best-fit line as a_A.

$$rA_{UV} = a_A m_A \quad (6\text{-}1)$$

The product of r and the area under the RI response (rA_{RI}) contains information about the aromatic and cyclohexyl masses (m_A and m_C, respectively), as denoted in Equation 6-2.

$$rA_{RI} = b_A m_A + b_C m_C \quad (6\text{-}2)$$

The RI constant for the aromatic ring (b_A) was obtained by passing solutions of known PS concentration through the RI detector and applying a linear fit to obtain b_A from the slope. The RI constant for the cyclohexyl ring (b_C) was obtained by passing solutions of highly hydrogenated (x_A>0.99) PS through the RI detector and obtaining b_C from the slope of the best-fit line.

Equation 6-1 can be divided by Equation 6-2 and rearranged so that the weight fraction of cyclohexyl rings (w_C) can be calculated using Equation 6-3.

$$w_C = \frac{A_{UV}\, b_A / a_A - A_{RI}}{\left(b_A / a_A - b_C / a_A \right) A_{UV} - A_{RI}} \qquad (6\text{-}3)$$

6.2.5. Differential Scanning Calorimetry

A TA Q2000 differential scanning calorimeter (DSC, TA Instruments, New Castle DE) was used to determine the T_g's of the polymer hydrogenation products. Nitrogen was used as the purge gas. Measurements were performed on approximately 5 mg of polymer sealed in a Standard Aluminum Pan (TA Instruments, New Castle DE). The polymers were heated at 4°C/min to 200°C, held isothermal for 5 minutes, cooled to 40°C at 4°C/min, held isothermal for 5 minutes, and heated to 200°C at 4°C/min. The T_g was determined from the second heat by the midpoint method.

6.2.6. Rheology Experiments

A TA Instruments ARES-M strain-controlled rheometer (New Castle, DE) was used to measure the shear storage and loss moduli (G' and G", respectively) of S-VCH polymers. The polymer samples were softened into disks (~11 mm in diameter and ~1.8 mm thick) by heating them to 160°C. The polymers were placed between 10 mm stainless steel parallel plates, and the data was collected at a frequency of 8 rad/sec while the polymer cooled from 160°C at 1°C/min. Strain sweeps conducted at 8 rad/sec showed

that the data was in the linear viscoelastic regime. The percent strain values ranged from 0.02% to 3.0%.

To determine T_g, a second-order polynomial was fitted to the first derivative of the log[G'(T)] versus T. The minimum of the polynomial was determined numerically and taken to be T_g. This value corresponds to the inflection on the log [G'(T)] versus T curve.

6.2.7. Hexane Extractions

The S-VCH products were dissolved in hexane in to a concentration of 0.04 g polymer/g hexane. This ratio was previously found to be suitable for the extraction of PS hydrogenation products [16]. The polymer was stirred in hexane for 3 days; then the undissolved polymer was separated from the supernatant. A few solutions were cloudy; they were centrifuged at 7000 rpm, which resulted in the aggregation of insoluble polymer and the clarity of the supernatant. The supernatant was drawn from the vial, and the hexane-soluble polymer was recovered by hexane removal through drying. The hexane-insoluble polymers were dissolved in THF and then dried. Both sets of polymers were dried in a vacuum oven under 25 in Hg.

6.3. Results and Discussion

6.3.1. Catalyst Evaluation

The use of heterogeneous nickel catalysts for PS hydrogenation has been shown to result in significant polymer backbone hydrogenolysis [4, 6, 7]. Platinum and palladium-based catalysts have resulted in little or no backbone scission [1, 5, 11, 17]. In this research, several commercially-available supported palladium, platinum, and ruthenium catalysts were tested for their abilities to hydrogenate the aromatic ring of PS. The hydrogenation activities of the catalysts were determined in 2 hour, 150^{o}C screening experiments. Agitation rate was maintained at 2500 rpm, catalyst to polymer ratio was 1:1 (g:g), and H_2 pressure was 800 psig.

The decreases in the activities of the 5% Pd/Al_2O_3 catalysts, which are shown in Figure 6.1, are partly due to the differences in the Pd dispersions, which are provided in Table 6.1. While it appears that the change in x_A associated with the 5% Pd/Al_2O_3-A and 5% Pd/Al_2O_3-E catalysts may be attributed solely to the two-fold difference in Pd dispersion, a first-glance comparison of the activities of the three catalysts for PS hydrogenation show a failure to obey the Madon-Boudart criterion [18]. Theoretically, the 100-fold difference in the Pd dispersions of the 5% Pd/Al_2O_3-S and 5% Pd/Al_2O_3-A catalysts should result in 5% Pd/Al_2O_3 being 100 times more active in hydrogenating PS. However, the 3-fold difference in catalyst activity suggests that mass transfer limitations may be influencing the observed behavior. This topic of mass transfer influence on PS hydrogenation will be discussed further in a later section.

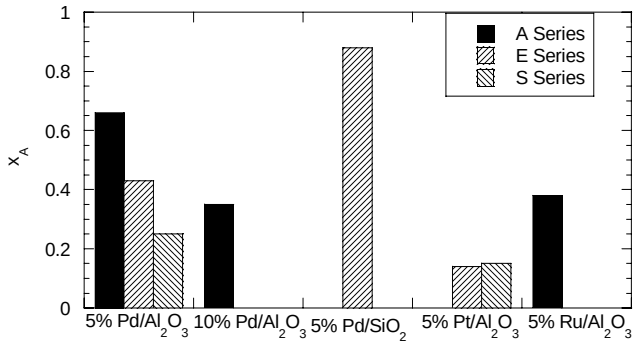

Figure 6.1. Catalyst Screening for PS Hydrogenation
(T=150°C, 2 hr., 3 wt% PS-DHN, 800 psig H_2, 1 g catalyst/g PS, 2500 rpm)

Figure 6.1 shows that the 5% Pd/Al_2O_3-A and 5% Pd/SiO_2-S catalysts were the most active in hydrogenating PS's aromatic rings. Therefore, they were chosen for further studies and will be known as 5% Pd/Al_2O_3 and 5% Pd/SiO_2 from this point forward.

6.3.2. Effect of Temperature

Polystyrene was hydrogenated at 90°C, 120°C, 150°C, and 180°C using 5% Pd/Al_2O_3 and 5% Pd/SiO_2. The change in aromatic ring concentration with respect to time was found to be first-order in aromatic ring concentration and first-order in catalyst concentration at low to moderate conversions. As expected, the rate of aromatic ring hydrogenation increased with reaction temperature. This is shown in Figures 6.2a and 6.2b by the increasing magnitude of the slopes of the best fit-lines to $-\ln(1-x_A)$ versus

C_{cat}*t data. The observed rate constants (k_{obs}) were taken as the slopes of the best-fit lines. Increasing the reaction temperature from 90°C to 180°C resulted in an approximate 24-fold increase in the rate of 5% Pd/Al_2O_3-catalyzed PS hydrogenation, as denoted by k_{obs}. The increase was even more dramatic with 5% Pd/SiO_2; k_{obs} at 180°C was 52 times larger than that obtained at 90°C.

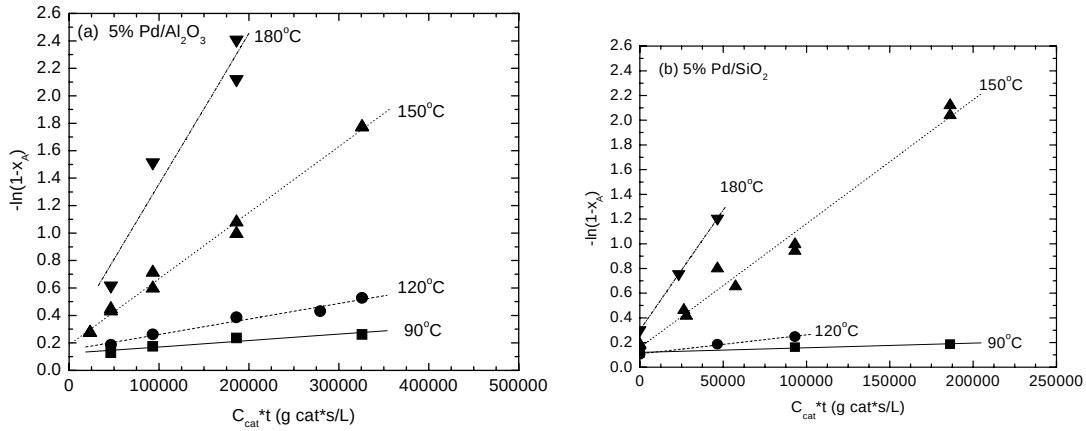

Figure 6.2. Effect of Temperature on PS Hydrogenation. (a) 5% Pd/Al_2O_3 (b) 5% Pd/SiO_2 (3 wt% PS-DHN, 800 psig H_2, 1 g catalyst/g PS, 2500 rpm).

The observed rate constants were then plotted as a function of inverse reaction temperature. The resulting Arrhenius plot is shown in Figure 6.3. The apparent activation energies (E_a), which were calculated from the slopes of the best-fit lines (which are equal to E_a/R where R is the ideal gas constant), are 49.9 kJ/mol for 5% Pd/Al_2O_3-catalyzed PS hydrogenation in DHN and 61.1 kJ/mol for 5% Pd/SiO_2. The latter value is comparable to that measured by Xu et al. (59.6 kJ/mol) for 5% $Pd/BaSO_4$-

catalyzed PS hydrogenation in DHN, which was reported to be conducted in the absence of mass transfer limitations [19]. The E_a values obtained in the present research suggest that the reactions were not conducted in the external mass-transfer limited regime since E_a>> 20 kJ/mol, which is typically used to approximate the activation energy of diffusive processes. However, the possibility of a significant pore-diffusion resistance cannot be eliminated based on the measured E_a's.

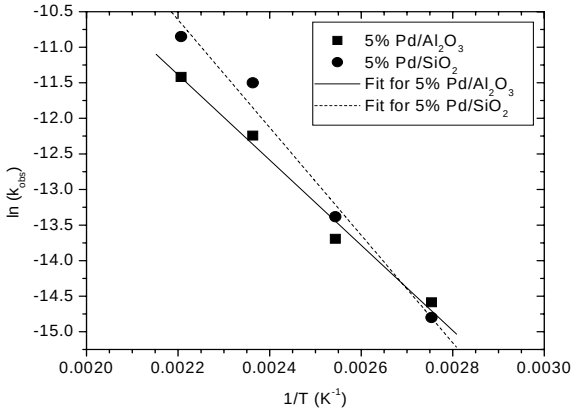

Figure 6.3. Arrhenius Plot for PS Hydrogenation.
(3 wt% PS-DHN, 800 psig H_2, 1 g catalyst/g PS, 2500 rpm).

6.3.3. Effect of Agitation Rate

At a reaction temperature of 150°C, a 5% $Pd/BaSO_4$ catalyst to polymer ratio of 1:1 (g:g) and agitation rates above 2000 rpm, gas-liquid mass transfer resistance was negligible in the hydrogenation of 3 wt% PS dissolved in DHN [19]. To ensure that an agitation rate of 2500 rpm was suitable for 5% Pd/Al_2O_3 and 5% Pd/SiO_2-catalyzed PS

hydrogenation at 150°C, the agitation rate was increased to 4000 rpm in 2-hour experiments. There was no change in the degree of hydrogenation (x_A=0.66 at 2 hours) with increased agitation rate, suggesting that gas-liquid mass transfer effects were negligible for 5% Pd/Al_2O_3-catalyzed PS hydrogenation at 2500 rpm. On the other hand, as shown in Figure 6.4, increasing the agitation rate above 2500 rpm resulted in the degree of hydrogenation decreasing for the 5% Pd/SiO_2-catalyzed reaction. These results were reproducible; however, the behavior is unexpected and warranted additional studies to determine if gas-liquid mass transfer resistance was significant.

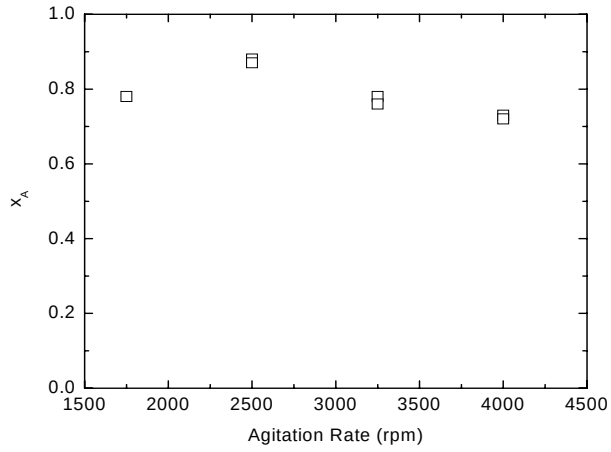

Figure 6.4. Effect of Agitation Rate on 5% Pd/SiO_2-Catalyzed PS Hydrogenation
(T=150°C, 3 wt% PS-DHN, 800 psig H_2, 1 g catalyst/g polymer)

6.3.4. Effect of Catalyst Concentration

The effect of varying catalyst concentration (from 0.5 g catalyst/g polymer to 2.5 g catalyst/g polymer) on PS hydrogenation kinetics was determined. Reaction temperature was maintained at 150^{o}C, hydrogen pressure was 800 psig, and the agitation rate was 2500 rpm. In order to discern whether gas-liquid mass transfer was a significant resistance for PS hydrogenation, initial observed rates of hydrogen consumption [$-r_{H2} = 3*(-r_A) = 3*k_{obs}C_{cat}C_A$] were plotted as a function of $C_{cat}*C_A$. The plot should be linear with a y-intercept of 0 if gas-liquid mass transfer resistances are not signficant. Liquid-solid and internal mass transfer resistances are encompassed in the observed rate constant, which should be related to the slope of the best-fit line. This analysis is similar to that which is conducted for a reaction in a catalyst particle that is first-order in H_2 concentration. The latter analysis has been described by other authors [20, 21]. The analysis for PS hydrogenation that is first-order in H_2 can be found in the Supplemental Information Section for comparison.

It was assumed that the rate of H_2 consumption was zero-order in H_2 concentration. This was based on the work of Xu et al. who demonstrated that the reaction was zero order in H_2 concentration at H_2 pressures greater than 500 psig [19]. To check the validity of this assumption for the present research, a series of experiments were run at a H_2 pressure of 1600 psig, 150^{o}C, 1 g catalyst/g PS. No changes in the aromatic ring conversion were observed from those obtained at 800 psig, 150^{o}C, so the zero-order in H_2 assumption is valid.

Figure 6.5 provides the results of plotting $-r_{H2}$ versus $C_{cat}*C_A$ for 5% Pd/Al_2O_3 and 5% Pd/SiO_2-catalyzed hydrogenations at 150°C. There is some scatter in the data. However, since the y-intercept of the best-fit line for the 5% Pd/SiO_2 is not zero, it is clear that there is some type of gas-liquid mass transfer resistance in 5% Pd/SiO_2-catalyzed PS hydrogenation. There does not appear to be any gas-liquid mass transfer resistance in 5% Pd/Al_2O_3-catalyzed PS hydrogenation since the data can be regressed through y=0 reasonably well. These results support the conclusion drawn from the agitation rate studies- external mass transfer resistance is not significant in 5% Pd/Al_2O_3-catalyzed PS hydrogenation, but it is significant in 5% Pd/SiO_2-catalyzed hydrogenation.

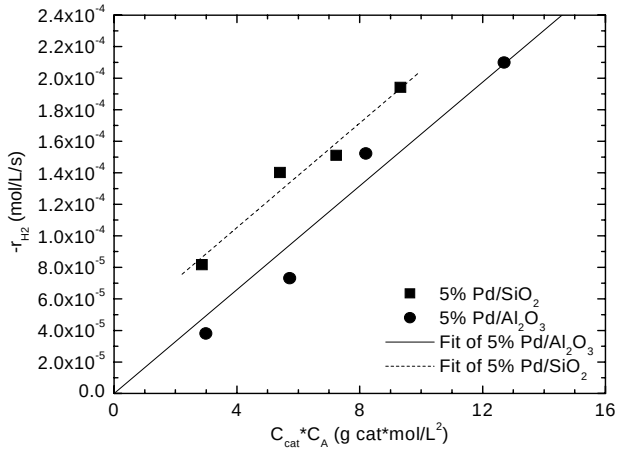

Figure 6.5. Effect of Catalyst Concentration on Pd-Catalyzed PS Hydrogenation
(T=150°C, 3 wt% PS-DHN, 800 psig H_2, 2500 rpm)

6.3.5. Molecular Weight Distribution

The molecular weight distributions were measured for the S-VCH copolymers formed at 150°C using 5% Pd/Al_2O_3 or 5% Pd/SiO_2. The slight broadening of the molecular weight distributions in Figure 6.6 illustrates the small amount of backbone scission that occurs as reaction time increases. The changes in the M_n's for the S-VCH created in this research are far less than what has been reported for nickel-catalyzed PS hydrogenation.

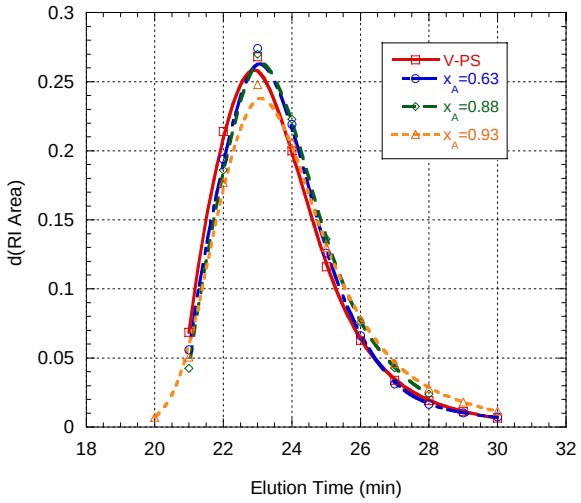

Figure 6.6. Gel Permeation Chromatograms of S-VCH from 5% Pd/SiO_2

Figures 6.7a and 6.7b show the concentrations of aromatic and cyclohexyl units in various fractions of a highly hydrogenated S-VCH (x_A>0.5). The lower molecular weight polymer, i.e., the polymer with longer elution time, is more hydrogenated than the high molecular weight polymer. For a 66% hydrogenated PS formed by 5% Pd/Al_2O_3-catalyzed hydrogenation, the cyclohexyl fraction increases from 0.2 as the molecular

weight of the polymer fraction decreases from about 500 kDa to about 10 kDa (Figure 6.7a). For a 5% Pd/SiO_2 polymer product with a similar overall degree of hydrogenation (x_A=0.63), the cyclohexyl fraction increases from about 0.4 to 0.9 as the molecular weight of the polymer fraction decreases from about 500 kDa to about 10 kDa. Because of the difference in the range of cyclohexyl fraction with similar overall x_A, these results indicate that the hydrogenation proceeds differently on the Al_2O_3 and SiO_2-supported catalysts. This topic will be further discussed in a later section of this paper.

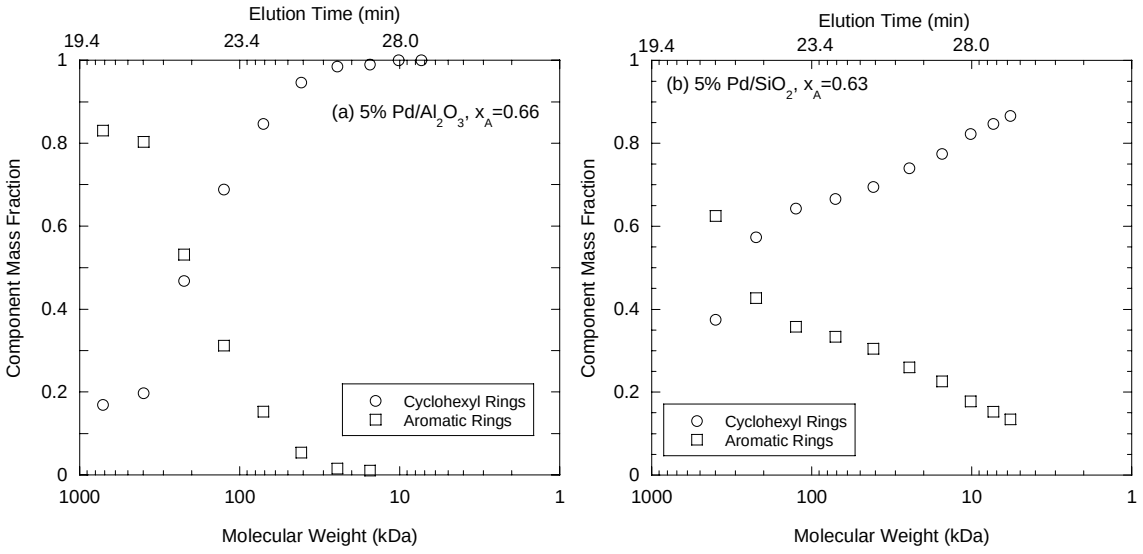

Figure 6.7. Deconvolution of GPC Distributions for (a) 5% Pd/Al_2O_3 Product, x_A=0.66 (b) 5% Pd/SiO_2 Product, x_A=0.63. Mobile Phase = THF.

As a check, the degrees of hydrogenation calculated from the areas under the GPC elution curves were compared to those obtained with UV analysis (with DHN as the solvent) conducted after the end of the reaction. They were found to be in good

agreement. For the examples shown, the x_A values obtained from the dilution of the polymer hydrogenation product-DHN solution yielded 0.66 for the 5% Pd/Al_2O_3 product and 0.63 for 5% Pd/SiO_2; the integration of the GPC results yielded comparable 0.70 and 0.65, respectively.

The aforementioned analyses were found to be applicable to S-VCH polymers with $x_A>0.5$; for $x_A<0.5$, the internal check of the x_A measured from GPC and UV did not equal one another. One possible explanation for this is that there is some randomness in the location of VCH units in S-VCH polymers with $x_A<0.5$ that distorts the GPC curves. It was found that a similar analysis that uses UV and light scattering (instead of RI) for deconvolution of copolymer composition did not work when there was random distribution of monomer units in the copolymer.

Nevertheless, these results provide confirmation that the lower molecular weight PS undergoes hydrogenation faster than their higher molecular weight counterparts. This may be due to the affinity of the low molecular weight polymer to adsorb onto the catalyst before the high molecular weight polymer. Kawaguchi et al.'s studies on the competitive adsorption of polystyrenes of different molecular weights onto porous SiO_2 [22] showed that the lower molecular weight polymer adsorbed before the higher molecular weight polymer. Burns and Carpenter found that more lower molecular weight PS adsorbed onto porous Al_2O_3 than high molecular weight polymer [23]. The lower adsorption value for the higher molecular weight polymer was attributed to the hindered diffusion that the larger polymer, i.e. the higher molecular weight sample, experiences

when it diffuses through a porous substrate. Consequentially, in this research, the polymer molecular weight distribution may affect polymer hydrogenation rates.

6.3.6. Catalyst Deactivation

At relatively short reaction times, PS hydrogenation at 150^{o}C was found to obey first-order kinetic behavior. As demonstrated in Figure 6.8, at longer reaction times, PS hydrogenation slowed appreciably and deviated from first-order behavior (solid lines). To demonstrate that a change in catalyst performance was occurring, PS was hydrogenated for a given time (2 hours for the 5% Pd/SiO_2-catalyzed reaction, 3.5 hours for the 5% Pd/Al_2O_3 reaction). The hydrogenated polymer solution was collected. A batch of fresh catalyst and the hydrogenated polymer solution were added to the clean reactor so that the catalyst to polymer ratio was 1:1 (by weight), and a second reaction was run at 150^{o}C. The results showed that the use of a fresh batch of catalyst in 2-step PS hydrogenations resulted in hydrogenation that matched or exceed what was predicted by the first-order model for each catalyst. These results suggest that there is a decrease in the concentration of active sites occurring at high aromatic ring conversions when a 1-step hydrogenation is used.

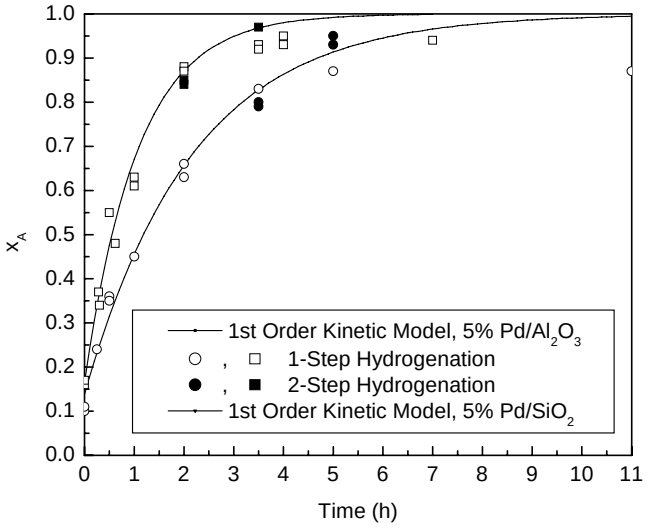

Figure 6.8. Effect of Fresh Catalyst on PS Hydrogenation
(T=150°C, 3 wt% PS-DHN, 800 psig H_2, 2500 rpm)

A simple model was used to describe the decrease in catalyst concentration that appeared to take place at longer reaction times in 1-step PS hydrogenation. Provided that the catalyst concentration decreased in a first order fashion, i.e., $\frac{dC_{cat}}{dt} = -k_d C_{cat}$, the expression for the disappearance of aromatic rings becomes

$$\frac{dC_A}{dt} = k'\left[C_{cat,0}\, exp(-k_d t)\right]C_A \qquad (6\text{-}4)$$

In Equation 6-4, k_d is the catalyst deactivation rate constant and $C_{cat,0}$ is the initial catalyst concentration. After substituting the aromatic ring concentration, Equation 6-4 was integrated to yield an expression in terms of the aromatic ring conversion x_A:

$$-\ln\left[\frac{1-x_A}{1-x_{A0}}\right] = \frac{k'}{k_d} C_{cat,0} \exp\left(-k_d t\right) \quad (6\text{-}5)$$

The model, which is represented by Equation 6-5, was then applied to all data for 5% Pd/Al_2O_3 and 5% Pd/SiO_2-catalyzed PS hydrogenation. The constants k' and k_d were determined by minimizing the sum of the square of the errors between the experimental and model values. As shown in Figure 6.9, the model reasonably fits the data. Furthermore, the rate constants for aromatic ring hydrogenation, which are provided in Table 6.2, are slightly higher than the values obtained in the analysis of the short-time region, which did not consider a decrease in catalyst concentration. The rate constant for 5% Pd/SiO_2 deactivation is roughly two times greater than the value for 5% Pd/Al_2O_3 deactivation rate constant, which is very similar to the difference in the observed rate constants for aromatic ring hydrogenation.

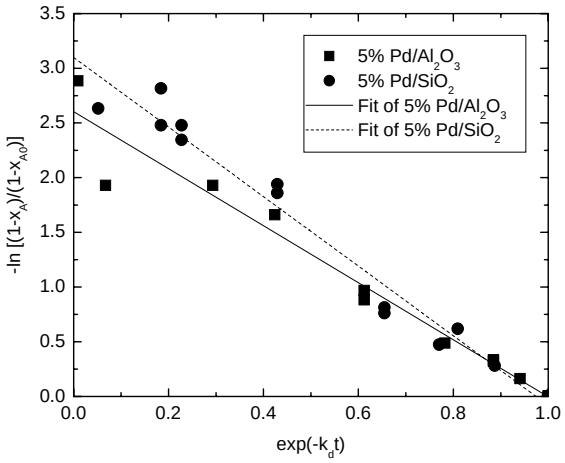

Figure 6.9. Model for Catalyst Deactivation. (T=150°C, 3 wt% PS-DHN, 800 psig H_2, 1 g catalyst/g PS, 2500 rpm)

Table 6.2. Model Parameters for Catalyst Deactivation During PS Hydrogenation

	k_{model} (L/g cat/s)	k_{obs} (L/g cat/s)	k_d (hr^{-1})
5% Pd/Al_2O_3	5.91 E-06	4.94 E-06	0.245
5% Pd/SiO_2	1.39 E-05	1.00 E-05	0.423

(T=150°C, 3 wt% PS-DHN, 800 psig H_2, 1 g catalyst/g PS, 2500 rpm)

The model mathematically describes the decrease in catalyst concentration, but it does not provide information on the physical mechanism. One potential source of the decreasing catalyst concentration is catalyst deactivation. Catalyst deactivation can be classified into three categories: chemical, mechanical, or thermal. Thermal deactivation is highly unlikely since the reaction temperature is far below what is typical for this route of deactivation. Chemical deactivation includes poisoning and changes of catalytic phases due to vapor-solid or solid-solid reaction. Catalyst poisoning, which occurs when reactants, products, or impurities strongly adsorb onto active sites, is a reasonable cause of the observed decrease in catalyst concentration since polymer molecules may be strongly and irreversibly adsorbing to catalytic sites. The occurrence of chemical deactivation by vapor-solid or solid-solid reaction is highly unlikely for PS hydrogenation in DHN. Mechanical causes of catalyst deactivation include fouling and attrition. Catalyst fouling is also a very likely scenario since the relatively large polymer coils can block active sites or pores.

To see if the decreases in catalyst concentration could be attributed to catalyst fouling, the BET surface areas of spent 5% Pd/Al_2O_3 and 5% Pd/SiO_2 catalysts were measured. As shown in Table 6.3, for samples outgassed at 115°C, which is below the polymers' decomposition temperatures, the BET surface areas were significantly less

than the value for the unused catalyst. Outgassing the spent catalysts at 300°C resulted in slight increases in the surface areas in both sets of catalysts. When outgassing was conducted at 300°C, residue was found on the wall of the sample tubes; the residue may be polymer degradation products. These results suggest that catalyst fouling by polymer blockage of pores is a reasonable hypothesis for the observed decreases in catalyst concentration.

Table 6.3. Characterization of Spent PS Hydrogenation Catalysts

Catalyst	Outgas Temp. (°C)	BET Surface Area (m^2/g)	Pore Volume (cm^3/g)
5% Pd/Al_2O_3, Unused	300	108	0.257
5% Pd/Al_2O_3, x_A=0.11	115	82, 80	0.21, 0.24
5% Pd/Al_2O_3, x_A=0.11	300	88	0.25
5% Pd/Al_2O_3, x_A=0.87	115	72, 86	0.30, 0.33
5% Pd/Al_2O_3, x_A=0.87	300	100	0.37
5% Pd/SiO_2, Unused	300	222	1.08
5% Pd/SiO_2, x_A=0.17	115	218, 211	1.36, 1.23
5% Pd/SiO_2, x_A=0.17	300	238	1.37
5% Pd/SiO_2, x_A=0.38	115	153	1.16
5% Pd/SiO_2, x_A=0.76	115	201, 182	1.27, 1.20
5% Pd/SiO_2, x_A=0.76	300	177, 190	1.08, 1.21

The observed decrease in active site concentration may also be influenced by the accessibility of catalytic sites in the interior of the catalyst particles to high molecular weight polymer. As indicated by the GPC results, the high molecular weight polymer is hydrogenated after the small molecular weight polymer. The higher molecular weight polymer may be precluded from the interiors of the 5% Pd/Al_2O_3 and 5% Pd/SiO_2

catalysts, thereby accessible catalyst concentration is reduced. Consequentially, an even further decrease in reaction rate may be observed.

6.3.7. Glass Transition Temperatures of S-VCH

The glass transition temperatures (T_g) of the S-VCH polymer products were determined from DSC measurements. As shown in Table 6.4, two T_g's exist in the moderately hydrogenated ($0.3<x_A<0.8$) S-VCH polymers formed in reactions where Al_2O_3 was the catalyst support. At low and extremely high ($x_A>0.8$) degrees of hydrogenation, only one T_g is present.

The existence of two T_g's in partially hydrogenated PS, which was confirmed by rheological measurements, is a novel feature of this research. It brings to light how polymer synthesis parameters, e.g., solvent and catalyst selection, may influence the properties of the copolymer products.

Two T_g's are indicative of polymer immiscibility. The immiscibility may be due to separate polymer chains, i.e., blends, or long polymer blocks that are insoluble with one another, e.g., block copolymers. Based on Sperling's comments on T_g behaviors in block copolymers [23], the existence of two T_g's and their inward shifts from the T_g's of the pure components (95-105^{o}C for PS, and 138-147^{o}C for PVCH) [1, 6, 7] are suggestive of styrene and VCH-rich phases. The topic of styrene and VCH-rich phases will be discussed in the next section.

Table 6.4. Glass Transition Temperatures for PS Hydrogenation Products

Catalyst Used	x_A	T_g (^oC)
5% Pd/Al_2O_3	0.24	103
	0.36	93, 126
	0.66	104, 129
	0.83	134
5% Pd/Al_2O_3(2.5)	0.99	128
5% Pd/SiO_2	0.37	95
	0.55	101
	0.63	103
	0.88	106
	0.93	122
5% Ru/Al_2O_3	0.38	103, 122
5% Pd/Al_2O_3-E	0.68	107, 122
5% Pd/Al_2O_3-S	0.18	103
65% Ni/SiO_2-Al_2O_3	0.99	139

All polymers were created in hydrogenations at 150^{o}C, 800 psig H_2, 3 wt% PS-DHN, 2500 rpm, 1 g catalyst/g polymer except for 5% Pd/Al_2O_3(2.5). The catalyst to polymer ratio was 2.5 g/g with all other reaction conditions the same.

Elias and Etter found two glass transitions in their 43 and 76% hydrogenated PS's. The lower T_g was around 75^{o}C while the higher T_g was approximately 100^{o}C. The authors attributed the higher T_g to PS sequences and the lower T_g to VCH sequences. The latter finding is supported by their measured T_g of 80^{o}C for fully hydrogenated PS (PVCH). These results- the presence of two T_g's and the T_g of PVCH- contrast with those reported by other researchers.

Abe and Hama [6] measured the T_g's of PS, fully hydrogenated PS, and three partially hydrogenated PS's (x_A ranging from 30 to 95%). The five partially hydrogenated PS's studied by Nakatani et al. were 10 to 92% hydrogenated [7]. Both

research groups reported a single T_g for each of their partially hydrogenated PS's. The contrast with the two T_g results obtained in the present research and to the work by the previous researchers may be attributed to the influence of catalyst and solvent on polymer product properties. Abe and Hama and Nakatani et al. used Ni catalysts and cyclohexane and methylcyclohexane, respectively, as the solvent in their hydrogenations. The present research was conducted with DHN and supported Pd catalysts.

Previous researchers have demonstrated that solvent selection affects polymer adsorption onto porous SiO_2 [22] and onto a metal substrate [26]. The adsorption affinity of a polymer onto a catalyst should affect hydrogenation mechanism, which in turn affects the reaction kinetics and the sequences of monomer units in the polymer product.

The influence of catalyst properties on the T_g of S-VCH with varying VCH content can further be seen by comparing the T_g results obtained for the polymers synthesized using the 5% Pd/SiO_2 catalyst to those made from the Al_2O_3-supported catalysts. Besides different reaction times, the only difference in the experimental parameters used to produce the data in Table 6.4 is the catalyst. For polymers with similar x_A's (x_A~0.65) made from three different catalysts, two T_g's were detected in the samples produced in hydrogenations with an Al_2O_3 support (5% Pd/Al_2O_3, x_A=0.66: 104^{o}C, 129^{o}C, 5% Pd/Al_2O_3-E, x_A=0.68: 107^{o}C, 122^{o}C). Only one T_g was observed in the sample generated from 5% Pd/SiO_2-containing reaction (5% Pd/SiO_2, x_A=0.63: 103^{o}C). The number of glass transitions in the 5% Pd/Al_2O_3, 5% Pd/SiO_2, and 5%

Ru/Al_2O_3 polymers with x_A~0.37 are the same as those that were found in the 65% hydrogenated polymers.

A single T_g was observed for each S-VCH polymer made in the 5% Pd/SiO_2-catalyzed reactions. For $x_A < 0.90$, the T_g's of the 5% Pd/SiO_2 products were comparable to the lower T_g values for the 5% Pd/Al_2O_3 products. At a high degree of hydrogenation (x_A=0.93), the T_g was far below the trends exhibited in previous reports [6, 7].

It is believed that the present T_g results demonstrate that metal crystallite size and polymer-catalyst support interactions influence the blocky polymer hydrogenation mechanism and thus the physical properties of the product polymer. The catalytic supports differ (Al_2O_3 versus SiO_2) and the average Pd crystallite sizes vary by roughly a factor of 4 (5.5 nm for 5% Pd/Al_2O_3 and 21 nm for 5% Pd/SiO_2). Theoretically, a larger metal crystallite size should result in blockier product polymers. However, metal-support interactions may play a role in the adsorption and reaction process and affect polymer blockiness.

For example, the reaction appears to proceed on Al_2O_3-supports in such a manner as to produce polymer chains that contain long blocks of hydrogenated polymer and long blocks of aromatic units. Phase separation, as observed in block copolymers produced by traditional methods, results in the presence of two T_g's. In the case of 5% Pd/SiO_2-catalyzed PS hydrogenation, the reaction proceeds in a more random fashion in which the saturated blocks of polymer are not as long as those produced when an Al_2O_3 support is used. Therefore, the chains are more miscible with one another, and one T_g is observed.

These results further support the hypothesis, which was first mentioned in the molecular weight distribution analysis section, that there is a difference in Pd/Al_2O_3- and Pd/SiO_2-catalyzed PS hydrogenation mechanisms.

6.3.8. Separation of S-VCH Polymers and Analysis

The S-VCH polymers from 5% Pd/Al_2O_3 and 5% Pd/SiO_2-catalyzed hydrogenations were separated into hexane-soluble and hexane-insoluble polymers as described in Section 6.2.7. Approximately 10 percent of the polymer was lost in the separation process. Figure 6.10 shows that the mass fractions of hexane-soluble polymers created using 5% Pd/Al_2O_3 and 5% Pd/SiO_2 increased with the overall degrees of hydrogenation. This behavior is reasonable since more VCH, which is hexane-soluble, is formed as the overall x_A increases. Furthermore, there is not much difference in the hexane-soluble polymers created from the two catalysts.

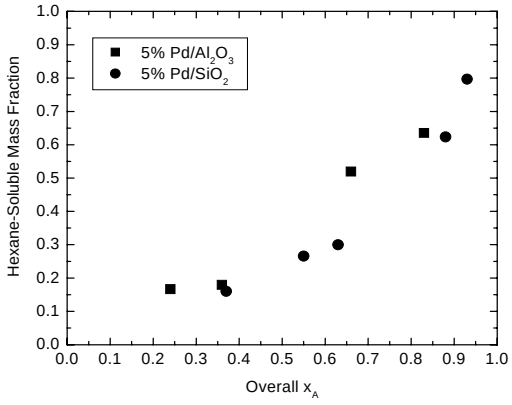

Figure 6.10. Hexane-Soluble Mass Fractions of S-VCH

The degrees of hydrogenation of the separated polymers were measured using UV-VIS spectroscopy. As shown in the second column of Table 6.5, the hexane-soluble polymer had high degrees of hydrogenation ($x_A \geq 0.85$). The x_A increased slightly with the overall degree of hydrogenation for the products from the 5% Pd/Al_2O_3-catalyzed reactions. The changes in x_A for the hexane-soluble S-VCH formed from the 5% Pd/SiO_2 catalyst are within experimental error, so the change is insignificant. The high degrees of hydrogenation associated with the alkane-soluble portions of polymer hydrogenation products are in good agreement with the polybutadiene hydrogenation studies conducted by Rosedale and Bates [9] and Cassano et al. [8]. These researchers observed two types of polymer chains in their hydrogenation products- a highly saturated polymer that was nearly 90% hydrogenated and the polybutadiene. The present results are also similar to the results obtained by Xu [16], whose hexane-soluble PS hydrogenation products had an average x_A of 0.80. The high aromatic ring conversions associated with the hexane-soluble portions and the increasing fraction of hexane soluble polymer (Figure 6.10) support the blocky polymer hydrogenation mechanism proposed by Rosedale and Bates.

The Tg's of the hexane-soluble polymers were measured using DSC. As shown in the third column of Table 6.5, with the exception of 5% Pd/Al_2O_3, $x_A=0.24$, only one T_g was observed in each of the extracted polymers. The presence of two T_g's in 5% Pd/Al_2O_3, $x_A=0.24$ may represent some point before the transition from long styrene sequences to long VCH sequences; the magnitude of change in the heat flow associated with the polymer transitioning from glassy to rubber state is proportional to the fraction

of polymer that possesses that T_g. In 5% Pd/Al_2O_3, x_A=0.24, the change in heat flow with the T_g at 104°C is much larger than the change observed at the T_g of 122°C.

Table 6.5. Properties of Extracted PS Hydrogenation Products

Catalyst Used	Overall x_A	x_A, Hexane Soluble	T_g, Hexane-Soluble (°C)
5% Pd/Al_2O_3	0.24	0.85	104, 122
	0.36	0.91	122
	0.66	0.93	122
	0.83	0.95	131
5% Pd/SiO_2	0.37	0.88	---
	0.63	0.90	122
	0.88	0.92	122
	0.93	0.88	127

The T_g's of the hexane-soluble polymers produced from the Al_2O_3-supported Pd catalyst are similar to the upper T_g's that was measured in the original polymer products (Table 6.4). In the original polymer, the PVCH-rich chains, which are hexane-soluble, and PS-rich chains may be miscible with one another. As a result, the T_g's may be a function of their miscibility.

6.4. Conclusions

Styrene-vinylcyclohexane copolymers can be synthesized through partial PS hydrogenation. Reaction parameters such as catalyst composition, temperature, and catalyst concentration influenced PS hydrogenation kinetics. The temperature

dependence of the observed rate of hydrogenation, as denoted by k_{obs}, obeyed Arrhenius behavior. The apparent activation energies of hydrogenation, which were 49.9 kJ/mol for 5% Pd/Al_2O_3 and 61.1 kJ/mol for 5% Pd/SiO_2, indicated that external mass transfer was not a controlling factor in PS hydrogenation. However, studies on the effects of agitation rate and catalyst concentration on the kinetics were suggestive of some external mass transfer influencing 5% Pd/SiO_2-catalyzed PS hydrogenation at 150^oC.

Polystyrene hydrogenation was found to deviate from first-order kinetic behavior at high aromatic ring conversions. The deviation was attributed to a decrease in catalyst concentration. It is believed that the decrease is primarily associated with polymer blockage of active sites and/or pores of the catalysts, as illustrated by the spent catalysts having lower surface areas than their unused counterparts.

Polystyrene hydrogenation is believed to occur in a blocky mechanism where the different interactions of 5% Pd/Al_2O_3 and 5% Pd/SiO_2 dictate the sequence lengths of hydrogenated and unhydrogenated units in the product polymer. As a result, the S-VCH polymers formed from these two catalysts exhibit different physical properties. The S-VCH polymers with moderate VCH contents that were produced using 5% Pd/Al_2O_3 possess two T_g's, which are indicative of immiscibility in the polymer chains. Contrastingly, the polymers formed when 5% Pd/SiO_2 is the catalyst have a single T_g. Polymers with a similar overall degree of hydrogenation that were formed from either Pd catalyst had very different distributions of aromatic and cyclohexyl portions at given elution times, i.e., molecular weights.

6.5. Acknowledgements

The authors would like to thank the Khan Research Group of the Department of Chemical and Biomolecular Engineering at North Carolina State University for the use of their DSC, TGA, and rheometer; the Genzer Research Group for the use of their GPC. This research was supported by Contract W911NF-04-D-0003 from the United States Army Research Office, Research Triangle Park, NC. Partial support was also provided by the STC Program of the National Science Foundation under Agreement No. CHE-9876674.

References

[1] D.A. Hucul, Hahn, S. F., Advanced Materials 12 (2000) 1855-1858.

[2] A. Iio, Yoshinari, M., Komiya, Z., Goto, K., Japan Synthetic Rubber Co., LTD., EP 317263, 1988.

[3] V. Wege, Bruder, F., Douzinas, K., Chen, Y., Bayer AG, DE 19921941, 2000.

[4] H.-G. Elias, Etter, O., J. Macromol. Sci., Part A 5 (1967) 943-953.

[5] M.D. Gehlsen, Bates, F. S., Macromolecules 26 (1993) 4122-4127.

[6] A. Abe, Hama, T., Polymer Letters 7 (1969) 427-435.

[7] H. Nakatani, Nitta, K-h., Soga, K., Polymer 39 (1998) 4273-4278.

[8] G.A. Cassano, Valles, E. M., Quinzani, L. M., Polymer 39 (1998) 5573-5577.

[9] J.H. Rosedale, Bates, F. S., Journal of the American Chemical Society 110 (1988) 3542-3545.

[10] G. Schulz, Worsfold, D. J., Polymer Communications 25 (1984) 206-207.

[11] J.S. Ness, Brodil, J. C., Bates, F. S., Hahn, S. F., Hucul, D. A., Hillmyer, M. A., Macromolecules 35 (2002) 602-609.

[12] L.B. Dong, McVicker, G. B., Roberts, G. W., Kiserow, D. J., In Preparation (2010).

[13] H.E. Adams, Separation Science and Technology 6 (1971) 259-273.

[14] Z. Fodor, Fodor, A., Kennedy, J. P., Polymer Bulleting 29 (1992) 689-696.

[15] S.D. Kim, Suwanmala, P., Klein, A., Sperling, L. H., Journal of Materials Science 2001 (2001) 2787-2793.

[16] D. Xu, PhD thesis, Department of Chemical and Biomolecular Engineering, North Carolina State University, Raleigh, 2005.

[17] M.D. Gehlsen, Weimann, P. A., Bates, F. S., Harville, S., Mays, J. W., Wignall, G. D., Journal of Applied Polymer Science, Part B: Polymer Physics 33 (1995) 1527-1536.

[18] R. J. Madon, Boudart, M., Ind. Eng. Chem. Fund. 21 (1982) 438-447.

[19] D. Xu, Carbonell, R. G., Kiserow, D. J., Roberts, G. W., Ind. Eng. Chem. Res. 42 (2003) 3509-3515.

[20] R.V. Chaudhari, Ramachandran, P. A., AIChE J. 26 (1980) 177-201.

[21] H.S. Fogler, Elements of Chemical Reaction Engineering, 4th Edition, Prentice Hall PTR, Upper Saddle River, NJ, 1999.

[22] M. Kawaguchi, Anada, S., Nishikawa, K., Kurata, N., Macromolecules 25 (1992) 1588-1593.

[23] H. Burns Jr., Carpenter, D. K., Macromolecules 1 (1968) 384-390.

[24] L.H. Sperling, Introduction to Physical Polymer Science, 4th ed., Wiley-Interscience, Hoboken, NJ, 2006.

[25] H.-G. Elias, in: J. Brandrup, Immergut, E. H., Grulke, E. A. (Ed.), Polymer Handbook, 4th ed., John Wiley & Sons, Hoboken, NJ, 1999, pp. 291-326.

[26] M. Kawaguchi, Hayakawa, K., Takahashi, A., Macromolecules 16 (1983) 631-635.

Supplemental Information

In the catalyst particle, the reaction of H_2 can be described as

$$-R_{H2} = \eta C_{cat} k_{H2} C_S \quad \text{(6-S-1)}$$

In Equation 6-S-1, η is the effectiveness factor, C_{cat} is the catalyst concentration, k_{H2} is the rate constant for H_2 consumption, and C_S is the H_2 concentration at the surface of the catalyst particle. The mass transfer of H_2 from the gas to liquid phase can be described by

$$-\boldsymbol{R_{H2}} = \boldsymbol{k_S A}\left(\boldsymbol{C_g} - \boldsymbol{C_b}\right) \qquad \text{(6-S-2)}$$

In Equation 6-S-2, k_S is the mass transfer coefficient for H_2 absorption, A is the bubble surface area, C_g is the H_2 concentration at the gas-liquid interface, and C_b is the bulk H_2 concentration. The rate of H_2 transfer through the bulk solution to the catalyst is

$$-\boldsymbol{R_{H2}} = \boldsymbol{k_{LS} a_p C_{cat}}\left(\boldsymbol{C_b} - \boldsymbol{C_s}\right) \text{ (6-S-3)}$$

where k_{LS} is the liquid-solid mass transfer coefficient and a_p is the external surface area of the catalyst. Equations 6-S-1 through 6-S-3 are added together and rearranged to the form:

$$\frac{-\boldsymbol{1}}{\boldsymbol{R_{H2}}} = \frac{\boldsymbol{1}}{\boldsymbol{k_S A C_g}} + \frac{\boldsymbol{1}}{\boldsymbol{C_g}}\left[\frac{\boldsymbol{1}}{\boldsymbol{k_{LS} a_p}} + \frac{\boldsymbol{1}}{\eta \boldsymbol{k'}}\right]\frac{\boldsymbol{1}}{\boldsymbol{C_{cat}}} \qquad \text{(6-S-4)}$$

A plot of $-1/R_{H2}$ versus $1/C_{cat}$ should be linear with a y-intercept of $\frac{1}{k_s A C_g}$. If this term is small compared to the second term on the right-hand side of Equation 6-S-4, the plot will appear to go through the origin. If the data presented in Section 6.3.4 is analyzed

using Equation 6-S-4, similar results to what was described in the main text of this article are reached- there is gas-liquid mass transfer resistance. This is shown in Figure 6-S-1.

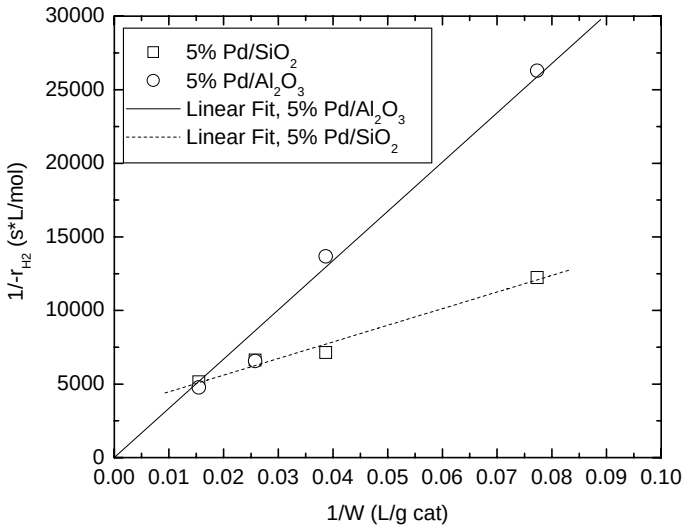

Figure 6-S-1. Analysis of Mass Transfer Resistances in PS Hydrogenation
(T=150^{o}C, 3 wt% PS-DHN, 800 psig H_2, 2500 rpm)

CHAPTER 7 :

CONCLUSIONS AND RECOMMENDATIONS

7.1. Conclusions

Polystyrene (PS) hydrogenation using various heterogeneous catalysts creates polymers with improved thermal and oxidative stability, higher glass transition temperature (T_g), and attractive optical properties. The large size of the polymer molecules imposes mass transfer limitations on heterogeneously-catalyzed polymer hydrogenation. Conducting the hydrogenation in a carbon dioxide (CO_2)-expanded solvent can reduce mass transfer limitations by lowering polymer solution viscosity and increasing polymer diffusivity.

The effect of CO_2 on the diffusion coefficient of a monodisperse, 308 kDa PS in decahydronaphthalene (DHN) was quantified at several temperatures and CO_2 concentrations. High pressure dynamic light scattering revealed that at a system pressure of 20.7 MPa, the infinite dilution diffusion coefficient of PS increased by a factor of 2.5 when CO_2 concentration was increased from 0 to 44 mol%. Solvent quality, as indicated by the dynamic second virial coefficient k_D, decreased at higher CO_2 concentrations. The hydrodynamic radius, R_H, of PS was not very sensitive to changes in CO_2 concentration.

Relatively high degrees of hydrogenation can be reached when mesoporous 5% Pd/Al_2O_3 or 5% Pd/SiO_2 is used as the catalyst for PS hydrogenation in neat DHN. The 5% Pd/SiO_2 is twice as active for PS hydrogenation as 5% Pd/Al_2O_3. However, the

palladium catalysts were not suitable for carrying out the same reaction in CO_2-expanded DHN because catalyst deactivation occurred and PS hydrogenation ceased. This deactivation occurs because of carbon monoxide (CO) poisoning of active Pd sites. The CO, which is formed from the reaction of CO_2 and H_2 in the reverse water-gas shift reaction, was detected in the gas phase at the end of the reactions.

In order to take advantage of the benefits on transport properties that are associated with a CO_2-expanded solvent, CO levels needed to be reduced. To accomplish this, a methanation catalyst was introduced into the reaction system. The use of a physical mixture of a hydrogenation catalyst (5% Pd/Al_2O_3 or 5% Pd/SiO_2) with a methanation catalyst (65% Ni/SiO_2-Al_2O_3 or 5% Ru/Al_2O_3) was effective in reducing CO levels but did not significantly improve PS hydrogenation. However, the use of a bimetallic catalyst, in which the hydrogenation metal and the methanation metal are located on the same support, e.g., $Pd/Ru/SiO_2$, reduced CO levels beyond detection limits, and PS hydrogenation levels in CO_2-DHN were comparable to the values obtained in neat DHN.

The rate of PS hydrogenation was found to be dependent on polymer molecular weight, with low molecular weight polymer being apparently more reactive than high molecular weight polymer. These observations were based on gel permeation chromatography (GPC) data of commercial grade PS hydrogenation products and on the kinetic data obtained for hydrogenation of a series of monodisperse PS's. For example, the hydrogenation rate of 24 kDa PS is nearly two orders of magnitude larger than the

rate for 160 kDa PS. The effect of polymer molecular weight is attributed to changes in the size of the polymer coil relative to the size of the catalyst pore, typically designated as λ. As the polymer size approaches that of the catalyst pore (λ ca. 0.70), polymer diffusivity significantly decreases. This behavior of the polymer diffusivity is very similar to that of the reaction rate.

While liquid-solid mass transfer resistances were not a controlling factor in this research, calculations show that internal mass transfer (pore diffusion) resistances significantly influence the kinetics of PS hydrogenation. Increases in the Weisz modulus are associated with increases in polymer molecular weight for the reaction in neat DHN. However, the addition of CO_2 resulted in decreases in the Weisz modulus, indicating that the presence of CO_2 reduced the internal mass transfer resistance. The increase in CO_2 concentration results in polymer-solvent interactions becoming less favorable. Consequentially, the polymer coils are smaller and are able to diffuse faster inside the catalyst pores. This has a positive impact on the observed hydrogenation rates.

The T_g's of partially hydrogenated PS's were measured. Moderately hydrogenated polymers from catalysts in which Al_2O_3 was the support possessed two T_g's. In contrast, only one T_g was observed in polymers with similar degrees of hydrogenation that were made from catalysts in which SiO_2 was the support. It is believed polymer-support and polymer-active metal interactions influence the sequence lengths of the saturated and unsaturated units in the polymer products.

The partially hydrogenated polymers were subjected to hexane extractions. The degrees of hydrogenation and T_g's of the hexane-soluble fractions were measured. The hexane-soluble polymers were found to be a minimum of 85% hydrogenated, which is similar to the results obtained in the analyses of polybutadiene hydrogenation products. The T_g's were found to be characteristic of VCH-rich chains since the values were higher than that of neat PS.

7.2. Recommendations

In order to reduce or eliminate internal mass transfer resistances in heterogeneous PS hydrogenation, macroporous catalysts should be used. Since there is a trade-off between metal loading and surface area/pore size of catalysts, an optimum balance of these two parameters should be found. Also, for reactions in a CO_2-expanded liquid, the effect of methanation metal concentration on PS hydrogenation should be determined for bimetallic catalysts.

Further characterization of product polymers is needed. This would provide a deeper understanding of the physical properties and how catalyst properties affect the polymers. The effect of catalyst on the T_g of partially hydrogenated PS should be further investigated. The sequence length distributions of unsaturated and saturated units should be measured; they would provide more definitive insight on the differences observed in the physical properties of the polymers made under different reaction conditions.

APPENDICES

APPENDIX A: REVERSE WATER-GAS SHIFT REACTION STUDIES

A.1. Introduction

The reverse water-gas shift (RWGS) reaction, which is shown in Equation A-1, generates carbon monoxide (CO), a known catalyst poison.

$$CO_2 + H_2 \leftrightarrow CO + H_2O \qquad \text{(A-1)}$$

The formation of CO via the RWGS reaction in hydrogenations containing dense phase CO_2 has been documented. For studies in a batch reactor, CO poisoning of active sites results in the cessation of the desired reaction [1-3], which in this research, is the hydrogenation of the aromatic rings of polystyrene (PS).

Palladium and platinum catalysts have been found to be suitable for accomplishing PS hydrogenation in a neat organic solvent [4-9]. However, when a carbon dioxide (CO_2)-expanded solvent is used, CO is generated via the RWGS reaction. One way to negate the effect of CO is to introduce a small amount of methanation catalyst to the reaction mixture. The methanation catalyst is used to convert CO to methane (CH_4) via the reaction shown in Equation A-2.

$$CO + 3H_2 \leftrightarrow CH_4 + H_2O \qquad \text{(A-2)}$$

This research explored the RWGS activity of supported palladium, ruthenium, palladium/ruthenium, and platinum/ruthenium catalysts at ambient pressure. The gas

phase was analyzed using mass spectrometry and provides information on the species that are produced when a mixture of CO_2 and H_2 are passed over the various catalysts.

A.2. Experimental

Commercially available 5% Pd/SiO_2 (Strem Chemicals, Newburyport, MA) and 5% Ru/Al_2O_3 (Sigma-Aldrich, Milwaukee, WI) catalysts were used as received. A homemade 1.6% Ru/4.2% Pd/SiO_2 catalyst and donated 5% Pd/5% Ru/SiO_2 and 5% Pt/5% Ru/SiO_2 (BASF Catalysts, LLC) were also the subjects of the study.

An Autosorb 1-C (Quantachrome Instruments, Boynton Beach, FL) was used to study the RWGS reaction. A 80:20 (mole basis) CO_2:H_2 mixture (Research Grade, Airgas National Welders, Charlotte, NC) was passed over 0.5 grams of catalyst that was loaded in the chemisorption cell. The cell was flushed with helium (Research Grade, Airgas National Welders, Charlotte, NC) for at least 15 minutes. The cell was heated to an average temperature of 150^{o}C under helium flow. The input gas was then changed to the CO_2:H_2 mixture. The outlet gas from the reactor was analyzed as a function of time. Table A-1 provides the fragments that were monitored using the mass spectrometer and their corresponding mass-to-charge ratios (m/e^-).

Table A-1. Mass Spectrometer Mass-to-Charge Ratios

m/e^-	Component	m/e^-	Component	m/e^-	Component
2	Hydrogen	15	CH_3*	28	CO, CO*
4	Helium	18	Water	44	CO_2
16	CH_4 or O				

It was not possible to differentiate between CO_2 and CO because CO_2 breaks into the same units as CO (m/e^-=16, m/e^-=28). Since m/e^- could be CH_4 or an oxygen fragment, CH_4 formation is observed at m/e^-=15.

A.3. Results and Discussion

Figures A-1 and A-2 show the results of passing the CO_2:H_2 mixture over the monometallic catalysts. The first dotted line in each figure represents the changeover from helium to the CO_2:H_2 mixture. The gas concentrations take a few minutes to stabilize. The profiles for the reaction over 5% Pd/SiO_2 (Figure A-1) do not contain any unexpected information. One thing to note is water (H_2O, m/e^-=18) evolvution for nearly an hour after the switchover to CO_2:H_2. No CH_4 formation is noted since the m/e^-=15 signal is very small (on the order of magnitude of 10^{-12} A) and constant.

As shown in Figure A-2, the data for reaction using 5% Ru/Al_2O_3 catalyst shows that CH_4 is formed after 15 minutes of CO_2:H_2 flow. This result is reasonable since ruthenium is a known methanation catalyst. Methane formation appears to be very sensitive to temperature. As noted by their oscillatory behavior, H_2O generation and H_2 flow are also sensitive to temperature and appear to be related to CH_4 generation. The large drops and increases in the ion current signal are associated with the acquisition software crashing.

The results of passing CO_2:H_2 mixtures over bimetallic catalysts are presented in Figures A-3 through A-5. The homemade 2% Ru/5% Pd/SiO_2 catalyst does not generate

CH_4 (Figure A-3). While this result supports the analyses of the gas collected from the reactor at the end of the experiments, it is a bit surprising because this catalyst is effective in hydrogenating PS in CO_2-DHN and the proposed mechanism of CO removal/improved PS hydrogenation is methanation of the catalyst poisoning by ruthenium. A scan of m/e^-'s ranging from 2 to 50 did not reveal the presence of any unexpected species. One possibility is that the generated CH_4 is in such low concentration that it is undetectable.

The behavior of the gas mixture over 5% Pd/5% Ru/SiO_2 (Figure A-4) and 5% Pd/5% Ru/SiO_2 (Figure A-5) is different from that of the homemade catalyst. Both of the commercial bimetallic catalysts generate CH_4 after 15 minute of CO_2:H_2 flow. The oscillation of water generation and H_2 flow with temperature are also visible; they also have an induction period. One unique feature is the drop in the H_2O signal after approximately two hours of CO_2:H_2 flow. There are also related decreases in the H_2 and CH_4 signals and are indicative of a change in activity of the catalyst. One possible reason for the induction period and the decrease in ion current is that the catalysts were used as received for these experiments. The catalysts may not have been fully reduced and therefore their performance was affected.

To test this theory, a corollary experiment was run. The 5% Pt/5% Ru/SiO_2 catalyst was subjected to the typical chemisorption pretreatment procedure. Helium was passed over the catalyst for 30 minutes at 120^{o}C, and the sample was evacuated for 30 minutes. After the sample was heated to 327^{o}C, H_2 was then passed over the catalyst for 2 hours. The sample was cooled to 150^{o}C, and the gas was then switched to CO_2:H_2, and

data were collected. As shown in Figure A-6, there is no induction period, and there is no drop in the H_2O and CH_4 signals after two hours of CO_2:H_2 flow. The catalyst does not appear to deactivate when H_2 reduction step is implemented, which contrasts with the case when the catalyst is used as received.

A.4. Conclusions

The reverse water gas shift reaction was studied by passing a mixture of CO_2:H_2 over a bed of catalyst. When the 5% Pd/SiO_2 or 2% Ru/5% Pd/SiO_2 catalyst was used, no CH_4 formation was observed. However, when 5% Ru/Al_2O_3, 5% Pd/5% Ru/SiO_2 or 5% Pt/5% Ru/SiO_2 was used as the catalyst, CH_4 was produced after a 15 minute induction period. There appeared to be a change in the activity of the 5%-5% bimetallic catalysts after two hours of exposure to CO_2:H_2. A subsequent experiment showed that reduced catalyst behaves differently than an as-received catalyst in the RWGS reaction. If possible, a reduction step should be implemented in the typical reaction procedure to obtain more efficient catalytic activity.

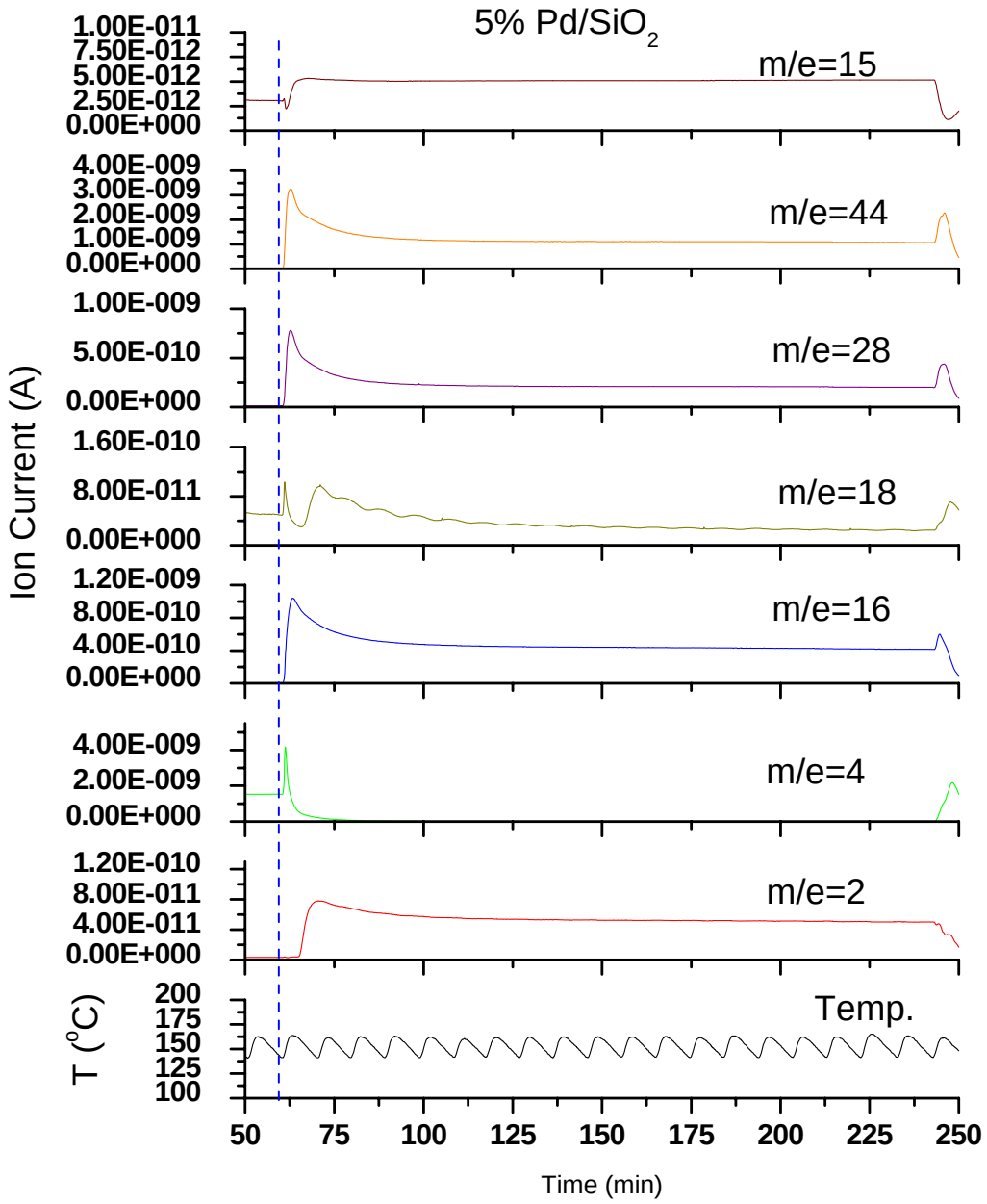

Figure A-1. Mass Spectrometer Response for RWGS Reaction over 5% Pd/SiO_2 ($T=150^{o}C$)

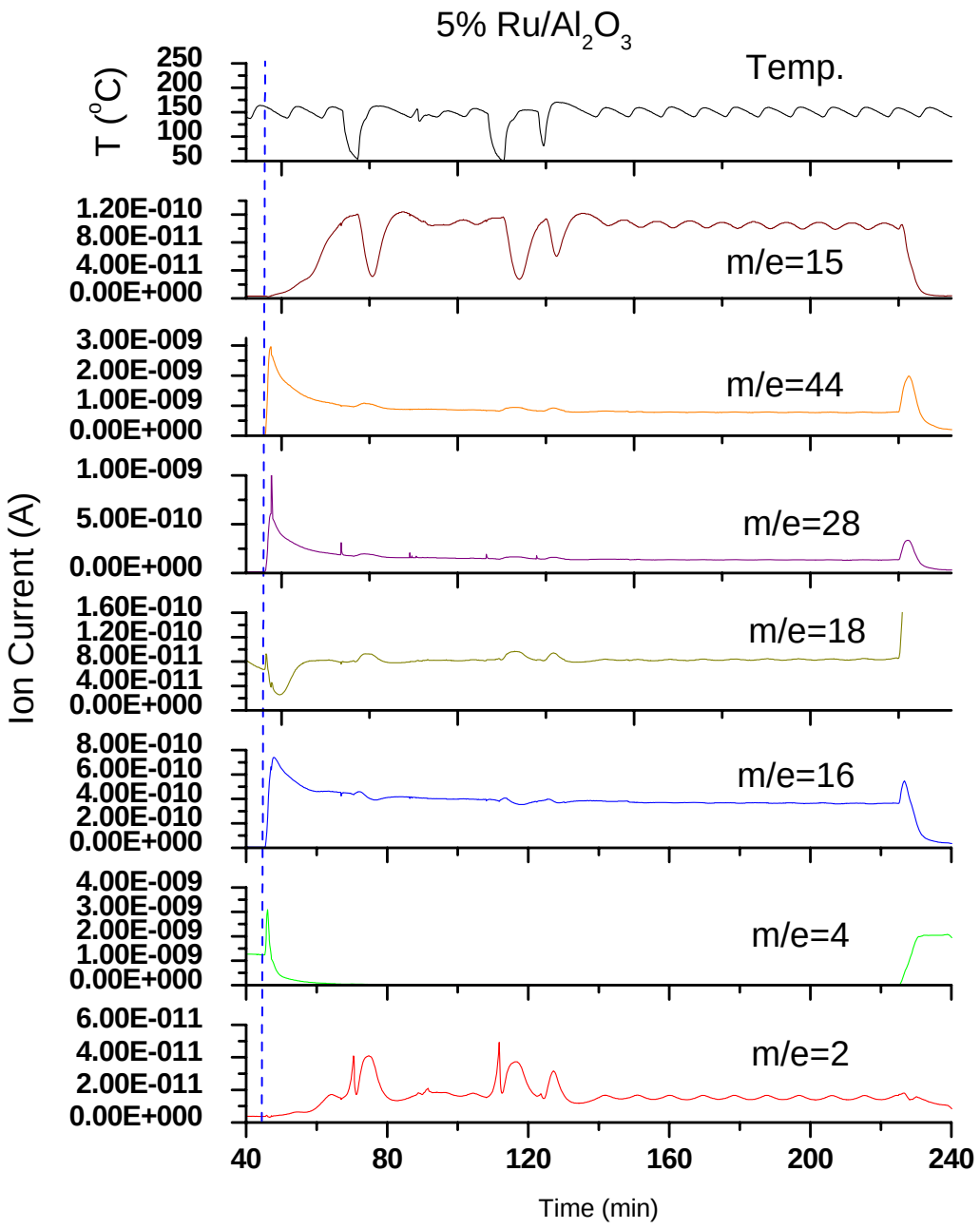

Figure A-2. Mass Spectrometer Response for RWGS Reaction over 5% Ru/Al_2O_3 (T=150°C)

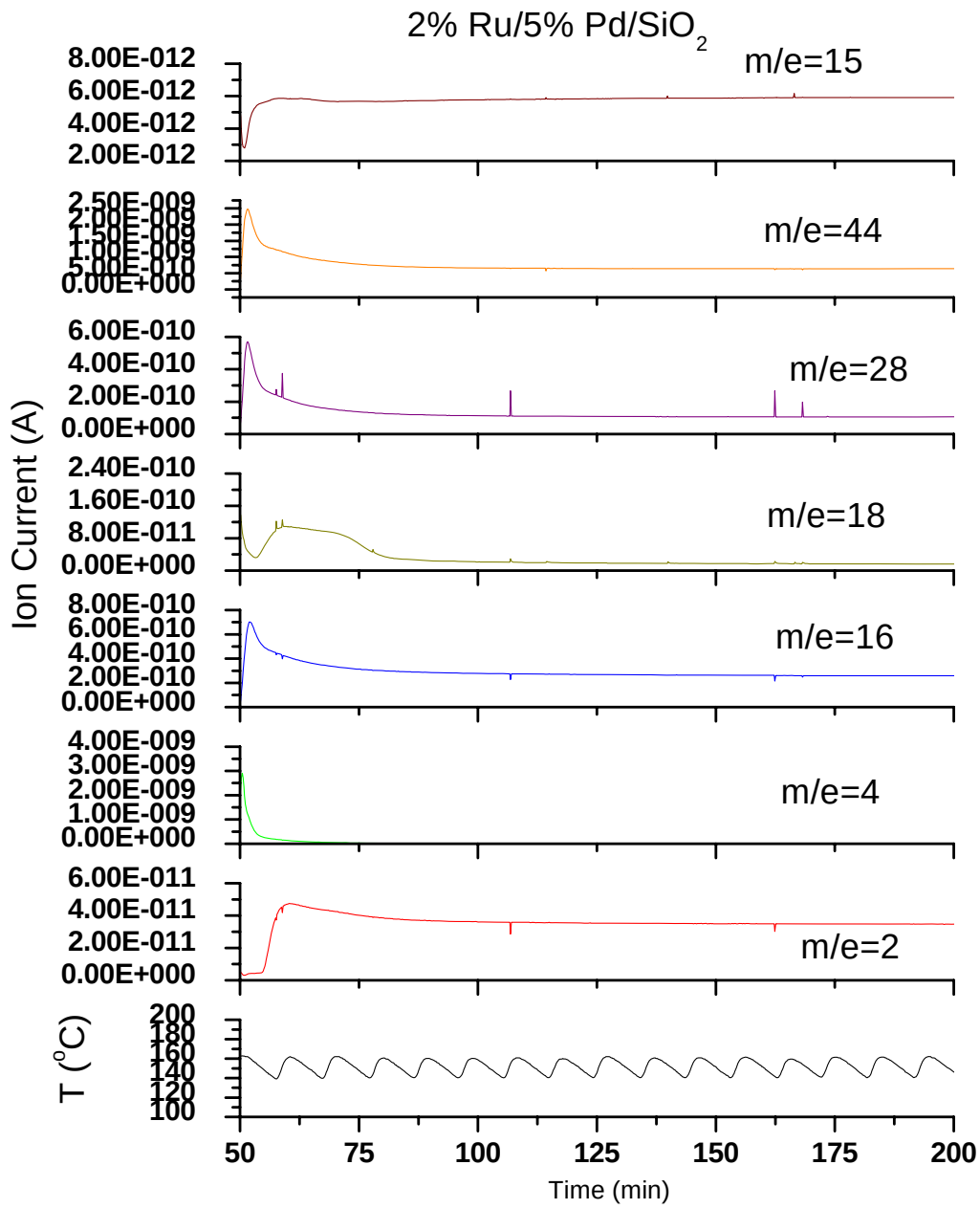

Figure A-3. Mass Spectrometer Response for RWGS Reaction over 2% Ru/5% Pd/SiO_2 (T=150°C)

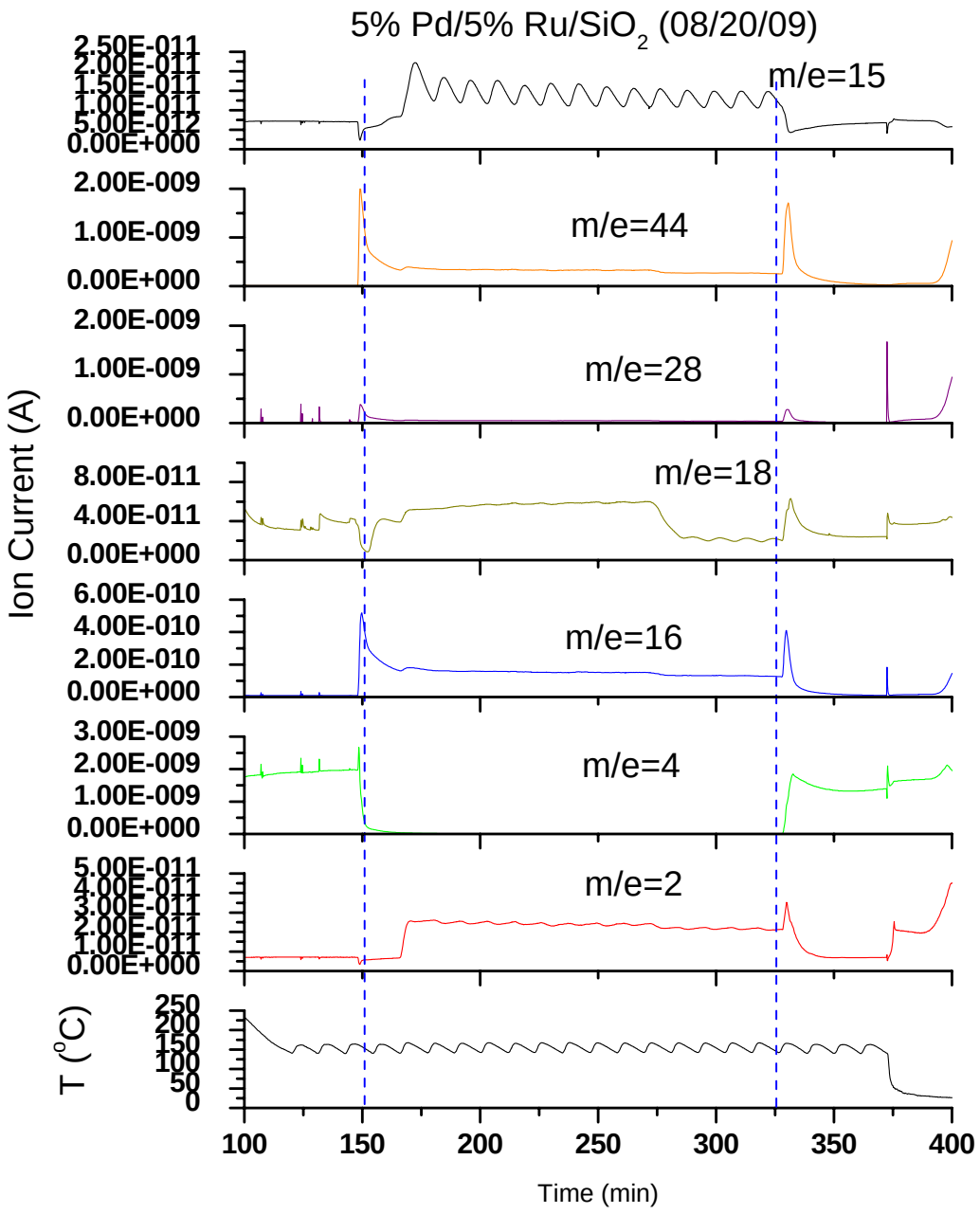

Figure A-4. Mass Spectrometer Response for RWGS Reaction over 5% Pd/5% Ru/SiO_2 (T=150°C)

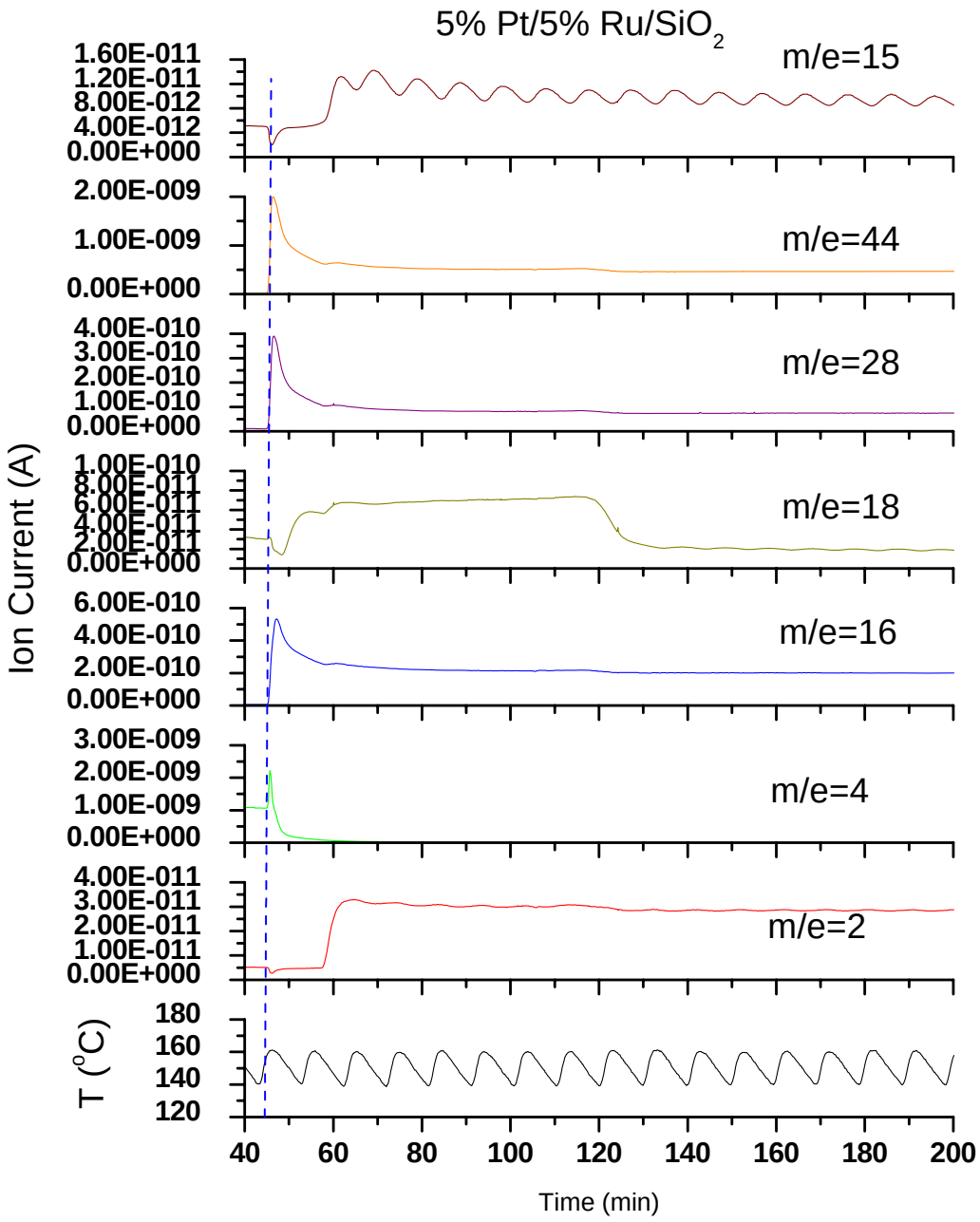

Figure A-5. Mass Spectrometer Response for RWGS Reaction over 5% Pt/5% Ru/SiO_2 (T=150°C)

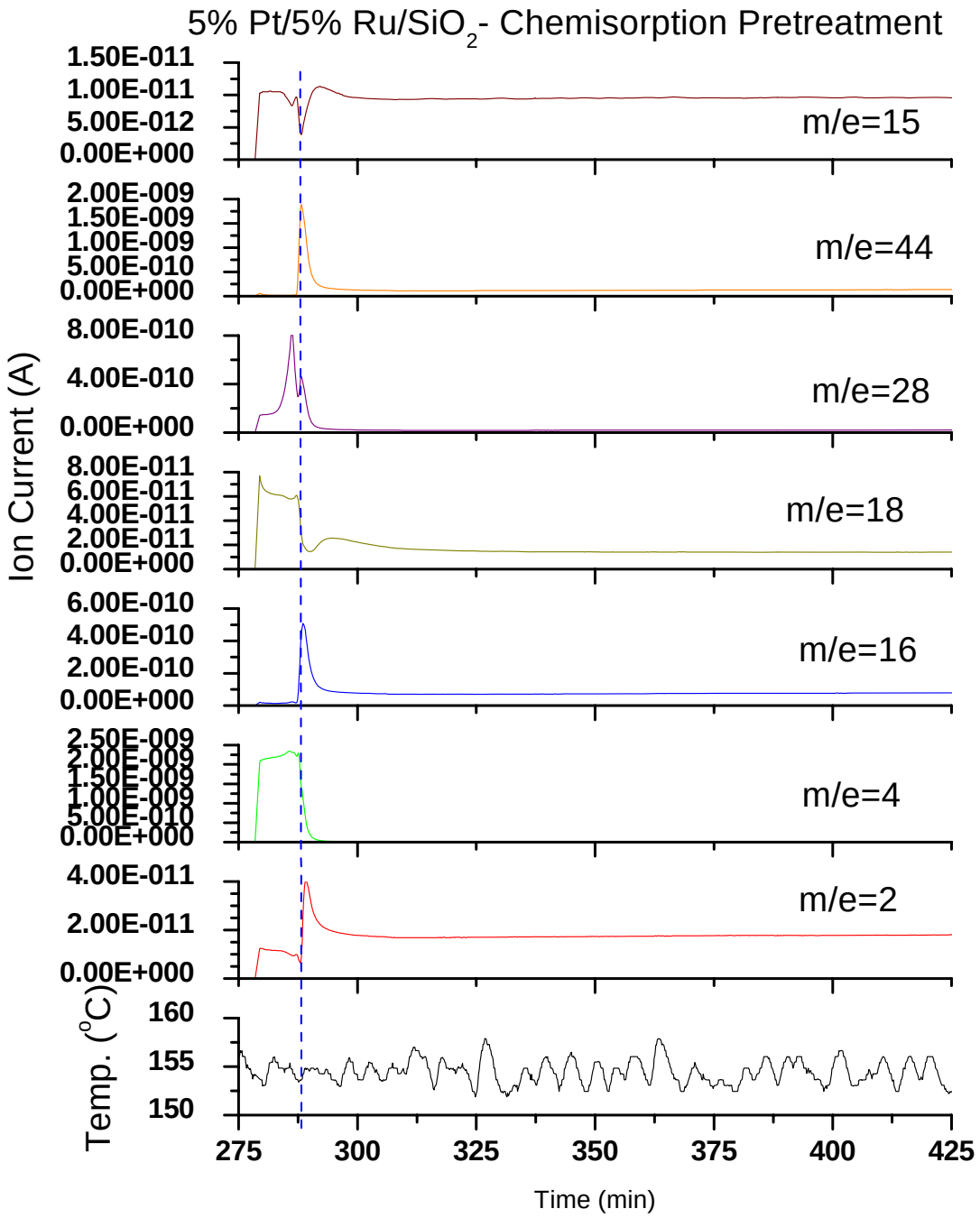

Figure A-6. Corollary Mass Spectrometer Response for RWGS Reaction over 5% Pd/5% Ru/SiO_2 (T=150°C)

References

[1] Minder, B.; Mallat, T.; Pickel, K. H.; Steiner, K.; Baiker, A. Catal. Lett. 34 (1995) 1-9.

[2] Ichikawa, S.; Tada, M.; Iwasawa, Y.; Ikariya, T. Chem. Commun. (2005) 924-926.

[3] Xu, D.; Carbonell, R. G.; Kiserow, D. J.; Roberts, G. W. Ind. Eng. Chem. Res. 44 (2005) 6164-6170.

[4] Gehlsen, M. D.; Bates, F. S. Macromolecules 26 (1993) 4122-4127.

[5] Gehlsen, M. D.; Weimann, P. A.; Bates, F. S.; Harville, S.; Mays, J. W.; Wignall, G. D. J. Appl. Poly. Sci. Part B: Polym. Phys. 33 (1995) 1527-1536.

[6] Xu, D.; Carbonell, R. G.; Kiserow, D. J.; Roberts, G. W. Ind. Eng. Chem. Res. 42 (2003) 3509-3515.

[7] Bussard, A.; Dooley, K. M. AIChE J. 54 (2008) 1064-1072.

[8] Hucul, D. A.; Hahn, S. F. Advanced Materials 12 (2000) 1855-1858.

[9] Ness, J. S.; Brodil, J. C.; Bates, F. S.; Hahn, S. F.; Hucul, D. A.; Hillmyer, M. A. Macromolecules 35 (2002) 602-609.

APPENDIX B: EFFECT OF PALLADIUM/RUTHENIUM RATIO ON POLYSTYRENE HYDROGENATION IN CO_2-DHN

B.1. Introduction

Catalyst deactivation has been observed in the batch hydrogenation of polystyrene (PS) in carbon dioxide (CO_2)-expanded decahydronaphthalene (DHN). As a result, the desired aromatic ring hydrogenation ceased. The catalyst deactivation has been attributed to the formation of carbon monoxide (CO) via the reverse water-gas shift (RWGS) reaction. Previous studies have shown that the use of a physical mixture of a Pd hydrogenation catalyst with a small amount of methanation catalyst was effective in reducing CO levels and allowing ring hydrogenation to proceed. While a supported nickel catalyst was previously used as the methanator, this research explored the use of 5% Ru/Al_2O_3 as the methanation catalyst for PS hydrogenation in CO_2-DHN.

B.2. Materials and Methods

Two catalysts, 5% Pd/Al_2O_3 and 5% Ru/Al_2O_3, were purchased from Sigma-Aldrich (Milwaukee, WI). Commercial grade PS with a number-average molecular weight of 130,000 g/mol and a weight-average molecular weight of 170,000 g/mol and anhydrous DHN, a 24/76 mixture of *cis* and *trans* isomers, were purchased from Sigma-Aldrich (Milwaukee, WI) and used as received.

A series of two-hour reactions were run in a slurry batch reactor (Autoclave Engineers, Erie PA). The temperature was maintained at 150^{o}C. Using UV-VIS spectroscopy, the aromatic ring concentration (C_A) was determined by measuring the absorbance at 261.5 nm. The aromatic ring concentration was then used to compute the degree of hydrogenation (x_A) by the formula: $x_A=1-C_A/C_{A0}$, where C_{A0} is the aromatic ring concentration at t = 0. The gas from the reactor was collected in a gas sampling bag. Carbon monoxide concentrations in the gas were analyzed by drawing gas through a Draeger CO detection tube (10/b, Draeger Safety, Pittsburgh, PA) using an accuro bellows pump (Draeger Safety, Pittsburgh, PA). Additional details of the reaction procedure may be found in Chapter 4.

B.3. Results and Discussion

A series of hydrogenations were run in which the catalyst to polymer ratio was maintained at 1:1 (g:g) while the Pd and Ru contents were varied. Figure B-1 shows the weak dependence of x_A on the Pd/Ru ratio for PS hydrogenation in neat DHN. The degrees of hydrogenation for the reaction in CO_2-DHN are consistently lower than those obtained in the neat organic solvent. The addition of Ru as a co-catalyst in the CO_2-containing reaction results in x_A steadily increasing from 0.16. However, the use of 5% Ru/Al_2O_3 as the sole catalyst for PS hydrogenation in CO_2-DHN is not as effective as using the physical mixture of supported Pd and Ru catalysts.

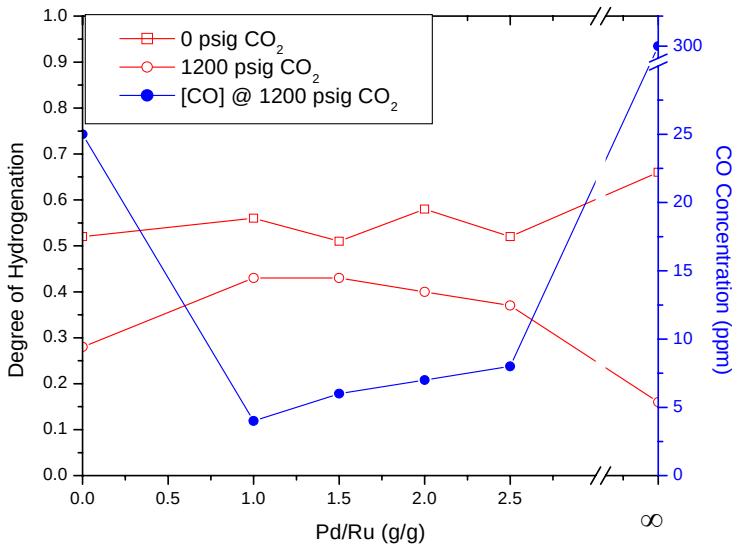

Figure B-1. Effect of Pd/Ru Ratio on PS Hydrogenation. (T=150°C, 2 hr., 3 wt% PS-DHN, 800 psig H_2, 1 g catalyst/g PS, 2500 rpm)

The behavior of x_A may be directly correlated to the CO concentrations of the gas collected at the end of the reactions in CO_2-DHN. The concentrations of the catalyst poison CO at the two extremes (Pd/Ru=0 or Pd/Ru=∞) were higher than the values obtained when catalyst mixtures were used. Consequentially, hydrogenation activity is lower since CO poisons hydrogenation sites.

The present results contrast with those obtained for PS hydrogenation in CO_2-DHN using a mixture of 5% $Pd/BaSO_4$ and 65% $Ni/SiO_2/Al_2O_3$ catalysts. In the previous work, CO levels were reduced *and* aromatic ring hydrogenation in CO_2-DHN was comparable to the values obtained for the reaction in neat DHN. Comparable levels of CO reduction were observed in this research. However, aromatic ring hydrogenation never matched or exceeded the values obtained for the reaction in neat DHN. As

demonstrated in Chapter 4, the Ru catalyst was more effective than Ni catalyst in methanating CO. The contrast between the observed behaviors is attributed to the differences between the Pd hydrogenation catalysts. As discussed in Chapter 4, it is believed that the use of mesoporous 5% Pd/Al_2O_3 resulted in internal mass transfer limitations for PS hydrogenation while the internal mass transfer resistance was very small or non-existent for the RWGS reaction. Consequentially, CO is formed and poisons sites for hydrogenation before it contacts the methanation catalyst and undergoes reduction.

APPENDIX C: SYNTHESIS OF PALLADIUM-BASED CATALYSTS FOR POLYSTYRENE HYDROGENATION

C.1. Introduction

The effect of pore diffusion resistances on the kinetics of heterogeneous polystyrene (PS) hydrogenation was shown in Chapters 4 and 5. The research demonstrated the need for using a macroporous support when high molecular weight PS is hydrogenated. Also, a bimetallic catalyst in which a hydrogenation metal such as palladium and a methanation metal such as ruthenium located on the same porous support must be used when the reaction is conducted in a carbon dioxide-expanded liquid.

In this work, several Pd/SiO_2 catalysts were prepared and tested for their hydrogenation activities. Additionally, two $Pd/Ru/SiO_2$ catalysts were made and used to hydrogenate PS in neat and CO_2-expanded decahydronaphthalene (DHN).

C.2. Materials and Methods

C.2.1. Materials

Palladium (II) nitrate hydrate (99.9% metals basis, Alfa Aesar, Ward Hill, MA) was used as received. Palladium (II) chloride (99.9% metals basis, Alfa Aesar, Ward Hill, MA) was used as received. Ruthenium (III) chloride hydrate was purchased from Strem Chemicals (Newburyport, MA) and used as received. Deionized ultra-filtered water was purchased from Fisher Chemical (Pittsburgh, PA) and used as received. Nitric

acid and hydrochloric acid were purchased from Alfa Aesar (Ward Hill, MA) and used as received. Ammonium hydroxide (10% v/v, Ricca Chemical, Arlington, TX) was used as received.

The Davicat SI 1410 SiO_2 support was donated by Grace-Davison. The BET surface area is 36 m^2/g. An average pore diameter of 122 nm was determined from intrusion volume obtained by mercury porosimetry. An ultra-wide pore SiO_2 was donated by Fuji-Silysia. The BET surface area was 7.9 m^2/g. The supplier provided an average pore diameter of 517 nm and an average particle size of 71 μm.

C.2.2. Catalyst Preparation

The incipient wetness impregnation technique was used to prepare the catalysts. The acidic catalyst precursor solution was created by adding a known amount of water to a vial containing the metal precursor before a small aliquot of acid was added. The next day, a volume of precursor solution that was equal to the pore volume of the support was added to the SiO_2, which had been dried in air overnight at 115°C. The mixture was stirred to distribute the precursor solution evenly in the support. The impregnated support was then dried overnight in air at 115°C before it was subjected to calcination and reduction steps. The sample was purged with nitrogen at room temperature and heated at 10°C/min to 500°C. The catalyst was calcined for 3 hours in air before being cooled to 327°C. The catalyst was then reduced with H_2 at 327°C for 2 hours.

The bimetallic catalysts were subjected to an ammonium hydroxide wash to remove any residual chlorides. A 5% (v/v) ammonium hydroxide solution was added to a jar containing the catalyst. The solution was tumbled for 24 hours before it was subjected to vacuum filtration. The catalyst was then rinsed with more ammonium hydroxide solution, then water, and then it was then dried in air at 115^{o}C for 24 hours. The washed catalyst was then subjected to calcination and reduction as described in the previous paragraph.

C.2.3. Catalyst Characterization

The BET surface areas and metal dispersions of the catalysts were measured using an Autosorb 1-C (Quantachrome Instruments, Boynton Beach, FL). The samples were outgassed at 300^{o}C for at least 1 hour before the surface areas were measured. For hydrogen chemisorption measurements, the catalysts were dried at 120^{o}C under helium flow. They were then reduced with hydrogen at 327^{o}C. Dual hydrogen isotherms were measured. The reported dispersion values of the monometallic catalysts are based on a Pd/H of 1:1. Dispersion values could not be calculated for the bimetallic catalysts because the calculation requires information that is unique to the catalytic metal. Hydrogen chemisorption does not differentiate between metals, so the monolayer uptakes of H_2 are reported for the bimetallic catalysts.

C.2.4. Polystyrene Hydrogenation

Polystyrene hydrogenation was conducted at 150^{o}C using a slurry batch reactor. Hydrogen pressure was maintained at 800 psig; an agitation rate of 2500 rpm was used. The degree of aromatic ring hydrogenation (x_A) was calculated from the aromatic ring concentration (C_A), which was obtained by measuring the absorbance at 261.5 nm using UV-VIS spectroscopy. Details of the reaction procedure may be found in Chapter 4.

C.3. Results and Discussion

Four 5% Pd/SiO_2 catalysts were synthesized by incipient wetness impregnation. The SiO_2 support with an average pore diameter of 122 nm was used in the monometallic catalysts. As shown in Table 1, the Pd loadings, which were measured using inductively coupled plasma-mass spectrometry (ICP-MS), were slightly below the target value of 5 wt%. The Pd dispersions are relatively low and can be correlated directly to their activities for PS hydrogenation. The most poorly dispersed catalyst has the lowest activity while the most highly dispersed catalyst has the highest activity. All of the values are far less than what was obtained for the commercially available 5% Pd/SiO_2 tested in Chapter 4. The commercial 5% Pd/SiO_2 catalyst has a smaller pore diameter (9 nm) than the SiO_2 used in this research.

Table C-1. 5% Pd/SiO_2 Catalysts for PS Hydrogenation

Sample	Pd Content (wt%)	Dispersion[a]	x_A[b]
1	4.41	3.2%	0.42, 0.31
2	3.42	0.8%	0.1
3	4.36	1.3%	0.12
4	4.07	1.7%	0.27

[a] Dispersion values measured by H_2 chemisorption, assuming Pd/H=1
[b] Reactions run for 2 hours at 150°C (3 wt% PS-DHN, 800 psig H_2, 2500 rpm)

The bimetallic catalysts, which were prepared using the SiO_2 with an average pore diameter of 517 nm, were used to hydrogenate PS dissolved in DHN and CO_2-DHN in 2-hour reactions. Table C-2 compares the results of hydrogenating PS using the 5% Pd/5%Ru/SiO_2 catalyst before and after the catalyst was subjected to an ammonium wash. The catalyst had a lower activity for PS hydrogenation post-wash; this is possibly due to some catalytic metal being lost during the wash step. The x_A's obtained when CO_2 was present are lower than those obtained in neat DHN. No CO was found in the gas phase from the "no wash" catalyst; 5 ppm was detected in the gas phase from the post-wash catalyst. It appears that the homemade 5% Pd/5% Ru/SiO_2 catalyst is not effective in hydrogenating PS in the neat or CO_2-expanded organic solvent.

Table C-2. PS Hydrogenation Using 5% Pd/5% Ru/SiO_2

Reaction Parameters	x_A
No CO_2, No Wash	0.35
1200 psig CO_2, No Wash	0.30
No CO_2, Wash	0.22
1200 psig CO_2, Wash	0.15

(T=150°C, 2 hr., 3 wt% PS-DHN, 800 psig H_2, 1 g catalyst/g PS, 2500 rpm)

Assuming equal Pd and Ru levels and monolayer metal coverage, the maximum metal loading on the 7 m^2/g-SiO_2 was determined to be 0.8 wt% for each metal. A nominal 1% Pd/1% Ru/SiO_2 catalyst was prepared and subjected to an ammonium hydroxide wash before screening tests were run. The resulting x_A's, which are given in Table C-3, show that the catalyst does not possess very much hydrogenation activity.

Table C-3. PS Hydrogenation Using 1% Pd/1% Ru/SiO_2

Reaction Parameters	x_A
No CO_2	0.11
1200 psi CO_2	0.08

(T=150^{o}C, 2 hr., 3 wt% PS-DHN, 800 psig H_2, 1 g catalyst/g PS, 2500 rpm)

The monolayer H_2 adsorption uptakes (μmol H_2/g cat) were measured. The uptake values were multiplied by the nominal total metal weight loadings to obtain a value in terms of moles H_2 per weight metal (N_m'). There is some error in the calculation since the actual metal weight loadings were not used, but the results, which are shown in Table C-4, provide first-pass knowledge of the metal dispersion. A lower N_m' value, as seen with the 5% Pd/5% Ru/SiO_2 catalyst, suggests a larger crystallite size since there is less exposed metal available for H_2 adsorption. Because there are two different metals present, each possessing their own size, no direct calculations of metal dispersion or metal crystallite sizes can be made. Nevertheless, the results are consistent with the belief that the 10% total metal weight loading would result in large crystallites since the maximum monolayer metal loading was determined to be 1.6 wt% on the support of

interest. Further catalyst characterization would provide more insight into the relationship between hydrogenation activity and catalyst properties.

Table C-4. Hydrogen Uptakes of Bimetallic Catalysts for PS Hydrogenation

Catalyst	N_m' (μmol H_2/g metal)
5% Pd/5% Ru/SiO_2	98
1% Pd/1% Ru/SiO_2	142

APPENDIX D: PRELIMIINARY MOLAR KERR CONSTANT CALCULATIONS FOR STYRENE-VINYLCYCLOHEXANE COPOLYMERS

D.1. Introduction

Polymer microstructure influences a polymer's macroscopic behavior and ultimately its end use [1]. The regiosequence (head-to-head, head-to-tail, tail-to-tail arrangement) and stereosequence (meso, racemic) of a polymer can affect its solubility and reactivity [2]. For copolymers, the sequence length distributions of the component monomers may also influence copolymer macroscopic behavior. Identifying these characteristics can lead to the development of tailored polymeric materials.

Infrared spectroscopy, nuclear magnetic resonance (NMR) spectroscopy, and mass spectroscopy are examples of techniques that have been used to characterize polymer microstructures [1]. In some cases, traditional methods such as NMR or pyrolysis/mass spectrometry are not able to identify sequence lengths in copolymers [3]. However, a property called the molar Kerr constant (mK) can be used to identify both the microstructure and sequence length distributions of copolymers. The determination of mK for polymers created under different reaction conditions (which is related to a sample's optical birefringence induced by a strong electric field) can provide insight on how reaction conditions affect the polymer product microstructure and sequence length distributions.

As discussed in Chapter 6, it appears that the physical properties of styrene-vinylcyclohexane (S-VCH) copolymers produced through polystyrene (PS) hydrogenation are sensitive to the catalyst used in PS hydrogenation. In this work, mK's for isotactic styrene-vinycyclohexane (S-VCH) chains consisting of 250 monomers were calculated. The calculations demonstrate the potential utility of mK in describing the differences in sequence lengths distributions of styrene and VCH in a copolymers created by PS hydrogenation.

D.2. Methodology

Molar Kerr constants for polymers are obtained from the Kerr constants of their dilute solutions. The Kerr constant is a parameter that is derived from inducing optical birefringence, or the electro-optic Kerr effect, in a normally isotropic polymer solution. The application of an electric field to a polymer dissolved in a solvent induces a birefringence that has been shown to be sensitive to tacticity, composition, and the sequence length distribution of a polymer. In order to use mK's to quantify sequence length distributions, a combination of theory and experiments must be used. This research presents preliminary work in developing a model for describing the mK's of S-VCH.

Theoretical calculation of mK's are rooted in Flory's rotational isomeric states (RIS) model, which has been used to determine other conformation dependent-properties such as dipole moments, mean square radii of gyration, and mean-squared optical

anisotropies [4]. The RIS model employs matrix multiplication methods as well as statistical mechanics to determine the probabilities of different conformations of a polymer. Details on the use of matrix multiplication methods to calculate conformation dependent properties can be found in Flory [4].

As shown in Equation D-1, mK is a function of the dipole moment (μ), traceless optical polarizability tensor $(\hat{\alpha})$, and the static polarizability tensor $(\hat{\alpha}')$ [5].

$$mK = \left(\frac{2\pi N_A}{15kT}\right)\left[\frac{\langle \mu^T \hat{\alpha} \mu \rangle_o}{kT} + \langle trace(\hat{\alpha}\ \hat{\alpha}') \rangle\right] \qquad \text{(D-1)}$$

Avogadro's number is represented by N_A, k is the Boltzmann's constant, and T is the absolute temperature. A generator matrix that is used to compute the average dipole moment contribution $(\langle \mu^T \alpha \mu \rangle)$ is 78 x 78 in size. Similarly, the generator matrix for the calculation of the average polarizability contribution $(\langle Trace(\hat{\alpha}\hat{\alpha}') \rangle)$ is 33 x 33 in size.

In order to fill in the matrices, the bond lengths, valence angles, and rotational states of the chemical bonds in a polymer chain must be known; some of the information may be found in Suter and Flory [6]. The conformational energies of three dyads (S-S, VCH-VCH, and S-VCH) were determined for this research. The conformation energies were used to determine the most favorable polymer conformations (based on energy minima) and to form the components of the generator matrices.

The conformational energies of PS and the use of the RIS model to study PS's conformation-dependent properties is well documented [7-9]. However, the use of the

RIS model to describe PVCH conformation is not well established. To the present knowledge, only isotactic PVCH has been modeled [10]. In order to calculate mK's for S-VCH copolymers, the conformational energies of an isotactic S-VCH dyad was calculated. Then the energies of S-VCH were combined with energies of the styrene and VCH dyads to calculate the dipole moment and polarizability contributions. The polarizability tensors for PS and cyclohexyl-based compounds can be found in several resources [11-13]. Using a MATLAB program, the contributions were substituted into Equation D-1 to compute mK for S-VCH polymers of differing styrene and VCH sequence lengths.

D.3. Results

Figures D-1 through D-3 show the mK's for isotactic S-VCH of varying VCH content at 27^{o}C. The number of consecutive styrene units is denoted by S*i* while the number of consecutive VCH units is denoted by VCH*j*. Figure D-1 shows the values of a polymer of 250 units that is 20% styrene. The blocky polymer (S50-V200) has a mK that is nearly an order-of-magnitude smaller than the mK for the (S1-V4) polymer. The mK for the blocky polymers stay fairly constant until the styrene sequence length decreases to 2 (S2-V8).

There is not much change in the mK for a 50:50 S-VCH polymer (Figure D-2) since there is just over a twofold difference in mK as the polymer sequence changes from blocky to alternating, but the general trend of the mK of a blocky copolymer being less

than that of an alternating copolymer is valid. Lastly, Figure D-3 shows the mK values for an isotactic S-VCH polymer that is 80% styrene. Only a small change in mK is noted as the S-VCH sequence length grows smaller. Again, the blockier polymer has lower mK's than its less blocky counterparts. It is not clear why the S4-V1 mK is lower than that of S8-V2.

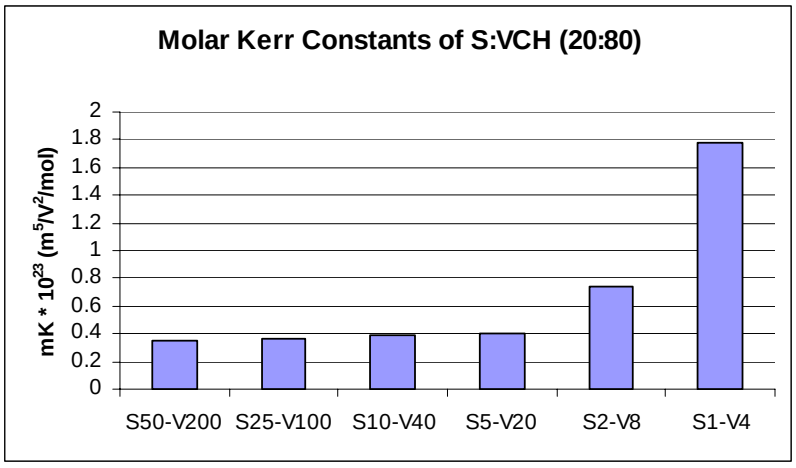

Figure D-1. Molar Kerr Constants for Isotactic S-VCH Copolymer, 20% Styrene (T=27°C, 250 monomers)

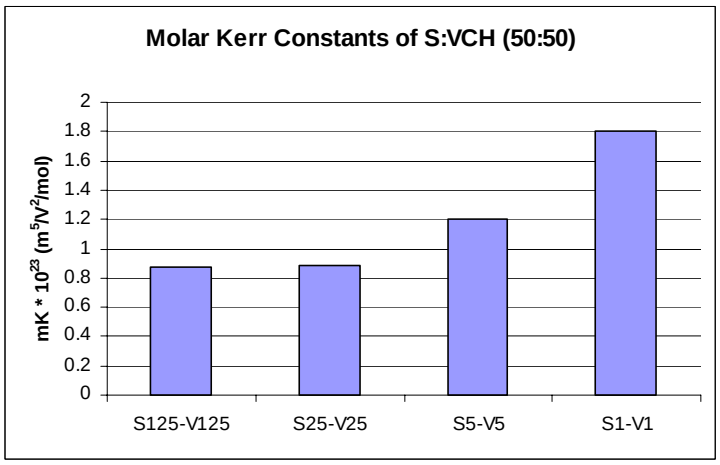

Figure D-2. Molar Kerr Constants for Isotactic S-VCH Copolymer, 50% Styrene (T=27°C, 250 monomers)

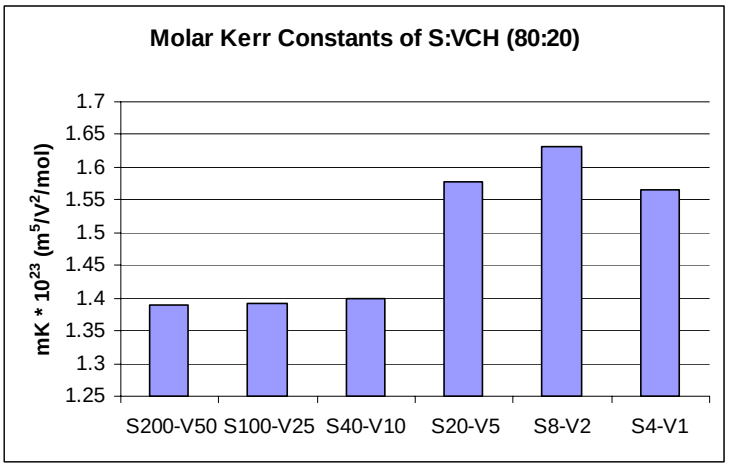

Figure D-3. Molar Kerr Constants for Isotactic S-VCH Copolymer, 80% Styrene (T=27°C, 250 monomers)

D.4. Acknowledgement

The MATLAB programming work of undergraduate research assistant Kevin Liang is gratefully acknowledged.

References

[1] Sperling, L.H. 2006. *Introduction to Physical Polymer Science*. 4th ed. 2006, Hoboken, NJ: Wiley-Interscience.

[2] Tonelli, A.E. *NMR Spectroscopy and Polymer Microstructure: The Conformational Connection*. 1989, Hoboken, NJ: Wiley-VCH.

[3] Zaikin, V.G.; Mardanov, R. G.; Kleiner, V. I.; Krentsel, B. A.; Plate, N. A. Journal of Analytical and Applied Pyrolysis, 1990. 17: 291-304.

[4] Flory, P.J. Macromolecules, 1974. 7: 381-392.

[5] Tonelli, A.E. Macromolecules, 1977. 10: 153-157.

[6] Suter, U. W.; Flory, P. Macromolecules, 1975. 8: 765-776.

[7] Fujiwara, Y.; Flory, P. Macromolecules, 1970. 3: 43-49.

[8] Yoon, D.Y.; Sundararajan, P. R.; Flory, P. J. Macromolecules, 1975. 8: 776-783.

[9] Li, X.; Yang, X.; Zhao, D.; Qian, R. Polymer, 1996. 37: 3929-3935.

[10] De Rosa, C.; Borriello, A.; Corradini, P. Macromolecules, 1996. 29: 6323-6327.

[11] Suter, U. W.; Flory, P. J. J. Chem. Soc. Farad. Trans. 2, 1977. 73: 1521-1537.

[12] Mattice, W. L.; Saiz, E. J. Polym. Sci. Part B: Polym. Phys, 1986. 24: 2669-2679.

[13] Navard, P.; Flory, P. J. J. Chem. Soc. Farad. Trans. 1, 1986. 82: 3367-3380.

APPENDIX E: POLYCARBONATE HYDROGENATION FEASBILITY STUDY

E.1. Introduction

The selective hydrogenation of the aromatic ring in poly(bisphenol A carbonate) BPA-PC, which is shown in Figure E-1, would create hydrogenated poly(bisphenol A carbonate), or HBPA-PC. The product polymer has better solvent resistance and higher softening temperature than BPA-PC [1].

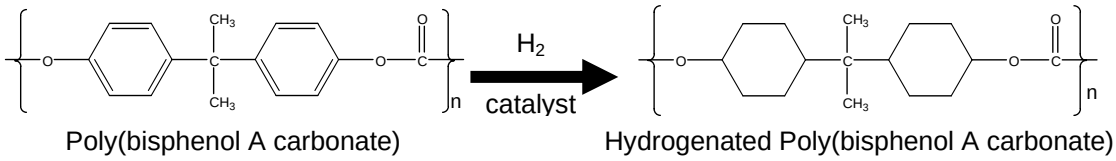

Figure E-1. Selective Hydrogenation of Poly(bisphenol A carbonate)

No attempts to hydrogenate BPA-PC are known. However, the desired copolymer product has been synthesized by other methods. HBPA-PC has been produced by phosgenation of hydrogenated bisphenol A (HBPA) [1] or melt transesterification of HBPA and diphenyl carbonate (DPC) [2]. Phosgenation of HBPA resulted in a polymer with a softening temperature (225 to 250^{o}C) that was on average 25 to 50^{o}C higher than that of BPA-PC. The product also exhibited solvent resistance to typical BPA solvents such as pyridine and dioxane [1]. A high molecular weight HBPA

polycarbonate (weight average molecular weight of 100,000) was formed from the melt transesterification process with zinc oxide serving as the catalyst [2].

Polycarbonate copolymers have been mentioned in literature. A Mitsubishi Gas Company patent discusses the synthesis of 2,2-bis[4-(4'-hydroxybenzoyloxy)cyclohexyl] propane, which is shown in Figure E-2, as a starting material for resins [3]. The dihydroxy compound is formed from the transesterification of HBPA and alkyl 4-hydroxybenzoate in the presence of a tin catalyst.

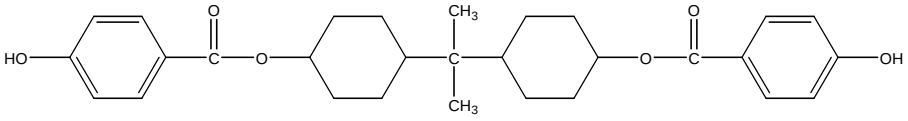

Figure E-2. 2,2-bis[4-(4'-hydroxybenzoyloxy)cyclohexyl]propane

Schnell referred to bisphenol A (BPA) and HBPA copolymers in his book on polycarbonates [4]. The French patent produced copolymers with 80 mole percent BPA to 20 mole percent HBPA and 50:50 mole percent mixture of the two [5]. In both cases, the melting range of the copolymer increased from that of BPA-PC. The German patent produced a 50:50 mole percent copolymer that had a higher melting range than the 50:50 copolymer produced in France [6].

E.2. Catalyst Selection

Potential catalysts for BPA-PC hydrogenation have been selected based on their abilities to selectively hydrogenate aromatic rings in the presence of carbonyl groups. Sud-Chemie's website names palladium as suitable for the desired application [7]. Other literature suggests ruthenium is suitable for the selective hydrogenation of aromatic rings in the presence of carbonyl groups.

The use of both catalysts is confirmed by research on model compounds such as dimethyl terephthalate (DMT). DMT hydrogenation has garnered industrial and academic interest. Palladium, ruthenium, rhodium, or combinations of the three catalysts have been used to hydrogenate the aromatic ring in DMT.

Eastman Kodak has patented several techniques for DMT hydrogenation [8-11]. The ultimate goal of their work is to form 1,4-dimethylcyclohexanedimethanol. As shown in Figure E-3, this is achieved in a series of reactions. The first reaction, which is the segment that parallels our research goal, uses Pd/Al_2O_3 to convert DMT to dimethyl-1,4-cyclohexanedicarboxylate (DMCD). This is achieved at temperatures between 150 and 275^{o}C and pressures between 3000 and 5000 psi.

Milder operating temperatures and pressures are used when other types of catalysts are used for DMT hydrogenation. For example, rhodium catalysts, sometimes tethered on Pd/SiO_2, have been used to hydrogenate DMT and other arene molecules such as methyl benzoate [12]. Reaction conditions for these catalysts were typically in the neighborhood of 70^{o}C and 60 psi [12, 13].

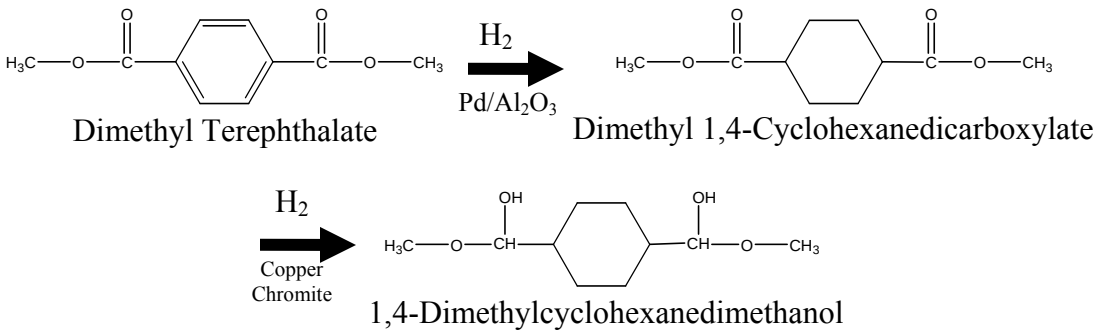

Figure E-3. Eastman's Dimethyl Terephthalate Hydrogenation

Supported ruthenium has been used to hydrogenate DMT. In one case, Ru/Al_2O_3 was used at 100 to 140°C and 700 to 800 psi to convert DMT to DMCD [14]. DuPont hydrogenated DMT to DMCD using 5 wt% Ru/C as a catalyst [15]. Pressure ranged from 500 to 1500 psig with a reaction temperature between 110 to 140°C. Ru/C has also been used to selectively hydrogenate the aromatic rings of neutralized trimellitic acid to cyclohexane-1,2,4-tricarboxylic acid using Ru/C as the catalyst [16].

E.3. Solvent Selection Studies

Three criteria exist for BPA-PC solvents: environmentally friendly character, relatively high boiling point (greater than 100°C), and no undesired reactivity with hydrogen. Literature identified several potential BPA-PC solvents. Qualitative solubility experiments narrowed the list to a few that were tested for reaction with hydrogen in the presence of the chosen catalysts. The solubilities of BPA-PC and HBPA have also been tested in the products of the solvent hydrogenation studies.

Literature indicates that halogenated hydrocarbons such as methylene chloride, chloroform, or fluorobenzene are suitable solvents for amorphous or crystalline BPA-PC [4, 17]. Not only are these compounds environmentally unfriendly, they have low boiling points and were therefore eliminated from further solvent studies. Other more environmentally friendly solvents are indicated by "*" in Table E-1.

The suitable BPA-PC solvents suggested by literature have at least one conjugated moiety, i.e., an aromatic ring and or a carbonyl group. The unsaturation allows for the possibility of solvent hydrogenation. With this in mind, "cousins" of the BPA-PC solvents were also tested for their abilities to dissolve BPA-PC. These cousins are forms of the solvents with different elements saturated, i.e., the aromatic ring and/or carbonyl group.

Both reactant and product solubility is important to the BPA-PC hydrogenation research. Ideally, the solubilities of the two components that comprise HBPA-PC (i.e., dicyclohexyl carbonate (hydrogenated diphenyl carbonate) and HBPA) would be determined in the potential solvents. However, only HBPA was commercially available.

The solubilities of BPA-PC (melt index= 10.5 g/10 minutes, Sigma Aldrich) and HBPA (Sigma Aldrich) were tested. All solvents were used as received. A known amount of solvent was added to a clean vial. An appropriate mass of solute was then added to the solvent in order to make a 5 weight percent solution. A magnetic stir bar was added to the vial, and the solutions were stirred for 24 hours. Qualitative observations on the dissolution (or lack of dissolution) were made. The solution

temperatures were then increased to 100°C, and additional observations were taken after 24 hours. The results of the solubility tests are given in Table E-1. The best solvents for BPA-PC contain the carbonyl functional group.

Table E-1. Results of BPA-PC and HBPA Solubility Experiments

	Room Temp.		100°C	
Solvent	**PC**	**HBPA**	**PC**	**HBPA**
Acetophenone*	P	P	Y	Y
Cyclohexyl Methyl Ketone	P	P, ~95%	P,~50%	Y
1-Cyclohexylethanol	N	Y	P	Y
Anisole*	P	P	Y	Y
Cyclohexanone*	P, ~75%	P	Y	Y
Cyclohexanol	P	Y	P	Y
n,n-Dimethylformamide*	P	Y	Y	Y
Benzaldehyde*	P, ~50%	P, ~75%	Y	Y
Cyclohexanal	P	P, ~90%	Y	Y
Cyclohexylmethanol	N	Y	P	Y
Cyclopentanone*	P, ~90%	P, ~75%	Y	Y
Cyclopentanol	N	Y	P	Y
n,n-Dimethylacetamide*	P	Y	Y	Y
Methyl benzoate*	P, ~50%	P	Y	Y
Methyl cyclohexylcarboxylate	P	P, ~75%	P, ~20%	Y
n,n-Dimethylcyclohexylamine	N	--	Y	--
Cyclohexane	N	--	Evaporates	--
Decahydronapthalene	N	--	N	--
Dicyclohexyl	N	--	N	--
Dicyclohexyl ketone	N	--	N	--

Key:
Target BPA-PC Concentration = 5 wt%
P = partial dissolution, Y = total dissolution, N = no dissolution.
Percentages indicate approximations of solute dissolved
* denotes literature suggested solvent

E.4. Solvent Hydrogenation Studies

After considering the Hazardous Materials Information System (HMIS) ratings for the three chemicals, additional solvent screening studies of acetophenone, methyl benzoate, and cyclopentanone have been conducted. Methyl benzoate is a GRAS (Generally Recognized As Safe) solvent while cyclopentanone has an HMIS rating of 1 (on a scale of 1 to 5 with 1 being the least harmful).

Solvent hydrogenation studies were conducted in the 50 mL batch reactor (Autoclave Engineers) that has been used for the group's polystyrene hydrogenation work. A typical 1-hour reaction was run at 90^{o}C at an agitation rate of 2000 rpm. One half gram of catalyst (1 wt% Pd/Al_2O_3, Alfa Aesar or 5 wt% Ru/Al_2O_3, Sigma Aldrich) was used per 25 mL of solvent. Hydrogen (National Welders) pressure was initially 1000 psig. If the pressure dropped significantly, hydrogen was added to the reactor to increase the pressure to 1000 psig.

All three potential solvents show some hydrogenation. Cyclopentanone was the least reactive potential solvent while acetophenone was the most reactive. The results of the methyl benzoate reactions were not reproducible. The analyses of the product solutions were conducted using the ReactIR system (Mettler-Toledo Autochem) available in the laboratory. A resultant spectrum was obtained by subtracting the neat solvent spectrum from the product spectrum. These resultant spectra indicated the disappearance of the carbonyl functional group (~1750 cm^{-1}) and the formation of alcohols (~3500 cm^{-1}) and cyclohexyl rings (~2940 cm^{-1}).

E.5. Solubilities of BPA-PC and HBPA in Hydrogenated Potential Solvents

The solubilities of BPA-PC and HBPA were tested in the hydrogenated potential solvents (HPS's). Initially, a mass of BPA-PC or HBPA was added to a HPS to constitute a one weight percent solute mixture. If the mass fully dissolved, enough BPA-PC or HBPA was added to form a five weight percent mixture. The results of the experiments are shown in Table E-2. Cyclopentanone was determined to be the most promising solvent and was used in further study.

Table E-2. Summary of Solubility Studies with Hydrogenated Potential Solvents

Hydrogenated Potential Solvent	1 wt% BPA-PC	≥ 5 wt% BPA-PC	1 wt% HBPA	≥ 5 wt% HBPA
Acetophenone	N	---	Y	N
Cyclopentanone	Y	Y	Y	N
Methyl Benzoate	N	---	N	---

Y = soluble at particular concentration; N = not soluble at particular concentration

E.6. BPA-PC Hydrogenation

The hydrogenation of one weight percent BPA-PC dissolved in cyclopentanone was attempted using the suggested Pd/Al_2O_3 or Ru/Al_2O_3 catalysts. Using a ratio of 2 grams of catalyst to 1 gram of polymer, the reaction was carried out at 90^{o}C and 2000 rpm. Initial hydrogen pressure was 1000 psig. Hydrogen was supplemented to the reactor if the pressure dropped below ~700 psig.

UV-VIS analyses of the product solutions from the Pd/Al_2O_3 or Ru/Al_2O_3 indicated the disappearance of the carbonyl group of BPA-PC (~337 nm). IR spectrum from the Pd/Al_2O_3 catalyzed hydrogenation indicates that the disappearance of the carbonyl functional group coincides with the formation of an alcohol group. No changes in the aromatic ring peaks occurred. When the reaction was catalyzed by Ru/Al_2O_3, the resulting IR spectrum shows much more prominent carbonyl disappearance and alcohol formation. Furthermore, the disappearance of the aromatic ring and the formation of the cyclohexyl rings were observed.

The preliminary studies on the heterogeneous hydrogenation of BPA-PC showed that the selective hydrogenation of the aromatic unit is difficult to control. A better understanding of the parameters that influence the heterogeneous polymer hydrogenation process would provide insight as to which catalyst support, catalytic metal, and solvent would facilitate the desired reaction while minimizing the undesired results.

References

[1] Goldberg, E. P. U. S. Patent 3157622. 1964.

[2] Yao, K. M.; Miyamoto, M.; Takegawa, I.; Aida, M. US Patent 6136946. 2000.

[3] Masumoto, M.; Asoh, T.; Ezaki, Y.; Aibe, H. US 4924025. 1990.

[4] Schnell, H. Chemistry and Physics of Polycarbonate. 1964, New York: Interscience Publishers

[5] Goldberg, E. P. France Patent 1198715. 1959.

[6] Schnell, H. B.; Schnell, H., Bottenbruch, L., Krimm, H., Fritz, G. Germany Patent 971777. 1959.

[7] Selective Hydrogenation of Different Functional Groups. http://www.sud-chemie.com/smcms/web/

[8] Akin, G. A. L.; Lewis, H. J.; Reid, T. F. US Patent 3334149. 1967.

[9] Gustafson, B. L. T.; Tennant, B. A.; Kuo, Y-J.; Price, T. W. US Patent 5286898. 1994.

[10] Gustafson, B. L. T.; Kuo, Y-J.; Tennant, B. A. US Patent 5319129. 1994.

[11] Tennant, B. A.; Williams, M. D.; Gustafson, B. L. US Patent 5399742. 1995.

[12] Gao, H.; Angelici, R. J. New J. Chem., 1999. 23: 633-640.

[13] Yang, H., Gao, H., Angelici, R. J. Organometallics, 2000. 19: 622-629.

[14] Lo, M-Y., Chang, M-Y. US Patent 6803341 B2. 2004.

[15] Foohey, W. L. US Patent 3027398. 1962.

[16] Jaffe, F. US Patent 3444237. 1969.

[17] Heiss, J. L. Polymer Engineering and Science, 1979. 19: 625-637.